ABSTRACT

Title of Thesis: COMMUNITY METABOLISM AND ENERGY TRANSFER IN THE CHESAPEAKE BAY TURBIDITY MAXIMUM IN 2007 AND 2008

Dong-Yoon Lee, Master of Science, 2010

Directed By: Professor Raleigh R. Hood
Marine-Estuarine-Environmental-Sciences

The estuarine turbidity maximum (ETM) is a zone of elevated organic matter concentrations and it is an important habitat for bacteria, zooplankton, and early-life-stages of fish. In an effort to identify the key mechanisms controlling production, we measured plankton community metabolism on a series of high-resolution spatial surveys in the upper Chesapeake Bay. The spatial patterns of metabolism revealed the highest primary production and community respiration rates downstream of the ETM region, and net heterotrophy in winter and spring. Also, strong correlations between plankton community metabolism and phytoplankton pigment concentrations, including chlorophyll-a and dinoflagellate indicating pigment peridinin, were observed. These correlations suggest that mixotrophic dinoflagellates were key organisms linking detrital and algal organic matter to higher trophic levels. It is hypothesized that the physiological advantages of mixotrophic dinoflagellates (i.e., autotrophic, heterotrophic) combined with the physical conditions in the ETM which enhance the quantity and quality of organic matter give rise to the high secondary production in the upper Chesapeake Bay.

COMMUNITY METABOLISM AND ENERGY TRANSFER IN THE CHESAPEAKE BAY TURBIDITY MAXIMUM IN 2007 AND 2008

By

Dong-Yoon Lee

Thesis submitted to the Faculty of the Graduate School of the
University of Maryland, College Park, in partial fulfillment
of the requirements for the degree of
Master of Science
2010

Advisory Committee:
Professor Raleigh R. Hood, Chair
Professor W. Michael Kemp
Professor Byron C. Crump

Acknowledgements

I would like to thank foremost my adviser, Dr. Raleigh Hood, for his advice, guidance, and patience throughout my graduate career. He has provided unlimited resources and knowledge which has been leading me from 'nothing' to 'understanding' of aquatic ecosystems. I am very sure this opportunity of working with him was invaluable experience in my life. I also want to thank Drs. Byron Crump and Michael Kemp, as my committee member, for supporting my research by providing lesson, honest comment, and suggestion. Without their encouragement and expertise, I would not accomplish my research with this much success.

Dr. Lou Codispoti and Vince Kelly deserve special thanks for teaching me precise titration method and chemical technique. I would like to express my gratitude to Dr. Larry Sanford for his expertise in physical computational modeling which allows me performing two additional models in this thesis. Dr. David Keller generously provided his phytoplankton pigment data and, as a friend, martial art practice with him at Horn Point Laboratory was one of my best recreational activities. I would also like to thanks Drs. Edward Houde, Michael Roman, Elizabeth North, Jamie Pierson and all students and research assistants in BITMAXII project for their friendship, help, comment, and encouragement.

I say thank all my friends and colleagues at Horn Point Laboratory. I also thank my parents, grandparents, parents-in-law, and brothers for their prayer. Lastly, I thank my lovely wife, Yoo-Kyung Song, for her prayer and love and I thank God for giving this opportunity and taking care of me always.

Table of Contents

List of Tables

List of Figures

Figure AIII.2: Average light intensity in the mixed layer depth. The average light was computed from January to May at the upstream, ETM, and downstream region. The light levels are gradually increasing from January to May in the three regions because of in part the seasonal increasing of light strength on the surface.

Figure AIII.3: Simulated phytoplankton (a), zooplankton (b), and dinoflagellate (c) biomass in the upstream, ETM, and downstream from winter to spring. Phytoplankton increased from the end of April in the upstream and ETM but from the middle of March in the downstream. Zooplankton biomass was more spatially contrast between the downstream and other two regions. The pattern of dinoflagellate biomass aligned best with that of dinoflagellate primary production and reached the maximum value in April.

Figure AIII.4: The fraction of energy sources for zooplankton (a) and mixotrophic dinoflagellate (b) in the downstream from winter to spring. Zooplankton had a high preference on dinoflagellate as a prey source from winter. The energy uptake for mixotrophic dinoflagellates is composed mainly of photosynthesis and bacteria ingestion.

Figure AIII.5: Primary production (a), community respiration (b), and net ecosystem metabolism (c) in the oligohaline of Chesapeake Bay from winter to spring. To calculate net ecosystem metabolism, which is estimated by subtracting community respiration from gross primary production, community respiration rates were multiplied by the depth of mixed layer at the upstream (7 m), ETM (15 m), and downstream (24 m). The trend of community metabolism having highest rates in the downstream during late spring is aligned with the field measurements.

General Introduction

The transition zone between seawater and freshwater is a universal characteristic of the upper reaches of estuaries and physical, chemical and biological dynamics of this zone have been studied extensively. Estuaries are often divided into three regions, for example, oligohaline, mesohaline, and polyhaline from low to high salinity regimes, and the oligohaline often covers the transition zone. Suspended sediment concentration is usually highest in the transition zone, and it is called estuarine turbidity maximum (ETM).

The highest concentrations of suspended particles that accumulate in the ETM can be attributed to physical and environmental influences. In Chesapeake Bay, the Susquehanna River at the head of the Bay is the major source of freshwater and sediment. Also, seawater intrusion, mainly through a deep shipping channel, sweeps estuarine bottom sediment back and forth along with the tides, and it resuspends sediments from the bottom. Due to rapid changes in salinity from the surface (freshwater) to the bottom (seawater), a strong salinity gradient prevents water and substrates from mixing over the strong pycnocline. The strength of pycnocline is mainly controlled by the magnitude of the river discharge (Sanford et al. 2001). In addition, the continuous supply of organic matter from aquatic and terrestrial sources accumulates in the ETM region. Allochthonous organic matter from anthropogenic sources, marsh detritus, or phytobenthic organisms from shallow environments, is continuously supplied to the ETM via the freshwater flow. Also, autochthonous organic matter derived from internal primary production also contributes to the

organic matter pool. These high concentrations of heterogeneous particles are turned into aggregates, which are colonized by bacteria. Not surprisingly, all this organic matter loading affects the structure and productivity of the ETM food web (Hollibaugh & Wong 1999).

Autotrophic production in the oligohaline of region of estuaries is often limited by light due to the elevated total suspended sediment (TSS) and/or by phosphorous limitation during winter-spring season due to much higher input of dissolved inorganic nitrogen (Fisher et al. 1992, Fisher et al. 1999). As a result of the resource limitation, low autotrophic production should cause the shortage of labile organic matter for herbivorous or omnivorous heterotrophs and result in low secondary production. However, ETMs are not only a region where there is high copepod biomass (e.g., *Eurytemora affinis*), but they are also an important spawning and nursery ground for anadromous striped bass *Morone saxatilis*. In fact, food availability for young fish larvae is one of the most crucial survival requirements, and it has been found that larval fish strongly depend on copepods biomass for food in the ETM region (North & Houde 2006). This suggests that copepods obtain sufficient energy in spite of the low primary production and successfully transfer energy to secondary producers. This paradoxical combination of low primary production with high copepod and fish larvae biomass suggests that there is a fundamental difference in the food web structure in these oligohaline areas compared to other aquatic regions that allows efficient energy transfer pathways.

Novel food webs and pathways of carbon and energy transfer have been proposed in other environments where there is a lack of autochthonous organic matter

input. For example, in a lake where autochthonous production is not sufficient to support secondary producers, allochthonous organic matter often subsidizes secondary production so that it exceeds the level of internal autotrophic production (Pace et al. 2007). In a similar way, allochthonous organic matter could directly subsidize copepod production in the upper Chesapeake Bay because abundant calanoid copepods are omnivorous. However, the importance of allochthonous organic matter for supporting the energy requirements of copepods is still debated for a number of reasons (Vincent et al. 1996, Islam et al. 2005, David et al. 2006). Firstly, size ranges of organic matter vary from a few microns to as big as zooplankton. Aggregation of organic matter via biologically, chemically, and physically-mediated processes is a commonly observed process in ETMs (Goldman 1984, Simon et al. 2002) that leads to the formation of successively larger particles that cannot be consumed by copepods. Since optimal prey size for *E. affinis* is limited by the morphology of feeding apparatus (Hansen et al. 1994) and is in the range of 19 to 33 μm (Richman et al. 1980), free-living bacteria, which are not associated with detritus, cannot be grazed by copepods. Secondly, calanoid copepods are capable of grazing selectively and have a grazing preference on more nutritious food items. Under extreme TSS-rich conditions as in the ETM environment, the clearance rate of calanoid copepods is significantly higher on phytoplankton than particulate organic carbon indicating selective grazing on preferred prey items (Tackx et al. 2003). Therefore, it is unclear whether or not calanoid copepods can take advantage of having abundant particulate allochthonous organic matter to fulfill their energy requirements and transfer energy to higher secondary producers.

Net ecosystem metabolism (NEM) can be used as an indicator for systematic responses to nutrient and organic matter enrichment and to estimate trophic status of an ecosystem. Calculated as the difference between gross primary production (GPP) and total respiration (R), it reveals the metabolic response of the entire community (NEM = GPP - R). In a positive NEM condition (net autotrophic), autotrophs produce more organic matter through assimilation of inorganic nutrient than the amount of organic matter consumed by heterotrophs. This, in turn, indicates a potential for net export of organic matter from the system. In contrast, in a negative NEM condition (net heterotrophic) community respiration is higher than gross primary production, indicating net import of organic matter, which is often observed in eutrophic ecosystems. NEM measurements are very powerful because they represent the net effects of complex individual processes, community interactions, geochemical processes, and anthropogenic influences that are often found in estuarine environments.

In the upper Chesapeake Bay, primary production and respiration have been measured in previous studies and net heterotrophy has been observed on an annual cycle (Boynton & Kemp 1985, Smith & Kemp 1995, Kemp et al. 1997). Kemp et al. (1997) used biogeochemical models to calculate NEM in the oligohaline region and reported maximal net heterotrophy in March and April when organic matter loadings are highest due to spring river discharge. These measurements are consistent with the high input of terrestrial organic matter and low light availability that is observed in the ETM region in the spring that should give rise to net heterotrophic conditions. However, physical and environmental forces vary in time and space and subsequent

biological productivity is strongly dependent on these forces in the ETM. Despite the apparent importance of the ETM for supporting secondary production, few studies have attempted to measure NEM variations in the ETM in the winter-spring season when secondary production is highest. Therefore, measurements of NEM were used to estimate the trophic status of the upper Chesapeake Bay and quantify the sources of organic matter that support secondary production. These measurements provide important insights into the systematic responses of the ETM environment to nutrient and organic matter enrichment and also shed light on the food web pathways which transfer energy from low to high trophic level producers.

Chapter 1: Community metabolism and energy transfer mechanism in the upper Chesapeake Bay 2007 and 2008

Abstract

The Chesapeake Bay estuarine turbidity maximum (ETM) at the interface between freshwater and seawater is a region of dynamic physical processes which cause the entrapment of sediment and organic matter originating from both the terrestrial and aquatic environments. The allochthonous organic matter is assumed to be a fundamental energy source supporting the estuarine food web resulting in high secondary production, which is largely driven by mesozooplankton in the Chesapeake Bay ETM region. However, the specific pathways by which this organic matter is transferred to higher trophic levels are not known.

Here we describe detailed studies of variability in plankton community metabolism and related measurements in the Chesapeake Bay ETM from multiple cruises in winter and spring of 2007 and 2008, which are aimed at better quantifying the structure of the estuarine food web. Measured quantities include oxygen primary production, respiration of the plankton community, light attenuation, and algal pigment concentration and species composition in transects through the ETM region. The measurements of oxygen production and consumption provide in-depth information on the relative contribution of autotrophic and heterotrophic processes at a variety of spatiotemporal scales. The relationships between these measurements,

and pigment concentration and compositions also provide insights into specific contributions from different phytoplankton groups in the ETM food web.

These measurements consistently reveal a classic minimum in carbon fixation via photosynthesis in the vicinity of the ETM. They also show that dramatic increases in primary production and community respiration downstream of the ETM were often associated with the presence of mixotrophic dinoflagellates but were not associated with diatoms. In contrast to upstream conditions, temporal variability in plankton community metabolism, primary production, respiration, and bacterial production were all higher downstream of ETM, which was driven by dynamic bio-physical interactions. The dinoflagellate contribution to primary production and respiration appears to be particularly large reflecting their mixotrophic feeding, by which they can obtain energy both autotrophically and heterotrophically. Although the diatom contribution to primary production was relatively small, it appears to have been an important carbon source for microbes. This study suggests that in the oligohaline region of Chesapeake Bay mixotrophic dinoflagellates supply most of the labile organic matter during late winter and spring and also provide a vector for transferring microbial production fueled by terrestrial and dissolved organic matter to secondary producers.

Introduction

Estuaries are influenced by physical, chemical and biological forces, which determine biogeochemical cycles and trophic interactions. Chesapeake Bay is the biggest and most extensively studied estuary in the United States (Kemp et al. 2005).

The Susquehanna River at the head of the bay is responsible for more than 50 % of freshwater input. This input has a distinct seasonal flow pattern with high discharge from late winter to spring and low to moderate discharge from summer to fall. The flow largely controls salinity gradients and therefore stratification, pycnocline depth, and the location of the turbid zone (Schubel & Pritchard 1986, Sanford et al. 2001). The bay can be separated into upper, middle, and lower regions by salinity regimes (i.e., oligohaline, mesohaline, and polyhaline, respectively). This study focuses on biological responses to physical, chemical and biological forcing in terms of plankton community metabolism in the oligohaline region.

In Chesapeake Bay the highest concentration of suspended particles is usually found at the limit of salt intrusion in the vicinity of the sharp salinity gradient where freshwater and saltwater converge. The region is called the estuarine turbidity maximum (ETM). The gravitational circulation induced by the composite influence of tidal exchange and freshwater discharge generates a two-layer circulation and entraps particles (Sanford et al. 2001). The trapping is primarily due to the convergence and recirculation at the interface between the down-estuary and up-estuary flows, but it is also influenced by a variety of factors such as stratification, resuspension, flocculation, tides, settling velocity, sedimentation rate, and wind (Schubel & Pritchard 1986, Sanford et al. 2001). In Chesapeake Bay, the area where the 1-psu isopycnal intersects the bottom is often a fairly good indicator of the location of ETM but it is not always associated with the 1-psu isopycnal or any specific location due to environmental variability and topographic influences (Sanford et al. 2001).

The oligohaline area receives high levels of organic matter loading from both terrestrial and aquatic sources. It is often hard to measure the quantity and quality of this organic matter due to the diverse origins and complex biochemical reactions that occur between dissolved and particulate organic matter and living organisms (Simon et al. 2002). It is, however, important to characterize and quantify this organic matter to understand better the interacting anthropogenic and natural influences on the estuarine food web. Achieving this understanding is also crucial for management of estuarine health and resources (e.g., hypoxic/anoxic events, benthic macrofauna, and fisheries). In lakes, stable isotope analysis of organic carbon has revealed that a greater fraction of heterotrophic metabolism is often fueled by terrestrial organic matter than by autochthonous primary producers when environmental conditions limit the autotrophic production (Findlay et al. 1991, Carpenter et al. 2005, Pace et al. 2007). In previous Chesapeake Bay studies, primary production rates and chlorophyll-a concentrations have been observed to be lowest in the oligohaline area (Smith & Kemp 1995, Kemp et al. 1997), presumably due to light limitation (Fisher et al. 1999), suggesting a higher contribution of terrestrial organic matter than internal loading for fueling estuarine food webs. However, the relative contributions from internal and external loading in the oligohaline area is complicated due to the continuous supply of nutrients and organic matter from rivers, the benthos, and shallow environments which further subsidize secondary production.

Understanding the sources of organic matter and food web dynamics (i.e., relative importance of autochthonous algal production versus allochthonous input) is important in the ETM because the region supports high larval recruitment of several

anadramous fish, such as striped bass *Morone saxatilis* and white perch *M. americana* (North & Houde 2003). It should also be noted that the mesozooplankton populations are dominated by the calanoid copepods *Eurytemora affinis* and *Acartia tonsa*, and the typical freshwater cladoceran *Bosmina longirostris* in the oligohaline (Roman et al. 2001, Winkler et al. 2003, David et al. 2006). As a part of a dynamic food web, Pomeroy (1974) and Azam et al. (1983) proposed 'microbial loop' theory which emphasizes the importance of microbial and detrital production pathways into the copepods and fish. Further, it was proposed that if bacteria and detritus are directly consumed by copepods, the shortened production pathway would result in higher energy conservation and transfer efficiency than those of the microbial loop and it is called 'microbial shunt' theory (Baross et al. 1994). The shunt theory is in part supported by the effective grazing capability of many copepods on a broad size spectrum of prey items including detrital organic matter with or without microbes (Heinle et al. 1977, Boak & Goulder 1983).

Terrestrial organic matter generally consists of a high fraction of refractory matter (Pace et al. 2004), but it is often augmented by bacterial production, which enhances the nutritional value (Goldman 1984, Crump & Baross 2000). When terrestrial loading to an aquatic system is high it may be possible to satisfy the carbon requirement of secondary producers with little or no primary production. However, Winkler et al. (2003) measured a sufficient amount of autotrophic production to fulfill the carbon requirement for copepods in the St. Lawrence River estuary and concluded that the system is strongly dependent on autochthonous autotrophic production. Further, since copepods are capable of grazing selectively on prey with higher protein

content such as protozoa (White & Roman 1992) and phytoplankton (Cowles et al. 1988), it is not clear whether copepods in systems with large allochthonous carbon sources satisfy their nutritional needs primarily from abundant detrital organic matter or from a combination of algal and detritus carbon. In addition, it has been shown that when copepods strongly depend on detrital organic matter, it can result in low survival and egg production rate (Heinle et al. 1977). It seems therefore, that even in aquatic systems with large allochthonous carbon sources, it is not always clear how significant these are in supporting secondary production.

Direct measurements of oxygen production and consumption have provided a powerful tool for estimating the relative contributions of autotrophic and heterotrophic processes in aquatic systems and therefore quantifying the relative importance of allochthonous versus autochthonous carbon sources in the food web. The so-called net ecosystem metabolism (NEM) can be estimated by subtracting community respiration from gross primary production (see methods below). Estuarine eutrophication due to anthropogenic disturbances often causes net negative ecosystem metabolism (also called net heterotrophy) implying that more organic matter is consumed by respiration than produced by autotrophic growth (Valiela et al. 1992, Hopkinson & Vallino 1995, Smith & Hollibaugh 1997). For this to happen there must be a net import of terrestrial organic matter and net export of inorganic nutrient into adjacent regions (Kemp et al. 1997). Previous studies have shown that primary production is highly correlated with euphotic depth (Wofsy 1983, Cole & Cloern 1987) and consequently is very low in the oligohaline area of Chesapeake Bay (Smith & Kemp 1995, Kemp et al. 1997). Community respiration is also often low in the

oligohaline (Smith & Kemp 2003) but more likely exhibits high spatial and temporal variations because of differences in uptake efficiency on terrestrial and autotrophic organic matter by heterotrophs. In general, NEM in the oligohaline is negative, i.e., net heterotrophic, though often with significant seasonal variations (Smith & Kemp 1995, Kemp et al. 1997, Caffrey 2004). In contrast, in areas where a wide variety of autotrophs flourish in the presence of abundant light and inorganic nutrient supplies the ecosystem can have positive net ecosystem metabolism (also called net autotrophy) implying that more organic matter is produced by local autotrophic growth than consumed by heterotrophic respiration. Therefore, net ecosystem metabolism can be used to assess the aggregate response of a wide variety of autotrophic and heterotrophic species in a community to environmental and anthropogenic influences which can reveal trophic status and health of an ecosystem (Caffrey 2004).

Here we describe results from oxygen production and respiration measurements from a series of high-resolution spatial surveys on the Chesapeake Bay ETM region. These measurements provide insight into the metabolic demands of different plankton communities in relation to salinity and turbidity. We speculate that the balance between autotrophic and heterotrophic processes can vary significantly with time and in space, especially during late winter and spring due to temporal variability in river flow and organic matter loading. Although the ETM plays an important role in the secondary production, it is not clear what are the major sources of the organic matter that fuel higher trophic level production (freshwater, marine, local). The objectives of this study are to use direct measurements of oxygen

production and consumption in combination with water quality and algal pigment data to: 1) characterize the spatial and temporal variability in primary production and respiration in the Chesapeake Bay ETM; 2) determine the sources of primary production that might fuel growth of higher-trophic-level organisms; and 3) identify any specific food web pathways through which algal or detrital production is transferred to higher trophic levels.

Methods

Study site

The oligohaline area of Chesapeake Bay encompasses 11 % of total Bay area and stretches from the Chesapeake Bay Bridge (lat: 38°59.8' N) to Havre de Grace (lat: 39°28.3' N) at the mouth of Susquehanna River, Maryland, 76 km along a shipping channel (defined as river-km; Fig. 1). Hereafter we refer to the area located between 0 to 30 river-km from the mouth of Susquehanna River as the "Upstream Region" (encompassing Stations 14a to 11), the area between 30 to 45 river-km as the "ETM Region" (encompassing Stations 10 to 08), and the area between 45 to 80 river-km as the "Downstream Region" (encompassing Stations 07 to 03). The channel is maintained by dredging, and it serves as a conduit for seawater intrusion (Sanford et al. 2001). A total of six cruises were conducted in the channel, two in late winter (22-26 February 2007 & 23-26 January 2008), two in early spring (9-15 April 2007 & 17-23 April 2008), and two in late spring (8-14 May 2007 & 16-22 May 2008). Hereafter, we refer to the cruises by season, i.e., late-winter, early-spring, and late-spring, instead of by specific dates/months. The timing of two spring cruises was

designed to maximize observations during the time periods of high river discharge and organic matter loading. Two axial surveys were performed at the beginning and end of each cruise. These consisted of 11 CTD (conductivity, temperature, and depth; Sea-Bird Electronics, Inc.) casts equipped with fluorescence, oxygen and optical backscatter sensors. All axial surveys were done in less than 8 h from 0600 to 1400. Immediately after each axial survey, the CTD data were processed using SBE Data Processing software to locate the center of ETM. Salinity and turbidity measured by CTD casts were mapped as contour plots using a MATLAB v7.5 (The MathWorks, Inc.). It should be noted that the actual scale of the x-axis (river distance) to y-axis (depth) on the contour plots is distorted by about 300:1.

Field sampling procedure

Five out of the 11 CTD stations were selected along axial surveys for water sample analyses within 8 h. At these five stations, which included two upstream of the ETM, one ETM, and two downstream of the ETM, plankton community metabolism was measured along with water quality, pigment analysis, and bacterial production using the following sampling procedure and methods. Water samples were collected with 10-L Niskin bottles mounted on the CTD at 0.5 m below the surface, the middle of pycnocline where salinity changes were most rapid, and 0.5 m above bottom during the up-cast of the CTD. At the freshwater end-member station where there was no pycnocline, mid-water samples were collected in the middle of water column. Under low light conditions we gently transferred water from each depth into a 24-L bucket equipped with a stir bar to ensure the homogeneity of water samples.

At least 10 minutes after the transfer samples for measuring oxygen production and consumption were siphoned through 70 cm Tygon laboratory tubing into replicated 60-ml biological oxygen demand (BOD) bottles, allowing the bottle to overflow three times its volume. Samples for initial O_2 concentration were fixed immediately. O_2 concentration was measured using the Winkler titration method (Carpenter 1965) with an automated photometric endpoint detection system having a minimum precision of 0.01 % (Sensoren Instrument System). Primary production and respiration were measured using the light-dark bottle oxygen method (Kemp et al. 1992) with samples incubated on rotating transparent and opaque flow-through incubators (12 rotations per minute) at ambient temperature on shipboard (±1 ℃ of in situ water temperatures), respectively, to prevent any biased rates due to settling of suspended sediment (Madden & Day 1992).

Primary production measurement

Net primary production rate was calculated as the difference in the means between initial and final O_2 concentrations measured in triplicate 60-ml BOD bottles, filled with surface water and covered with neutral-density screens allowing passage of 37, 17, 11, 6, and 2 % of surface irradiance for 24 h. Underwater irradiance levels were measured using a PRR-600 spectral radiometer (Biospherical Instruments, Inc.) or Secchi Disc depth following CTD casts. Secchi depth was used on only one cruise in late spring 2008 when the radiometer malfunctioned. The Lambert-Beer Law was used to calculate diffuse attenuation coefficients (k; unit: m^{-1}) and euphotic depths (1 % of surface irradiance level) from the irradiance measurements:

$$I_d = I_0 \, e^{-kd}$$

where I_0 is the light intensity at the surface, I_d is the light intensity at depth, and *d* is depth. Theoretical depths of the five simulated in situ light levels were also calculated with this equation for vertical integration. For late spring 2008, *k* was derived from Secchi Disc depth using an empirical relationship:

$$k = 1.7 / Z_{sd}$$

where Z_{sd} is Secchi Disc depth (Parsons et al. 1984). Then, the mean volumetric rates of net primary production (mg O_2 m^{-3} h^{-1}), measured at each light level, were integrated vertically over the euphotic depth using a trapezoidal method (g O_2 m^{-2} d^{-1}). However, please note that we chose to integrate primary production over the 1 % surface irradiance level for the reason of convenience. In reality, vertical mixing of organisms in a mixed layer would cause rapid changes of vertical position of phytoplankton and may alter integrated primary production rates. However, the mixed layer depth appeared to vary seasonally and spatially and could be hard to decide by seeing snap shots of salinity distribution because of rapid changes of salinity distribution. Gross primary production at each station was determined by adding community respiration rate in the euphotic zone to the net primary production assuming constant daily respiration (Hopkinson et al. 1989).

Respiration measurement

Community and picoplankton (the latter defined as plankton filtered through 3-μm polycarbonate membrane filter; Sieburth et al. 1978) respiration rates were measured on surface, middle, and bottom water samples as decreases in O_2 concentration in replicated (triplicate) dark BOD bottles. The picoplankton filtration was done using a reverse gravity method (Crump et al. 1998). BOD bottles were incubated for a period of either 12 h in late-winter or 6 h in early- and late-spring. Volumetric respiration rates were calculated by subtracting oxygen concentration of samples incubated in the dark from the initial concentration. Respiration rates (mg O_2 m^{-3} h^{-1}) at the three depths were multiplied by the depth (m) of each region (from surface to the middle of surface/middle sampling depths, from the middle of surface/middle to the middle of middle/bottom sampling depths, and from the middle of middle/bottom sampling depth to bottom, respectively) and then summed over the water column (mg O_2 m^{-2} h^{-1}). In order to account for the 5-fold difference in the water column depth between the seawater end-member (furthest down-estuary) and freshwater end-member (furthest up-estuary) in along-axis respiration rate comparisons, we divided the vertically-integrated respiration rate at each station by the water column depth at each station which gives an estimate of the mean water column respiration rate (g O_2 m^{-3} d^{-1}).

Size-fractionated respiration measurement

We performed size-fractionated respiration rate measurements at the freshwater and seawater end-members and in the ETM to find the quantitative

significance of different size groups in total community respiration. Standard forward filtration was used in 2007, i.e., gently pouring water through a sequence of filters, whereas reverse filtration was used in 2008. Water samples were screened through 20, 10, and 3 μm nitex mesh and collected in stirrer-equipped buckets that were cleaned and dried. Picoplankton respiration rate (<3 μm filtered) represents the oxygen demand of free-living bacteria, cyanobacteria, and other small heterotrophs and autotrophs which are mostly composed of prokaryotes. Among picoplankton, free-living bacteria which are not associated with detrital particles often tend to dominate metabolic activities in the Chesapeake Bay (Smith & Kemp 2001). Oxygen consumption by less than 10 μm size group includes heterotrophic flagellates, ciliates, and microprotozoa (Hopkinson et al. 1989). Oxygen consumption by less than 20 μm excludes oxygen consumption by macrozooplankton, mesozooplankton, large ciliates, protozoa and large phytoplankton. The measurement of both community and size-fractionated respiration assumes that oxygen concentrations decrease linearly over time as reported in previous studies (Smith & Kemp 2001, Preen & Kirchman 2004) and tested in this study (see Appendix I). Incubation methods were the same as for the normal respiration rate measurement.

Bacterial production measurement

Bacterial production rates of the same water samples were estimated by Dr. Crump (Horn Point Laboratory, Cambridge, MD, USA). Bacterial production rate was estimated using incorporation rate of ^{3}H-leucine into macromolecules during 1 h incubation (Kirchman 1993). ^{3}H-leucine incorporation rate was converted into

production rate using a ratio of cellular carbon to protein of 0.86, a fraction of leucine in protein of 0.073, and an intracellular leucine isotope dilution of two (Crump et al. 2007). These measurements were made on unfiltered and 3-μm-filtered water to distinguish between particle-attached and free-living bacteria, respectively (Crump et al. 1998). To compare the relative magnitude of organic matter production by bacteria (μg C l^{-1} h^{-1}) and autotrophs (g O_2 m^{-2} d^{-1}), a photosynthetic quotient of 1.2 (moles of O_2 produced : moles of CO_2 assimilated; Smith & Kemp 1995) was assumed to convert to the same carbon units (mg C m^{-2} d^{-1}). Note that primary production was integrated over euphotic depth whereas bacterial production was integrated over the entire water column, as respiration rates were integrated.

Phytoplankton pigment analysis

Phytoplankton pigment data of the same water samples were estimated by Dr. Keller (Horn Point Laboratory, Cambridge, MD, USA). Samples for high performance liquid chromatography (HPLC) pigment analysis were collected by filtering water under low light conditions through 25 mm GF/F filters. The filters were frozen and stored at -80 °C using either liquid nitrogen or a low temperature freezer. Upon return to shore HPLC pigment analysis was performed by Horn Point Laboratory analytical services according to the methods of Van Heukelem and Thomas (2001). The following pigments (and their associated phytoplankton groups or degradation sources) were used in statistical analyses presented in this paper: chlorophyll-a, peridinin (dinoflagellates), fucoxanthin (diatoms), alloxanthin (cryptophytes), zeaxanthin (cyanobacteria), chlorophyllide-a (found in senescent

diatoms), pheophorbide-a (resulting from digestive breakdown of chlorophyll by protozoans), pheophytin-a (degraded chlorophyll found in zooplankton fecal pellets and sediments), and total pheophytin (the sum of degraded pigments).

Long-term irradiance data analysis

Long-term observations of light attenuation coefficients (k) from 1990 to 2006 were obtained from the Chesapeake Bay Program to calculate a monthly climatology of euphotic depth for comparison with the euphotic depths estimated using the irradiance measurements collected on the 2007 and 2008 cruises. Three stations, CB2.1 (Turkey Point Light; 10 river-km), CB3.1 (Tolchester Beach; 40 river-km), and CB3.3C (Chesapeake Bay Bridge; 74 river-km), represent the regions of our field stations at the freshwater end-member, ETM, and seawater end-member, respectively. These monthly average k values were used to calculate euphotic depths in each month using the Lambert-Beer Law. Note that k values were not monitored at CB2.1 and CB3.1 in February and November, so a linear interpolation was used to estimate these.

Statistical analysis

Pearson's correlation analysis and simple linear regression analysis were extensively used in this research. Also, data for 2007 and 2008 were pooled into one data set if measured mean rates were not significantly different between the two years to estimate the general patterns of plankton community metabolism and their relationships to environmental properties (ANOVA, $\alpha = 0.05$). Multiple regression

analysis was not employed because there is substantial collinearity among some of the variables measured. Although significant correlations in simple linear regression analysis do not necessarily indicate casual relationships (Boynton & Kemp 2000), the analysis still gives useful and straightforward information on correlations among variables and their statistical significance. When significant correlations were found between salinity and phytoplankton pigments, which is commonly found in estuaries, partial correlation analysis was used keeping the salinity effect constant. This allows interpretation of correlations among biological variables without the potentially confounding influence of correlations with salinity. All statistical tests were performed using the statistical software package SAS (SAS Institute, Inc.). Data point outliers were excluded based on the Cook's D test statistic. The points excluded from data reported here include one community respiration rate and two picoplankton respiration rates measured in early spring 2007 that were an order of magnitude higher than the mean respiration rate on the same axial survey.

Results

The average river discharge from January to May in 2008 (2,001 $m^3 s^{-1}$) was higher than the long-term average of the same period from 1967 to 2008 (1,678 $m^3 s^{-1}$). In contrast, the average discharge in 2007 was very close to the long-term average (1,679 $m^3 s^{-1}$) (Fig. 2). Salinity and turbidity distributions varied by season but short-term variations were also observed between two axial surveys in the same cruise (Fig. 3). In general, seasonal changes in the river flow clearly dictated the shape and strength of the salinity gradient, which, in turn, controlled the location and

concentrations of suspended sediment. Despite resuspension of sediments from the bottom layer in the ETM region, the continuous supply of detritus from river appeared to control the light availability near the surface. Euphotic depths measured during this study steadily increased downstream which agrees with the long-term averages of euphotic depths estimated using data collected by Chesapeake Bay Program (Fig. 4). Substantial interannual variations of euphotic depth, which are controlled by the timing and magnitude of river discharge, were found between the two years in this study, i.e., the seasonal mean euphotic depths were shallowest in early-spring in 2007 but in late-spring in 2008.

Spatiotemporal variability in plankton community metabolism

The average rate of gross primary production ranged from 0.20 to 7.72 g O_2 m^{-2} d^{-1} and the rates consistently increased downstream and from late-winter to late-spring (Fig. 5). Community respiration ranged from 0.03 to 0.90 g O_2 m^{-3} d^{-1} and picoplankton respiration ranged from 0.02 to 0.33 g O_2 m^{-3} d^{-1} and both had similar spatial and temporal trends to that of gross primary production (Fig. 6). All but one site at the freshwater end-member in late-winter were net heterotrophy with NEM varying from +0.06 to -12.48 g O_2 m^{-2} d^{-1} (Fig. 7). The spatial and temporal trends of NEM were also similar to that of gross primary production, with net heterotrophy increasing downstream and from late-winter to late-spring. The average rate of total bacterial production (the sum of particle-attached and free-living bacteria) ranged from 78.03 to 872.61 mg C m^{-2} d^{-1} from late winter to late spring and the rate increased downstream as well (Fig. 8). Average surface chlorophyll-a concentration

ranged from 2.70 to 32.15 μg l^{-1} and the mean concentrations at surface, middle and bottom depths increased downstream (Fig. 9a).

Late-winter (defined as January and February)

The average river discharge in late–winter of 2007 (1,198 m^3 s^{-1}) was lower than that of 2008 (1,871 m^3 s^{-1}), which was higher than the long-term average (1,369 m^3 s^{-1}). Water temperatures ranged from -0.8 to 9.4 ℃ (Fig. 2). In late-winter 2007 relatively weak salinity gradients and more well-mixed water-columns were observed compared to those of 2008 due to a combination of low river discharge and low air temperatures. As a result, the interface where the 1-psu isohaline meets the bottom was located upstream of the ETM in 2007 (Fig. 3a & b). Turbidity, measured by optical backscatter, was higher throughout the water column in late winter 2008 when average river discharge was higher (Fig. 3g & h). It should be noted, however, that the strength and location of the ETM was highly variable depending to a large extent on the phase of the tides. Euphotic depths ranged from 1.7 to 3.8 m in 2007 and from 1.8 to 3.7 m in 2008 and constantly deepened downstream (Fig. 4).

The two-year mean of gross primary production in late-winter ranged from 0.22 to 2.01 g O_2 m^{-2} d^{-1} (Fig. 5). In addition, the two-year mean of community respiration ranged from 0.03 to 0.19 g O_2 m^{-3} d^{-1} and the mean of picoplankton respiration ranged from 0.02 to 0.06 g O_2 m^{-3} d^{-1} in late-winter (Fig. 6a & b). Overall, net ecosystem metabolism resulted in net heterotrophy ranging from +0.06 to -1.42 g O_2 m^{-2} d^{-1} (Fig. 7). Integrated carbon production from bacteria and phytoplankton ranged from 147.26 to 950.69 mg C m^{-2} d^{-1} and there was a higher contribution of

autotrophic carbon in the ETM and downstream as opposed to upstream where these contributions were approximately balanced (Fig. 8a). Chlorophyll-a concentration at the surface ranged from 5.72 to 21.44 μg l^{-1} increasing downstream which were comparable to depth-averaged chlorophyll-a concentration (Fig. 9a). It caused the mean primary production rate per biomass (assimilation number) to range from 0.04 to 0.10 g O_2 (mg Chlorophyll-a)$^{-1}$ d^{-1} which are not significantly different from stations ($p > 0.05$; Fig. 9b).

Early-spring (defined as March and April)

Early-spring typically had higher river discharge due to vernal warming and snow melt. The mean of river discharge was 2,518 m^3 s^{-1} in 2007 and 2,449 m^3 s^{-1} in 2008 which were higher than the long-term average of 2,156 m^3 s^{-1} and the two-year mean of water temperatures ranged from 1.9 to 17.8 ℃ (Fig. 2). In both 2007 and 2008 the high river discharges caused sharp salinity gradients, and strong horizontal pycnocline was observed throughout the ETM and downstream region between 5 to 10 m deep (Fig. 3c, d, i & j). The high river input pushed the 1-psu isohaline downstream. In both years the highest concentrations of suspended sediment were found downstream below the pycnocline between 25 and 40 river-km. Euphotic depths ranged from 1.6 to 3.8 m in 2007 and from 2.2 to 3.7 m in 2008, and were shallowest in the ETM region in 2007 but in the upstream in 2008 (Fig. 4).

The two-year mean of gross primary production ranged from 0.20 to 2.38 g O_2 m^{-2} d^{-1} and the lowest mean rate was found in the ETM but it was not significantly different from the rates measured upstream (Fig. 5). The two-year mean of

community respiration ranged from 0.20 to 0.55 g O_2 m^{-3} d^{-1} and that of picoplankton respiration ranged from 0.07 to 0.33 g O_2 m^{-3} d^{-1} (Fig. 6a & b). Thus, net ecosystem metabolism resulted in net heterotrophy ranging from -1.04 to -7.40 g O_2 m^{-2} d^{-1} which became significantly lower downstream than late-winter (Fig. 7). Integrated carbon production from bacteria and phytoplankton ranged from 261.92 to 1,274.87 mg C m^{-2} d^{-1} (Fig. 8b). Although the overall mean contribution by the two communities was relatively balanced, the contribution from bacterial production was much higher (76 %) than primary production in the ETM. Chlorophyll-a concentration at the surface ranged from 2.70 to 21.76 μg l^{-1} increasing downstream with minimum upstream and in the ETM which were also similar to the depth-averaged concentration (Fig. 9a). It caused the mean assimilation number ranged from 0.07 to 0.16 g O_2 (mg Chlorophyll-a)$^{-1}$ d^{-1} (Fig. 9b). As in late-winter, differences in the assimilation number observed along the transects were not statistically significant ($p > 0.05$).

Late-spring (defined as May)

Unlike the previous two periods, late-spring did not have a distinct peak in river discharge in 2007 and 2008. The mean river discharge in 2007 of 963 m^3 s^{-1} was lower than in 2008 of 1,365 m^3 s^{-1} and also lower than long-term mean of 1,339 m^3 s^{-1} (Fig. 2). Water temperature ranged from 14.0 to 23.6 ℃ (Fig. 2). A weaker salinity gradient was observed in 2007 compared to 2008, which was likely the result of the lower river discharge. In both years high concentrations of suspended sediment were

observed in a broad region from 30 to 50 river-km (Fig. 3e, f, k & l). Finally, euphotic depths ranged from 3.1 to 4.4 m in 2007 and from 1.5 to 3.5 m in 2008 (Fig. 4).

The two-year mean of gross primary production was highest throughout the transects in late-spring, ranging from 1.21 to 7.72 g O_2 m^{-2} d^{-1} (Fig. 5). The two-year mean of community respiration ranged from 0.20 to 0.90 g O_2 m^{-3} d^{-1} and picoplankton respiration ranged from 0.07 to 0.18 g O_2 m^{-3} d^{-1} (Fig. 6a & b). Net ecosystem metabolism revealed strong net heterotrophy downstream ranging from -0.76 to -12.48 g O_2 m^{-2} d^{-1} (Fig. 7). Integrated carbon production of bacteria and phytoplankton ranged from 516.72 to 3,285.13 mg C m^{-2} d^{-1} and the contribution of autotrophic carbon was greater than 65 % at all stations along the transect (Fig. 8c). Chlorophyll-a concentration at the surface ranged from 5.89 to 32.15 μg l^{-1} with the highest values downstream which were also similar to the depth-averaged concentration (Fig. 9a). Also, the mean assimilation number ranged from 0.19 to 0.28 g O_2 (mg Chlorophyll-a)$^{-1}$ d^{-1} (Fig. 9b). Once again, differences in the assimilation number observed along the transects were not statistically significant ($p > 0.05$).

Statistical analysis for gross primary production

Pearson's correlation coefficients were calculated to examine the relationship between gross primary production, environmental variables (temperature, TSS and euphotic depth) and phytoplankton community composition (as indicated by HPLC pigments, peridinin, fucoxanthin, alloxanthin and zeaxanthin) in surface water. Although correlation coefficients and statistical significance vary by seasons, the results derived using the entire data set captured general patterns and magnitudes of

correlations between variables (Table 1). The analysis revealed that gross primary production was significantly correlated with several environmental and biological factors. However, there are also significant correlations between salinity and most of the phytoplankton pigments (except cyanobacteria) so it can be problematic interpreting the result because common relationships between salinity and gross primary production and salinity and phytoplankton pigments may contribute to the correlations between gross primary production and phytoplankton pigments.

Partial correlation analysis, keeping salinity constant, was therefore employed and resulted in an overall decline in the correlation coefficients for all variables but significant relationships were still found except with cryptophytes indicating pigment, alloxanthin (Table 1 upper right in italics). Among the environmental variables, temperature was the most important factor explaining 58% of the variability in GPP, suggesting that there was thermal kinetic control of phytoplankton production. Total suspended sediment (TSS) and euphotic depth both also explained a significant amount of the variability in GPP (31 and 32% respectively) but they had different signs, i.e., TSS was negatively correlated and euphotic depth was positively correlated, presumably because high TSS concentrations result in lower light availability which lowers GPP (Xu et al. 2005). It should be noted, however, that TSS and euphotic depth were not correlated with GPP on the any of the individual cruises (data not shown), suggesting that seasonal changes in TSS and euphotic depth (rather than spatial changes) were driving these correlations. Among the pigments, chlorophyll-a, peridinin, fucoxanthin, and zeaxanthin were all significantly correlated with gross primary production indicating that changes in total phytoplankton

abundance and specifically the abundance of individual phytoplankton groups were driving changes in GPP. The phytoplanktons were also strongly correlated with salinity suggesting that salinity control/stress can be an important factor determining phytoplankton community composition (Brand 1984).

Season by season regression analyses revealed that chlorophyll-a concentration explained 72% of the variation of GPP in late-winter, 40 % in early-spring, and 91 % in late-spring (Fig. 10). Significant fractions of gross primary production were also explained by dinoflagellate and diatom concentrations. Dinoflagellates explained 70% of GPP in late-winter and 77 % and late-spring but only 3 % in early-spring (Fig. 11). This low correlation in early-spring is consistent with the relatively low correlation between chlorophyll-a and GPP in the same period (Fig. 10) and the highest correlation between chlorophyll-a and peridinin among all of the variables (Table 1). In contrast to dinoflagellates, diatoms variability explained a relatively small amount of the variability in gross primary production, i.e., 2 % in late winter, 27% in early-spring and 40% in late-spring (Fig. 12). The stronger correspondence between GPP and diatoms compared to dinoflagellates in early-spring was in part caused by the increase in diatom concentrations upstream which corresponded to an increase in GPP upstream (Fig. 13b). These patterns also suggest that in early-spring diatoms originated from both the seawater and freshwater end-members but dinoflagellates only originated from the seawater.

Statistical analysis for community respiration

As with GPP, statistical analyses between respiration rates, pigments, and environmental parameters were performed to determine which variables drive the respiration rate variability. Here also, partial correlation was used because there are significant correlations between salinity, respiration and most of the pigments. Temperature is considered to be one of the most important variables influencing respiration of bacteria (Apple et al. 2006), plankton (Sampou & Kemp 1994), and entire estuarine community (Caffrey 2004). It is therefore not surprising that a significant partial correlation was found between temperature and both community and picoplankton respiration with all of the data combined (Table 2). However, temperature was not significantly correlated with respiration on the any of the individual cruises (data not shown) suggesting that seasonal changes in temperature (rather than spatial changes) were driving these correlations. TSS was inversely correlated with community respiration on all of the individual cruises (data not shown) and in the entire data set (Table 2). This is unexpected because TSS should provide substrates for particle-attached bacteria, which are more productive than free-living bacteria on a per-cell basis in terms of both respiration and production (Crump et al. 1998). Although Griffith et al. (1994) observed the highest number of bacteria in the oligohaline region of Chesapeake Bay perhaps due to high concentrations of organic substrates, total bacterial production in the Chesapeake Bay ETM was relatively low compared to downstream in this study (Fig. 8). In contrast, positive partial correlations between TSS and degraded pigments including pheophorbide-a,

pheophytin-a, and total pheophytin suggest that the ETM was a site for deposition of degraded pigments (Table 2).

Partial correlation analyses revealed that chlorophyll-a, dinoflagellates, pheophytin-a, and bacterial production were all positively correlated with community respiration. The same variables, except chlorophyll-a and dinoflagellates, were correlated with picoplankton respiration (Table 2). The pigment concentrations (Fig. 13) and the statistical correlation results (between chlorophyll-a and several pigments in Table 2), suggest that dinoflagellates were generally the most abundant phytoplankton species in the study region and that they accounted for a large fraction of community respiration as well. Variations in chlorophyll-a concentration explained 62 % of the variations in community respiration in late-winter, 32 % in early-spring, and 77 % in late-spring, while 62, 5, and 71 % of the variability in community respiration were explained by dinoflagellate in the same periods, respectively (Fig. 14). These results suggest that variations in the dinoflagellate populations played a very large role in driving community respiration at least during the late-winter and late-spring. In addition, larger y-intercepts were found as water temperature increased indicating that more heterotrophic organisms other than dinoflagellates contributed to respiration in warmer water (Fig. 14). Thus it appears that phytoplankton, and specifically dinoflagellates, were responsible for driving much of the primary production and respiration rate variability in the ETM region. The significant correlation between dinoflagellates and cryptophytes (Table 2) also reveals a spatial co-occurrence between the two communities in the upper Chesapeake Bay which may

represent a predator (dinoflagellates) and prey (cryptophytes) interaction (Li et al. 2000).

Size-fractionated respiration

The size-fractionated measurements revealed that the results could be biased by filtration artifacts (e.g., breaking particles, disturbing organisms, or decreasing predation), which sometimes resulted in community respiration rates (i.e., unfiltered water) that were lower than the rates measured on filtered water. This problem was often found when water was filtered through the 63 μm screen but this seldom happened after filtration through the smaller screens. In the following summary, if the difference between two neighboring groups was statistically different ($p < 0.05$) and the respiration rate was bigger after filtration, then the result was not included. In summary, statistically significant differences in respiration rate were not found in different size fractions at the freshwater end-member. This may be in part caused by the fact that respiration rates in each size class were too low to allow detection of significant differences with oxygen measurement technique. The measurements carried out on ETM surface water resulted in highly variable results from which it was difficult to draw any specific conclusions. In contrast, consistent results were obtained from the measurements carried out on the ETM bottom water and on the seawater end-member (Fig. 15). Specifically, in the early and late-spring period, approximately 50 % of community respiration was performed by organisms in the size range between 3 and 10 μm in the ETM bottom and downstream.

Phytoplankton pigments composition

The phytoplankton communities in the study area were generally dominated by dinoflagellates (as indicated by peridinin) and diatoms (as indicated by fucoxanthin), with substantial spatial and temporal variations. Alloxanthin (indicating the presence of cryptophytes) and zeaxanthin (indicating the presence of cyanobacteria) were also consistently measured, but the concentrations of these pigments were low compared to dinoflagellates and diatoms and so were considered to be negligible in explaining primary production and respiration rate variability. The mean surface chlorophyll-a concentrations were always highest downstream though sometimes chlorophyll-a concentrations increased upstream from the ETM, e.g., in early-spring (Fig. 9a). In contrast, mean dinoflagellate concentrations were always highest downstream and lowest at the freshwater end-member (Fig. 13). The mean diatom concentration was also always highest downstream except in the early spring when concentrations increased upstream from the ETM. Thus it appears that diatoms and dinoflagellates contributed to the downstream increases in chlorophyll-a whereas freshwater diatoms were responsible for the upstream increase in chlorophyll-a in early-spring. The mean dinoflagellate and diatom concentrations in early-spring were significantly lower than the other two periods (dinoflagellates: $p < 0.01$; diatoms: $p < 0.05$; $n = 60$, ANOVA).

Discussion

The purpose of this study is to estimate plankton community metabolism and investigate the fundamental structure of the estuarine food web in the Chesapeake

Bay ETM area in relation to environmental and biological influences during the winter-spring period. We consistently observed higher metabolic rates and stronger net heterotrophy downstream of the ETM. These elevated rates were associated with higher pigment concentrations and increased primary production and bacterial production rates. In contrast, the ETM region (25-40 river-km where the bottom topography rapidly shoals upstream) had relatively low primary production and respiration rates. Despite of the direct input of allochthonous organic matter along with river input, low plankton community respiration and primary production rates were generally observed upstream of the ETM and these rates were less variable in time compared to the downstream region.

Most of these metabolism results are comparable to previous studies in the upper Chesapeake Bay. Although the average of gross primary production in late-spring was about 2-fold higher than that observed in previous work in the upper bay (Smith & Kemp 1995& 2003, Kemp et al. 1997), it was caused by spatial discrepancy of defined seawater end-member stations between literatures. Since the axial transect surveys in this study were composed of a considerably larger number of stations than any previous efforts it provides a unique, high-resolution picture of plankton community metabolism variability in the ETM of Chesapeake Bay. It should be noted that the transects were performed in the mainstem and so do not capture ecosystem metabolism in the shallow areas where benthic metabolism occurs.

Environmental factors controlling primary production

The data suggest that spatial variations in primary production within the oligohaline area of Chesapeake Bay cannot be explained only by light availability. Near-surface assimilation numbers did not drop significantly in the ETM region on any of the cruises (Fig. 9b), suggesting that the phytoplankton there were not compromised physiologically, and were therefore not much affected by nutrient limitation either. Increases in euphotic depth downstream were not correlated with gross primary production on any of the individual cruises (data not shown), but were weakly correlated when all data were considered (Table 1). These results are in contrast to results of previous studies in the Chesapeake Bay (Harding et al. 1986, Fisher et al. 1999), other estuaries (Cloern et al. 1983, Irigoien & Castel 1997), and simulation models (Peterson & Festa 1984, Cole & Cloern 1987), which have pointed to light limitation as the most likely factor driving variations in primary production in the ETM region. This would, however, very likely be true if primary production was compared throughout the entire bay due to significantly shallower euphotic depths in the oligohaline compared to the meso- and polyhaline regions (see Fig. 2 in Smith & Kemp 1995). These results suggest that factors other than light or nutrient limitation are perhaps equally or more important for explaining the variations in primary production.

Relatively high inputs of dissolved inorganic nitrogen (nitrate + nitrite + ammonium; DIN) compared to phosphorus (soluble reactive phosphate; SRP) from the surrounding watershed caused the DIN/SRP ratios to exceed 100:1 in all cruises, which is far greater than the Redfield ratio of 16:1 (Crump et al. in preparation). In

addition, high inputs of silicate (dissolved silica; DSi) caused DSi/SRP ratios to exceed 50:1, which is also far greater than the Redfield ratio of 16:1 (data not shown). These ratios are comparable to those found in a previous study where the high values were attributed to the influences of high DIN and DSi loads from river discharge, and high DIN loads from direct rainfall, and wastewater treatment plants (Fisher et al. 1992). A steady decline of DSi was observed in late-winter as salinity went up, which appears to have been caused by simple mixing rather than nutrient uptake by diatoms. Therefore, it appears that phosphorus was likely the limiting nutrient in the oligohaline region, but it does not explain the spatiotemporal variation of primary production within the region because this nutrient appears to be limited uniformly in both space and time.

The dominant phytoplankton species were composed of the dinoflagellates *Heterocapsa rotundatum* (also known as *Katodinium rotundatum*), *Prorocentrum minimum*, and *Karlodinium micrum* (see Keller et al., in prep. for more detailed discussion and analysis of the floristic patterns). These are mixotrophic (autotrophic and phagotrophic) organisms that are all capable of grazing on bacteria (Jeong et al. 2005), cryptophytes (Li et al. 2000), and diatoms of various sizes and shapes. As Tyler and Seliger (1978) described, subsurface maximum concentrations of mixotrophic dinoflagellates were observed throughout pycnocline from downstream stations (76 river-km) to the just seaward of the ETM (40 river-km).

The role of dinoflagellates

The correlation analyses using the entire data set clearly indicate that autochthonous organic matter originated from dinoflagellates were an important source of carbon to the ecosystem in the oligohaline region during the winter-spring period, which may be attributable to the physiological attributes of these organisms (Table 1). Variations in dinoflagellate populations (as indicated by peridinin concentration) alone explained much of the variability in primary production with the second highest correlation, following the highest correlation with total chlorophyll-a (Table 1). Regression analyses in each of the cruises also revealed that dinoflagellates were highly correlated with gross primary production except in early-spring (Fig. 11) when the mean dinoflagellate concentrations were lowest (Fig. 13).

Dinoflagellates found in Chesapeake Bay are highly adaptable to environmental changes (e.g., salinity, light availability, and nutrients) and many can switch between heterotrophic and autotrophic feeding modes, i.e., they are mixotrophic (Stoecker 1998). It has been demonstrated that dinoflagellates can cause winter-spring blooms in the upper Chesapeake Bay (Sellner et al. 1992) even after a lengthy transport from the mouth of the bay, often under the compensation depth (Tyler & Seliger 1978). It has been suggested that there are a number of possible mechanisms that can prolong the viability of dinoflagellates under low light condition (Wofsy 1983, Cole et al. 1992) in addition to heterotrophic feeding. These include reduced grazing pressure and increased photosynthetic efficiency. However, grazing pressure appears to increase in the lower oligohaline region of Chesapeake Bay where high microzooplankton concentrations have been found (Johnson et al. 2003).

Harding (1988) found that dinoflagellates, specifically *P. minimum,* that migrate vertically in Chesapeake Bay, are capable of enhancing the efficiency of light harvest by increasing chlorophyll-a and peridinin per cell, and the initial slope of photosynthesis-light curve (α). Most of all, however, the phagotrophic capability of phototrophic dinoflagellates is particularly beneficial to dinoflagellates because it can provide both carbon and nutrients in low light and low nutrient conditions. This feeding strategy has been found in many dinoflagellate species in diverse environments (Sanders 1991, Stoecker et al. 1997).

The role of diatoms

The correlation results suggest that the contribution of diatoms to primary production was generally less than that of dinoflagellates. Concentrations of diatom were generally lower than those of dinoflagellate (Fig. 13) and they were not correlated with gross primary production on any of the cruises (data now shown), but they were significantly correlated in the entire data set as revealed in the partial correlation analysis (Table 1). Moreover, when the salinity effect is not removed, fucoxanthin concentrations significantly explained variations in gross primary production in early and late-spring (Fig. 12). This suggests that diatoms were more sensitive to salinity changes than dinoflagellates and that mortality due to salinity stress strongly affected the fate of diatoms in the oligohaline.

It should also be noted that this sensitivity might lead to underestimation of the contribution of diatoms to secondary production. Salinity changes are most rapid in the oligohaline and they can influence the fate of phytoplankton because the

optimal salinity ranges of phytoplankton are species specific (Brand 1984). Although the estuarine phytoplankton community has a wider salinity tolerance compared to oceanic and coastal species (Brand 1984), it is clear that different phytoplankton communities were responsible for autotrophic production in the different salinity regimes that we sampled, i.e., freshwater diatoms dominated the flora in the freshwater to oligohaline transition and marine/estuarine dinoflagellates dominated the flora in the oligohaline to mesohaline transition (Keller et al., in preparation). The transition between these two dominant floral groups was abrupt and it generally happened across the 0 to 1 isohalines in the ETM region (Fig. 13). It suggests that diatom mortality rates were high in this region, likely due to osmotic stress. Similarly, in the Schelde Estuary, freshwater phytoplankton communities showed the weakest ability to adapt to seawater and rapidly disappeared and were replaced by estuarine species when salinity increased to more than 0.5 (Muylaert et al. 2000). Thus, physiological (cellular lysis) and physical (sinking loss) processes may prevent diatoms from producing organic matter in the ETM. However, cell death increases dissolved organic matter release, which is eventually consumed by bacteria and microheterotrophs and thus contributes to secondary production.

Underestimation of the contribution of diatoms to secondary production might also be caused by the exclusion of benthic diatoms in the analysis. Benthic diatoms cannot inhabit the deep shipping channel in Chesapeake Bay because there is not sufficient light on the bottom to support photosynthesis. This impediment is worsened in the oligohaline due to high concentrations of TSS, which cause rapid light attenuation. However, we observed what appeared to be high concentrations of

filamentous algae and chain forming diatoms beneath >5 cm-thick ice cover in the upper estuary on the late-winter cruise in 2007, but not in 2008. Diatoms released from ice as it melts can be exploited by both pelagic and benthic grazers (Ichinomiya et al. 2009). Pierson et al. (in preparation) compared the production of copepods in late-winter in 2007 and 2008 and found that upstream of the ETM daily production of copepods was significantly higher in 2007. If there was rapid and selective grazing on diatoms by abundant copepods (Roman et al. 2001) and microzooplankton (Sherr & Sherr 2007, Ichinomiya et al. 2009), a significant fraction of attached diatoms might be consumed by the pelagic species. Although surface ice formation in the oligohaline Chesapeake Bay is not an annual event, further study is needed to estimate the contribution of ice-attached diatoms.

Comparison between primary and bacterial production

The contributions of phytoplankton and bacteria to total production varied in time and space, but primary production in general contributed more organic carbon than particle-attached and free-living bacteria combined (Fig. 8). This is in contrast to the findings of Findlay et al. (1991) who observed higher bacterial production than phytoplankton production in the tidally-influenced area of the Hudson River estuary. In the Hudson River, high TSS concentrations lead to rapid light attenuation, with diffuse attenuation coefficients (k) reaching values of 10 m^{-1} during spring runoff (Cole et al. 1992). In contrast, the maximum k measured in our study was 4.4 m^{-1} in early-spring. In addition, dinoflagellates, which require strong stratification of the water column in order to use it as a migration pathway (Tyler & Seliger 1978), would

likely not reach to the oligohaline of Hudson River estuary because the water column in the oligohaline is well-mixed (Fisher et al. 1988). We therefore speculate that the smaller *k* values and strong stratification in Chesapeake Bay are key factors that promote higher primary production than bacterial production in the oligohaline.

As with phytoplankton, bacteria originating from the freshwater would likely suffer from osmotic stress. Painchaud et al. (1987) described massive losses of riverine bacteria as they flow into the salinity convergence zone in the St. Lawrence Estuary. This zone of high bacteria and phytoplankton mortality very likely provides an important source of organic carbon for the ETM region. This idea is supported by the fact that the relationship between dissolved organic matter and salinity in the ETM region of Chesapeake Bay is best fit with a convex 2nd order polynomial function, indicating net DOM production in the ETM region, which was accompanied by decreases in particulate organic matter and chlorophyll-a concentrations (see Fig. 5 in Fisher et al. 1998, Crump et al., in preparation). This is in contrast to the idea that the production of dissolved organic matter in the ETM region is derived in large part from bacterial colonization and dissolution of detritus from allochthonous sources. This idea seems to be contradicted by the fact that picoplankton respiration rates were relatively low in the ETM region (Fig. 6b). All of these lines of evidence suggest that a more probable explanation is that the ETM region is an area of high salinity stress that causes the death of phytoplankton and bacteria, which increases dissolved organic matter concentrations. However, heterotrophic activities in the ETM are relatively weak compared to the downstream region where environmental conditions are more favorable for both autotrophic and heterotrophic growth.

Phytoplankton and degraded pigments analyses

Surprisingly high correlations were found between community respiration and chlorophyll pigments, which strongly suggest that "autotrophic organisms" were responsible for not only the primary production in the oligohaline region, but also a large fraction of community respiration (Fig. 14, Table 2). These correlations could potentially be explained by very tight coupling between autotrophic production and heterotrophic consumption, e.g., microzooplankton consumption of labile organic matter freshly exuded from phytoplankton. However, except in early-spring the high chlorophyll-a concentrations downstream of the ETM were largely due to the presence of mixotrophic dinoflagellates, (as indicated by high concentrations of peridinin and confirmed by microscopy). It therefore seems more likely that the combined autotrophic and heterotrophic capability of these dinoflagellates explains why there were such strong correlations between dinoflagellates, primary production and community respiration. Size-fractionated experiments also support this conclusion, i.e., there were significant declines in the respiration rate between the 10 to 3 μm-filtered samples in the ETM bottom water and downstream region which is consistent with a major contribution of mixotrophic dinoflagellates to total respiration (Fig. 15). The dinoflagellates *H. rotundatum* and *P. minimum,* which have equivalent spherical diameters of 5.8 and 12.1 μm, respectively (Jeong et al. 2005), likely passed through the 10 μm-screen and but were caught on 3 μm-screen in the size-fractionated measurements. Apparently, these organisms are quite flexible with the ability to adapt to new environmental conditions (salinity tolerance) and food sources (autotrophic

and heterotrophic) to fulfill their energy requirements (Sellner et al. 1991, Stoecker 1998).

It should be noted that high contributions of size-fractionated respiration rates between the 10 to 3 μm-filtered samples to total respiration rates can be caused by mixotrophic dinoflagellates and particle-attached bacteria as well. To find the contribution of each community (i.e., bacteria versus dinoflagellates), we assumed that only bacteria and mixotrophic dinoflagellates caused the respiration in the <10 μm-size samples and picoplankton respiration was only resulted from free-living bacteria. Then, the free-living bacterial production rates were linearly regressed with picoplankton respiration rates to calculate bacterial production (BP) and respiration (BR) efficiency. As a result, computed bacterial growth efficiency (BGE; BGE = BP/(BP+BR)) were 0.45 in late-winter, 0.19 in early-spring, and 0.21 in late-spring, appeared to be regulated by temperature (Apple et al. 2006). We also assumed that particle-attached bacteria had the same bacterial production and respiration efficiency with free-living bacteria. Then, total bacterial respiration rates, converted from total bacterial production rates, were compared with total community respiration (Fig. 16). Based on the calculation using the slopes of graphs, total bacteria community contributed approximately 19, 63, and 38 % of total community respirations in late-winter, early-spring, and late-spring, respectively. On the other hand, the average fraction of <10 μm respiration to total community respiration rates in the Figure 14 is 85 % in the average of two figures. As a result, the contribution of mixotrophic dinoflagellates to total community respiration was approximately 66 % in late-winter, 22 % in early-spring, and 47 % in late-winter. Therefore, the respiration of

mixotrophic dinoflagellates was higher than that of total bacteria except in early-spring when total community respiration was as low as the late-winter respiration.

The high correlations between community respiration and chlorophyll pigments also suggest that the ETM trapped TSS and degraded pigments except the senescent diatom indicating pigment, chlorophyllide-a, which had a positive relationships with chlorophyll-a (Table 2). The distribution and concentration of pheopigments in the ETM is very likely dictated by physiological stress, physical entrapment, and heterotrophic consumption (Welschmeyer et al. 1984, Miller & Moran 1997, Lemaire et al. 2002). The different spatial distribution of chlorophyllide-a in contrast to other pheopigments indicates that diatoms experienced more physiological stress rather than heterotrophic grazing. That is, rapid salinity changes may have played an important role of forming chlorophyllide-a, perhaps due to the low tolerance of diatoms to salinity changes discussed above. Although the dissolved organic matter released from diatoms is known to be rapidly utilized by microbial communities (Fuhrman et al. 1980, Bauerfeind 1985), this is not consistent with the correlation results which reveal a negative relationship between chlorophyllide-a and community respiration when all data are considered (Table 2). However, further analyses between chlorophyllide-a (x-axis) and community respiration (y-axis) in each cruise revealed positive logarithmic relationships with $r^2 = 0.35$, 0.32, and 0.50 in late-winter, early-spring, and late-spring, respectively (graphs not shown). These logarithmic relationships were only observed between chlorophyllide-a and respiration (they were not observed between the other degradation products and respiration) and they considerably improved the coefficients of determination

compared to linear regression analyses. These correlations suggest that senescent diatoms do provide an important food source for heterotrophs, but the reason for the logarithmic relationship is unclear.

Mixotrophic dinoflagellates and implications for estuarine food web

The physiological advantages of mixotrophic dinoflagellates appear to play an important role in the estuarine food web and the microbial loop in the Chesapeake Bay ETM. The downstream of the ETM is particularly rich in inorganic and organic nutrients, it contains high densities of bacteria and zooplankton, and there is more light. It is likely that the mixotrophic dinoflagellates transported from the lower Chesapeake Bay were living under low light conditions and would therefore have depended significantly on heterotrophic growth for survival. Presumably, upon arrival in the lower oligohaline region, where there are high nutrient concentrations and available light, these dinoflagellates would switch from heterotrophic to autotrophic growth. However, it should be noted that the duration of switching can vary depending on the mixotrophic species and also light, nutrient and food availability. Switching can take more than 24 h in some species (Sanders et al. 1990). It is therefore likely that individual dinoflagellates possess different degrees of mixotrophic balance, from primarily heterotrophic to intermediate to primarily autotrophic. It is also unclear whether or not the physiological change is unidirectional from heterotrophic to autotrophic because there are abundant bacteria and cryptophytes that dinoflagellates can feed on. Regardless, it seems likely that different mixotrophic states will exist in these dinoflagellate populations at least

during winter-spring due to the continuous transport of the organisms from the down Bay. This mixture of mixotrophic dinoflagellates can therefore provide both a source of labile organic matter from photosynthesis as well as consuming small heterotrophs.

Organic matter from diverse phytoplankton groups, bacteria, and external loading can give rise to abundant and diverse zooplankton populations (Roman et al. 2001, Pace et al. 2004). The mesozooplankton in the oligohaline region of many estuaries is dominated by the calanoid copepods and typical freshwater cladocera with the relative dominance varying in both space and time. These organisms are important consumers of organic matter and they are an important food source for fish larvae and higher trophic levels (North & Houde 2003, 2006). Presumably, mesozooplankton can fulfill their carbon requirements in the ETM region by selectively grazing on phytoplankton, by filtering out detrital organic matter with bacteria, or by grazing on microzooplankton (Van den Meersche et al. 2009). The low primary production in the Chesapeake Bay ETM suggests that copepod diets are, indeed, composed of a variety of food items, rather than selective grazing on phytoplankton. Kleppel (1993) emphasized that the nutritional requirements of copepods can be satisfied by grazing on diverse food items. Interestingly, dinoflagellates are estimated to have about twice the caloric content (the sum of protein, carbohydrate, and lipid) of diatoms of equivalent volume (Hitchcock 1982). Moreover, copepod egg production has been shown to be highly correlated with the ingestion of dinoflagellates or dinoflagellates in combination with other organisms than diatoms alone (Kleppel et al. 1991). It has also been shown that, due to the high grazing ability and preference for dinoflagellates by copepods, most dinoflagellate

biomass is consumed in the water column and sinking loss to the bottom is negligible (Sellner et al. 1991, 1992). All of these lines of evidence support the idea that dinoflagellates play a key role in the food web of the oligohaline Chesapeake Bay not only as an important organic matter producer and consumer, but also as a food source for copepods and higher trophic levels.

Upstream of the Chesapeake Bay ETM, high concentrations and continuous supplies of inorganic and organic nutrients along with bacteria and TSS presumably provide carbon sources for omnivorous mesozooplankton (Roman 1984). Although the production of diatoms in this region was much lower than that of dinoflagellates downstream of the ETM, they likely also provide an important carbon source for micro- and mesozooplankton. High river discharge in the shallow upstream region would rapidly flush diatoms and bacteria along with TSS and inorganic nutrients into the ETM region where changes in salinity and physical mechanisms further break down and trap particulate and dissolved organic matter. Although biological responses (i.e., community respiration and bacterial production) measured in the ETM were much lower than downstream, physical processes in the ETM were very likely crucial for preserving inorganic nutrients (i.e., high TSS and light limitation decrease nutrient uptake by phytoplankton) and supplying organic matter into the downstream region. Sudden emergence of dinoflagellates into a deeper euphotic layer where there are abundant nutrients likely accelerated the production of dinoflagellates. In addition to microzooplankton grazing on small heterotrophs, mixotrophic dinoflagellates having heterotrophic/phagotrophic ability can link bacterial production into higher secondary producers. Azam et al. (1983) emphasized that the

ecological interactions between commensalism, competition, and predation result in dynamic microbial loop. This study suggests that these three factors are seamlessly intermingled in the oligohaline Chesapeake Bay.

Conclusion

The estuarine circulation facilitates the transport of dinoflagellates from the down-bay or tributaries to the lower oligohaline region where optimal nutrient and light conditions support high autotrophic production downstream of the ETM. In this region heterotrophic respiration were also enhanced by both internal and external organic matter loading. The results presented in this paper clearly show that the oligohaline Chesapeake Bay is net heterotrophy in winter-spring and it strongly suggests that higher respiration compared to primary production in the downstream region was largely due to dinoflagellate respiration. Mixotrophic dinoflagellates appear to play a particularly important role in the oligohaline Chesapeake Bay, producing and consuming labile organic matter, and potentially providing a key pathway for carbon and energy transfer from low to high trophic levels. Specifically, the autotrophic ability of these dinoflagellates combined with their ability to graze on small autotrophs, heterotrophs, and bacteria may provide a mechanism for tight coupling between primary producers and copepods because they have a high nutritional value and are of optimal size for ingestion by copepods.

Tables

	Salinity	GPP	Temperature	TSS	Euphotic depth
GPP	0.46 **	-	*0.58* **	*-0.31* *	*0.32* *
Temperature	-0.24	0.39 **	-	*-0.34* **	*0.32* *
TSS	-0.21	-0.37 **	-0.27 *	-	*-0.61*
Euphotic depth	0.60 **	0.51 **	nr	-0.60 **	-
Chlorophyll-a	0.65 **	0.80 **	nr	-0.23	0.43 **
Dinoflagellate	0.57 **	0.73 **	nr	nr	0.29 *
Diatom	0.34 **	0.43 **	nr	-0.37 **	0.40 **
Cryptophyte	0.54 **	0.35 **	nr	nr	0.48 **
Cyanobacteria	nr	0.54	0.32 **	nr	nr

	Chlorophyll-a	Dinoflagellate	Diatom	Cryptophyte	Cyanobacteria
GPP	*0.74* **	*0.64* **	*0.33* *	*nr*	*0.58* **
Temperature	*0.25*	*nr*	*nr*	*0.21*	*0.35* **
TSS	*nr*	*nr*	*-0.33* *	*nr*	*nr*
Euphotic depth	*nr*	*nr*	*0.26* *	*0.23*	*nr*
Chlorophyll-a	-	*0.83* **	*0.39* **	*nr*	*0.43* **
Dinoflagellate	0.89 **	-	*nr*	*nr*	*nr*
Diatom	0.50 **	nr	-	*nr*	*0.55* **
Cryptophyte	0.45 **	0.27 *	0.21	-	*nr*
Cyanobacteria	0.36	nr	0.54	nr	-

Table 1: Correlation matrix of salinity and environmental and biological variables at surface with gross primary production. In italics (upper right): partial correlation coefficients excluding salinity influence if any. nr = no relationship if $r < 0.2$; ** $p < 0.01$, * $0.01 < p < 0.05$; $n = 60$. Pearson's correlation coefficient was used to examine the relationship between gross primary production, environmental variables and phytoplankton community composition in surface water.

	Salinity	T.Resp	Pico.Resp	Temperature	TSS
T.Resp	0.34 **	-	*0.56* **	*0.58* **	*-0.28* **
Pico.Resp	nr	0.57 **	-	*0.39* **	*nr*
Temperature	nr	0.47 **	0.35 **	-	*nr*
TSS	nr	-0.27 **	nr	nr	-
Chlorophyll-a	0.53 **	0.55 **	nr	nr	nr
Dinoflagellate	0.42 **	0.51 **	nr	nr	nr
Diatom	0.44 **	0.22 **	nr	nr	nr
Cryptophyte	0.43 **	0.27 **	nr	nr	nr
Cyanobacteria	nr	nr	0.31 **	nr	0.58 **
Chlorophyllide-a	0.47 **	nr	nr	-0.27 **	nr
Pheophorbide-a	0.69 **	nr	nr	nr	0.45 **
Pheophytin-a	0.48 **	0.44 **	0.32 **	0.23 **	0.41 **
T.Pheophytin	0.34 **	nr	nr	nr	0.66 **
T.Bacteria	nr	0.47 **	0.29 **	0.34 **	nr
F.L.Bacteria	nr	0.61 **	0.48 **	0.47 **	-0.22 **

	Chlorophyll-a	Dinoflagellate	Diatom	Cryptophyte	Cyanobacteria
T.Resp	*0.46* **	*0.43* **	*nr*	*nr*	*nr*
Pico.Resp	*nr*	*nr*	*nr*	*nr*	*0.30* **
Temperature	*nr*	*nr*	*nr*	*nr*	*nr*
TSS	*nr*	*nr*	*nr*	*nr*	*0.59* **
Chlorophyll-a	-	*0.90* **	*0.30* **	*0.38* **	*nr*
Dinoflagellate	0.92 **	-	*nr*	*0.25* **	*nr*
Diatom	0.46 **	nr	-	*nr*	*0.32* **
Cryptophyte	0.52 **	0.39 **	nr	-	*nr*
Cyanobacteria	nr	nr	0.32 **	nr	-
Chlorophyllide-a	0.54 **	0.45 **	0.48 **	0.40 **	nr
Pheophorbide-a	0.27 **	nr	0.50 **	0.23 **	0.52 **
Pheophytin-a	0.34 **	nr	0.42 **	0.34 **	0.62 **
T.Pheophytin	nr	nr	0.22 **	nr	0.57 **
T.Bacteria	nr	nr	0.20 *	0.22 **	0.20 **
F.L.Bacteria	nr	nr	0.34 **	nr	0.22 **

Table 2 (continued to next page)

	Chlorophyllide-a	Pheophorbide-a	Pheophytin-a	T.Pheophytin	T.Bacteria	F.L.Bacteria
T.Resp	*-0.23* **	*nr*	*0.33* **	*nr*	*0.44* **	*0.60* **
Pico.Resp	*-0.27* **	*nr*	*0.29* **	*nr*	*0.27* **	*0.47* **
Temperature	*-0.22* **	*nr*	*0.36* **	*nr*	*0.37* **	*0.49* **
TSS	*nr*	*0.63* **	*0.47* **	*0.70* **	*nr*	*-0.23* **
Chlorophyll-a	*0.39* **	*nr*	*nr*	*-0.23* **	*nr*	*nr*
Dinoflagellate	*0.31* **	*-0.24* **	*nr*	*-0.28* **	*nr*	*nr*
Diatom	*0.35* **	*0.30* **	*0.26* **	*nr*	*nr*	*0.32* **
Cryptophyte	*0.25* **	*nr*	*nr* *	*nr*	*nr*	*nr*
Cyanobacteria	*nr*	*0.66* **	*0.67* **	*0.59* **	*nr*	*0.21* **
Chlorophyllide-a	-	*nr*	*-0.21* **	*nr*	*nr*	*nr*
Pheophorbide-a	0.40 **	-	*0.62* **	*0.73* **	*nr*	*nr*
Pheophytin-a	nr	0.73 **	-	*0.60* **	*0.37* **	*0.47* **
T.Pheophytin	nr	0.73 **	0.66 **	-	*nr*	*nr*
T.Bacteria	nr	0.20 *	0.41 **	nr	-	*0.62* **
F.L.Bacteria	*nr*	*nr*	0.47 **	nr	0.63 **	-

Table 2: Correlation matrix of salinity and environmental and biological variables at surface, middle, and bottom water with respiration rates. In italics (upper right): partial correlation coefficients excluding salinity influence if any. nr = no relationship ($r < 0.2$); ** $p < 0.01$, * $0.01 < p < 0.05$; n = 180 but n = 165 for the two bacterial production. (T.Resp: total community respiration; Pico.Resp: picoplankton respiration; T.Pheophytin: total pheophytin; T.Bacteria: total bacterial production; F.L.Bacteria: free-living bacterial production).

Figures

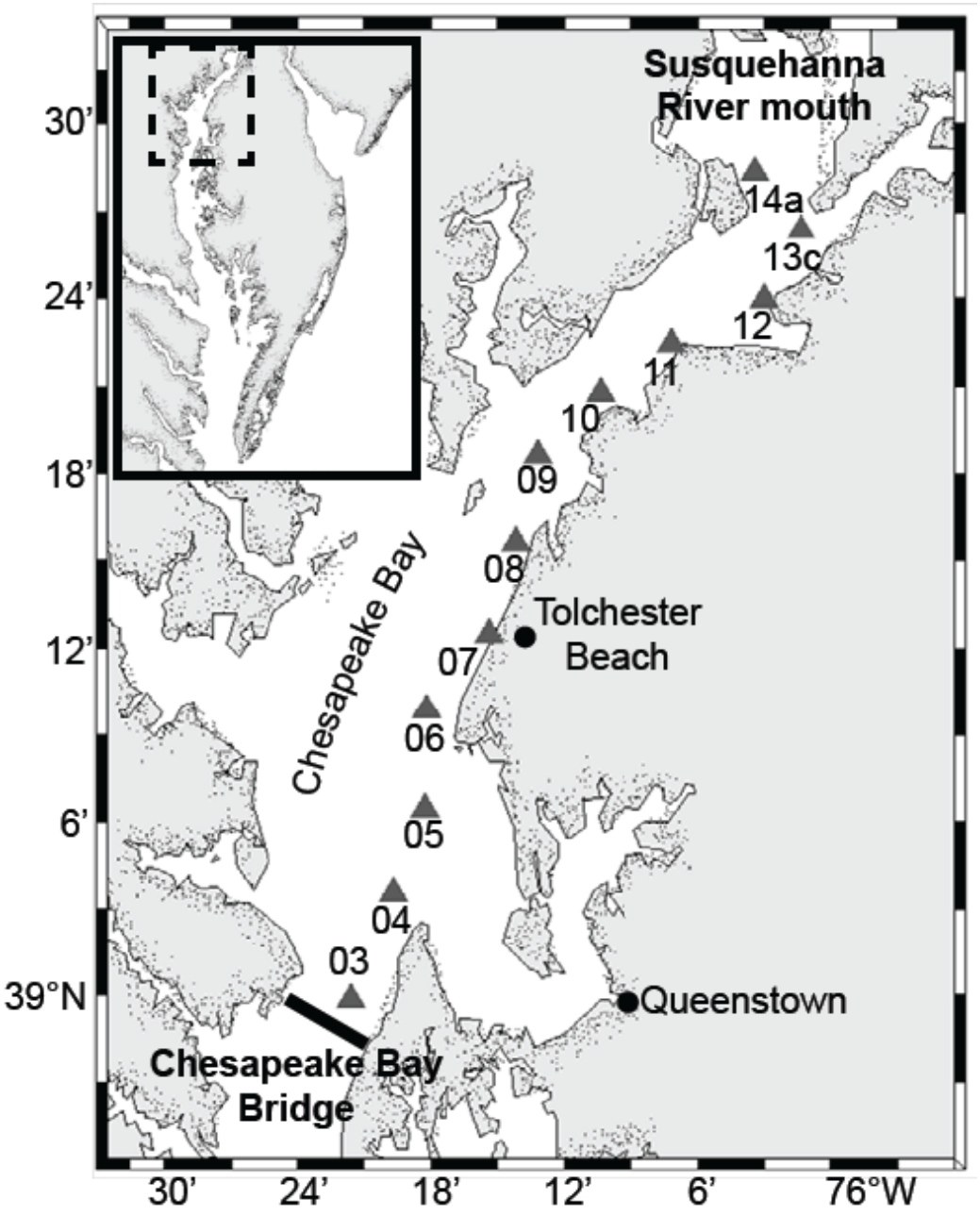

Figure 1: The oligohaline area of Chesapeake Bay which is 76 km along a shipping channel (defined as river-km) and stretches from the Chesapeake Bay Bridge (lat: 38°59.8' N) to Havre de Grace (lat: 39°28.3' N) at the mouth of Susquehanna River, Maryland, USA. CTD profile casts were made at a total of 11 stations from Station '03' near the Chesapeake Bay Bridge to Station '14a' near the Susquehanna River mouth within 8 h from 0600 to 1400. Water samples were collected from five stations among the 11 stations, representing two downstream, one estuarine turbidity maximum (ETM), and two upstream stations.

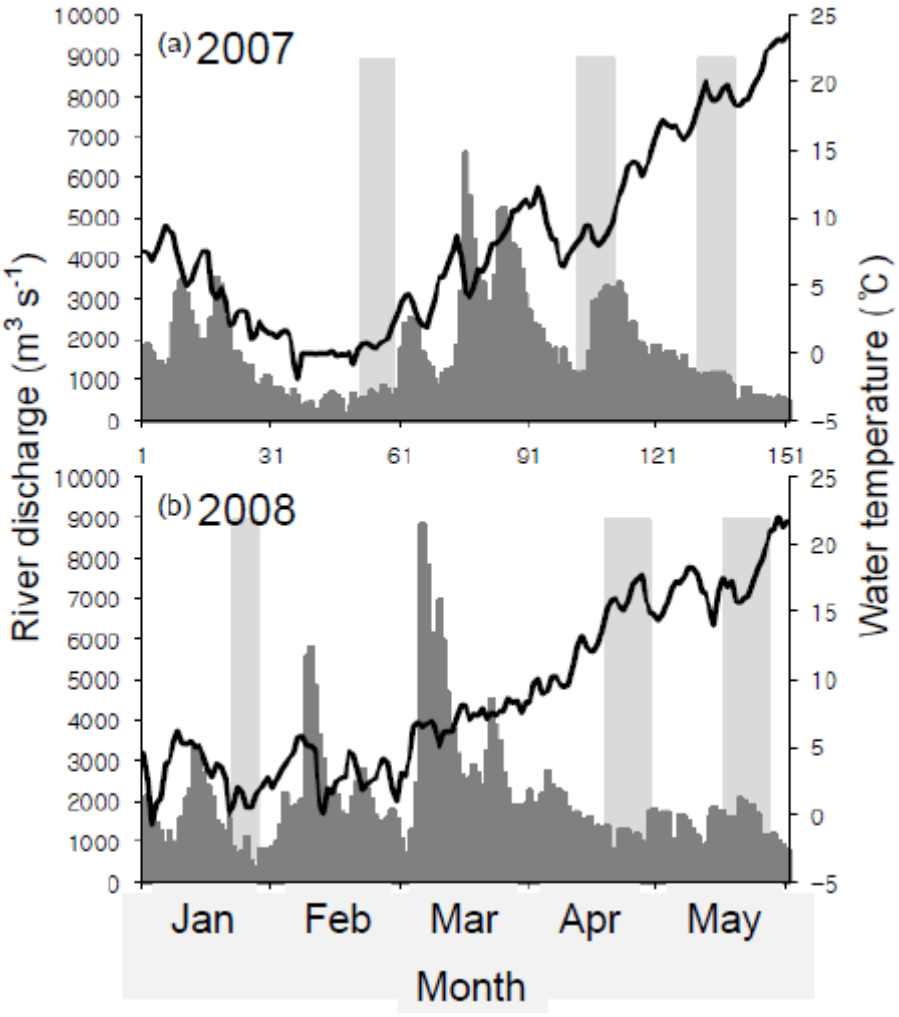

Figure 2: Daily river discharges at Conowingo Dam near the mouth of Susquehanna River (dark gray bar graphs; US Geological Survey) and water temperature at Tolchester Beach (black lines; Chesapeake Bay Program) in 2007 (a) and 2008 (b). Pale gray bars indicate the periods of research cruises.

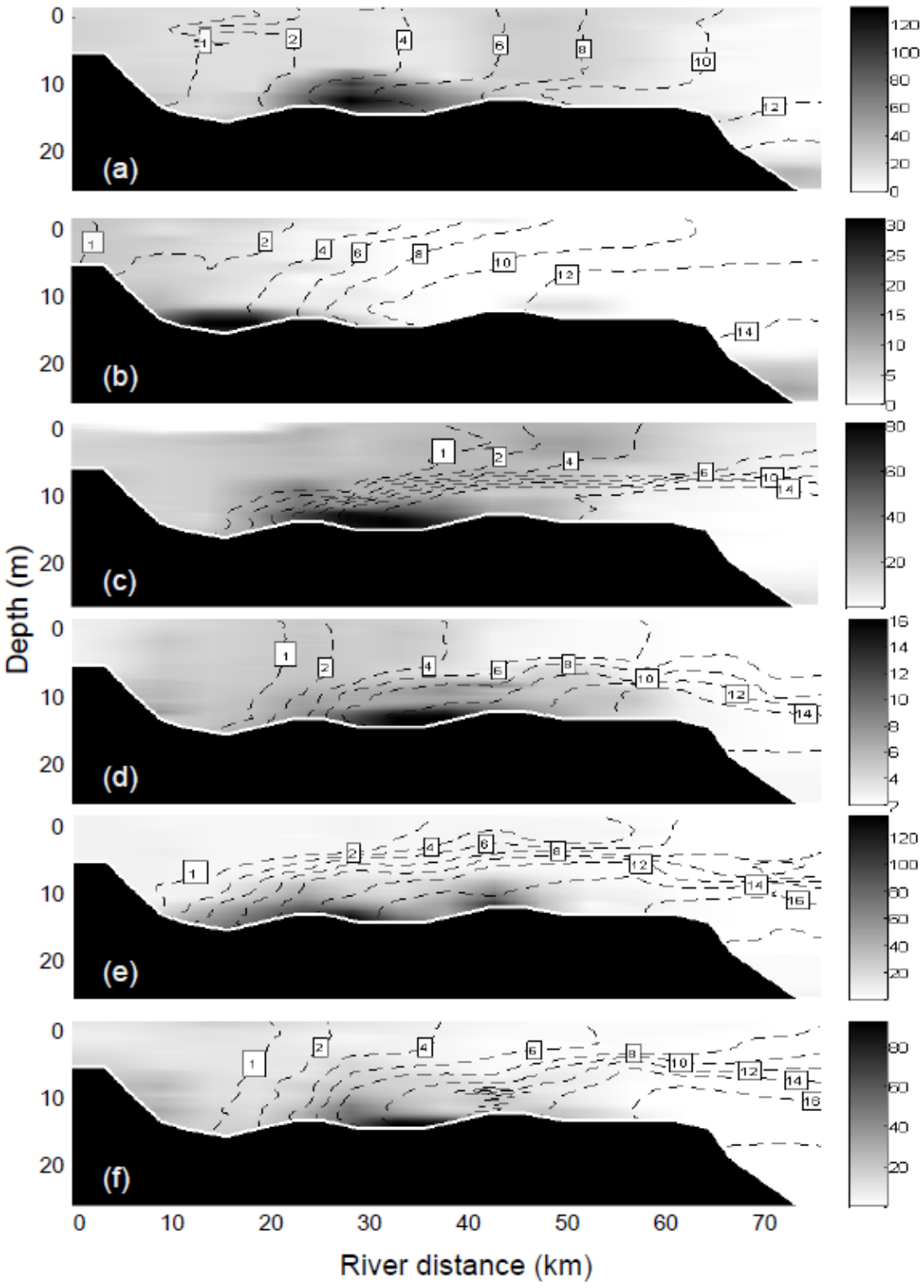

Figure 3 (continued to next page)

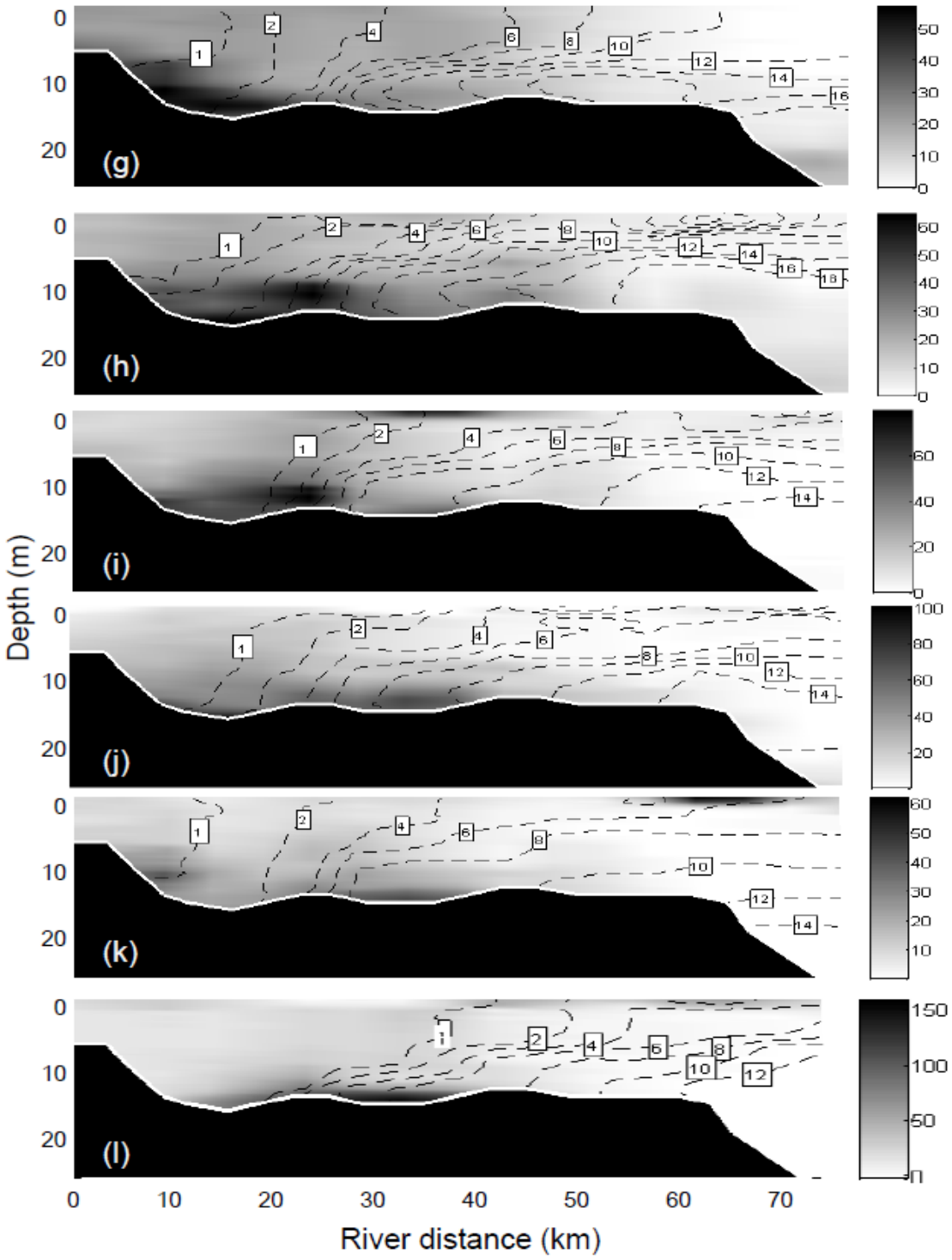

Figure 3: Contour plots of salinity (lines; unit: PSU) and turbidity (colors; unit: NTU) measured during 11 CTD casts on two axial surveys per cruise. Late-winter (a & b), early-spring (c & d), and late-spring (e & f) in 2007 and late-winter (g & h), early-spring (i & j), and late-spring (k & l) in 2008. The X-axis of each plot presents distances from the mouth of Susquehanna River (0 river-km) to the Chesapeake Bay Bridge (80 river-km) along the shipping channel.

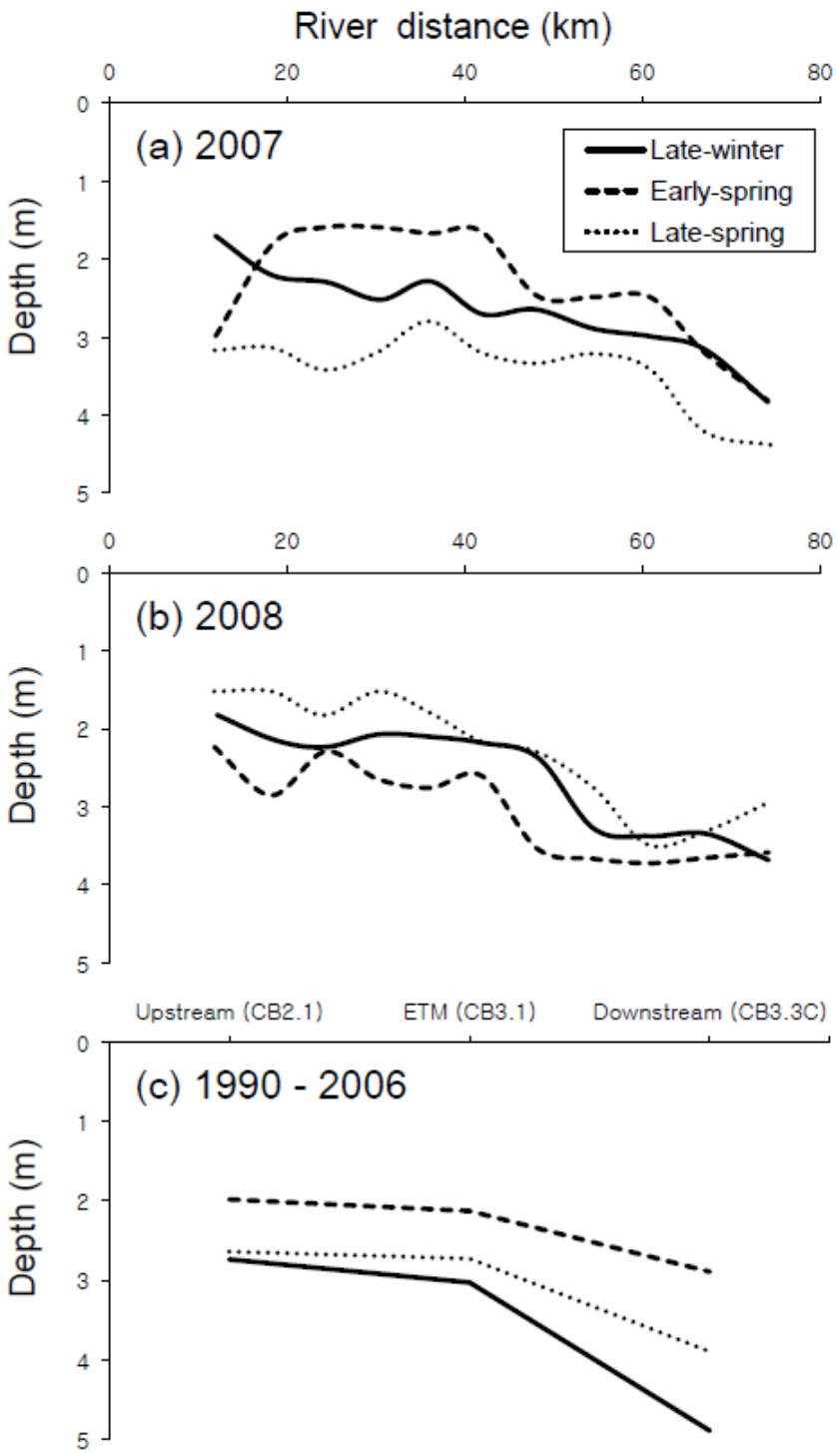

Figure 4: Average euphotic depth (1 % of surface irradiance level) along the mainstem of Chesapeake Bay in 2007 (a) and 2008 (b), and the long-term monthly averages from 1990 to 2006 (c). The estuarine turbidity maximum was located approximately at 35 river-km (a & b) and station CB3.1 (c).

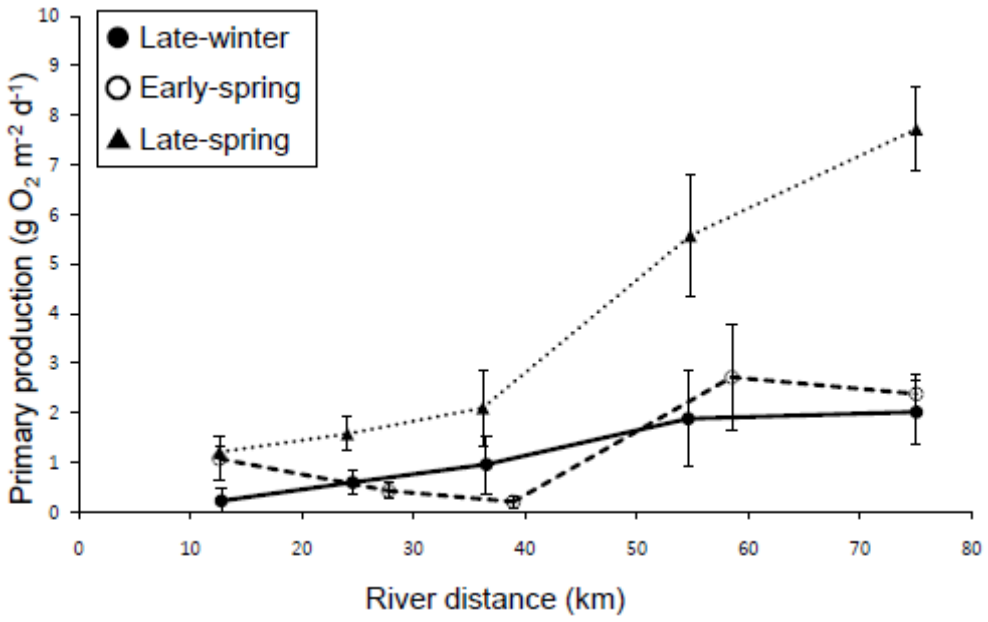

Figure 5: The mean of gross primary production (± SE) integrated over euphotic depths in 2007 and 2008 at five stations along the mainstem of Chesapeake Bay. The estuarine turbidity maxima were located between 30 and 40 river-km.

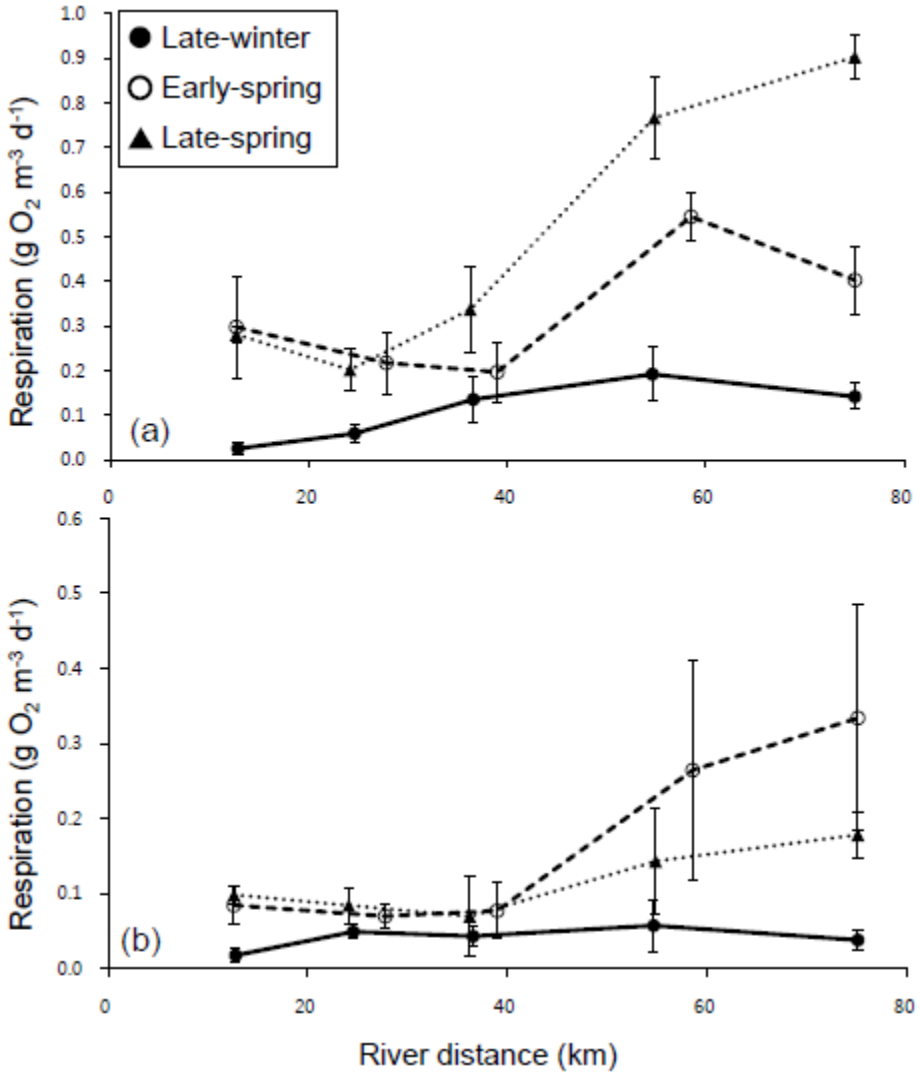

Figure 6: The mean of community respiration (a) and picoplankton respiration (b) in 2007 and 2008 at five stations along the mainstem of Chesapeake Bay (± SE). The estuarine turbidity maxima were located between 30 and 40 river-km.

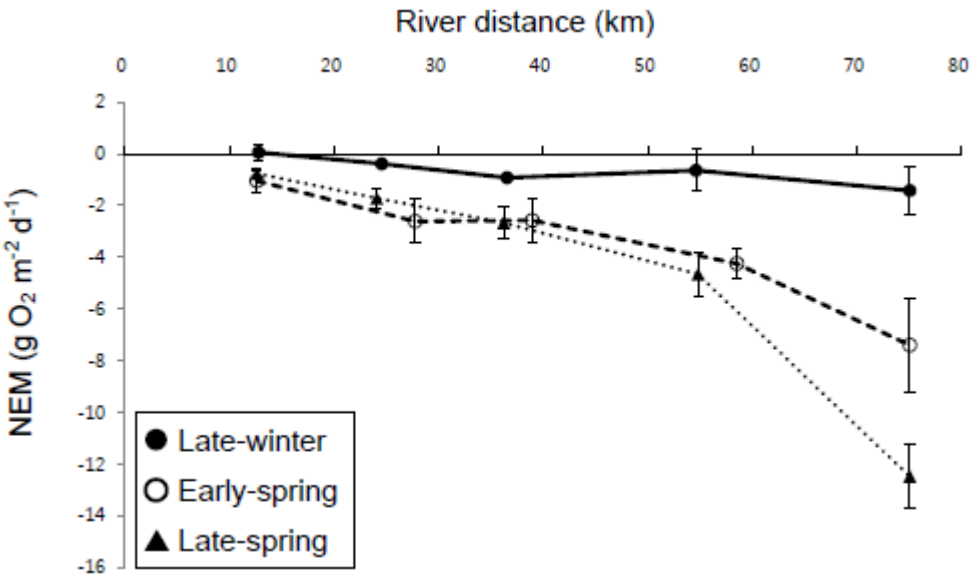

Figure 7: The mean of net ecosystem metabolism rates in 2007 and 2008 at five stations along the mainstem of Chesapeake Bay (± SE). The estuarine turbidity maxima were located between 30 and 40 river-km.

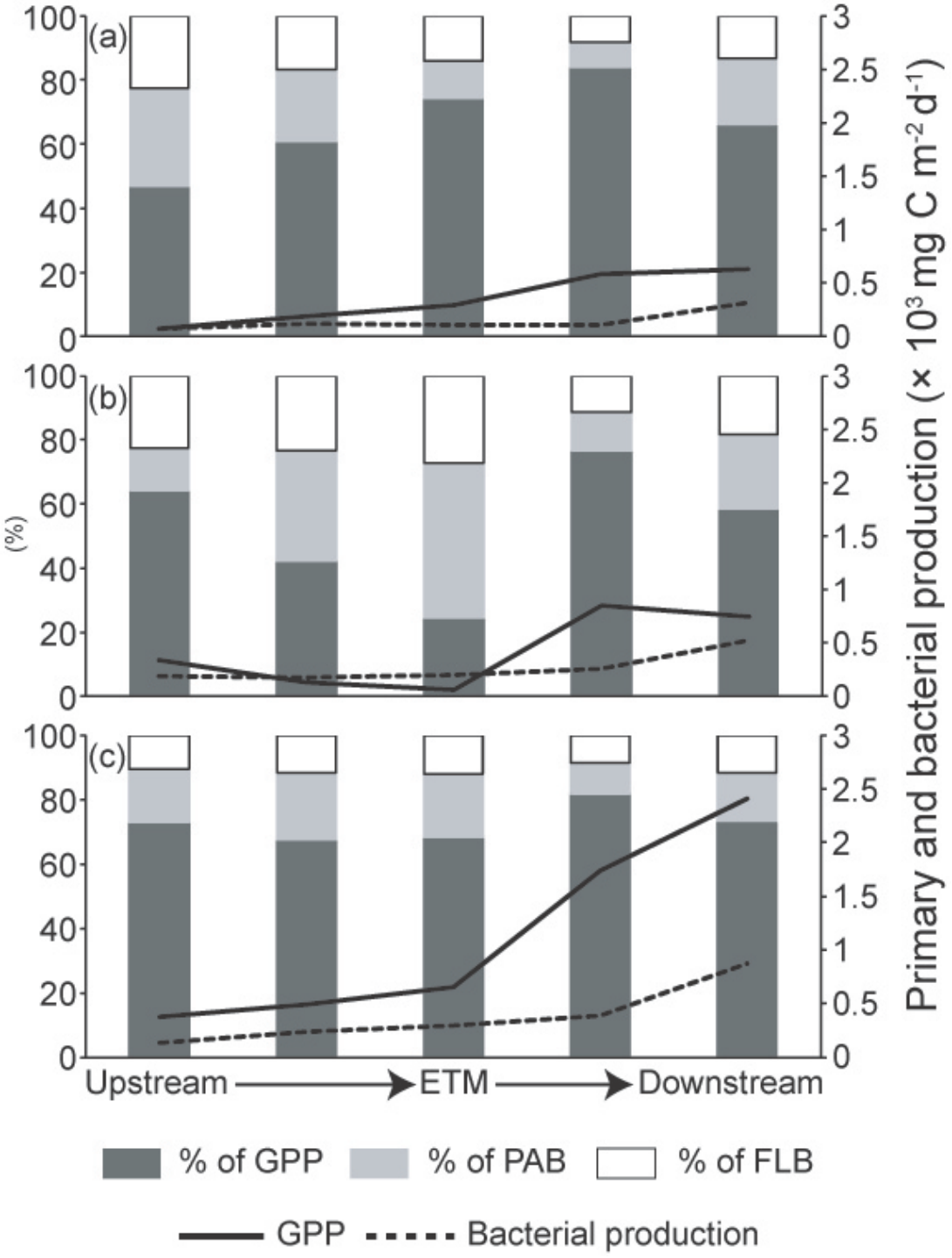

Figure 8: Percentages of two-year carbon production rates by phytoplankton (black areas), particle-attached bacteria (gray areas), and free-living bacteria (white areas) in late-winter (a), early-spring (b), and late-spring (c) (left y-axis). Line graphs indicate the sum of the three production rates (right y-axis).

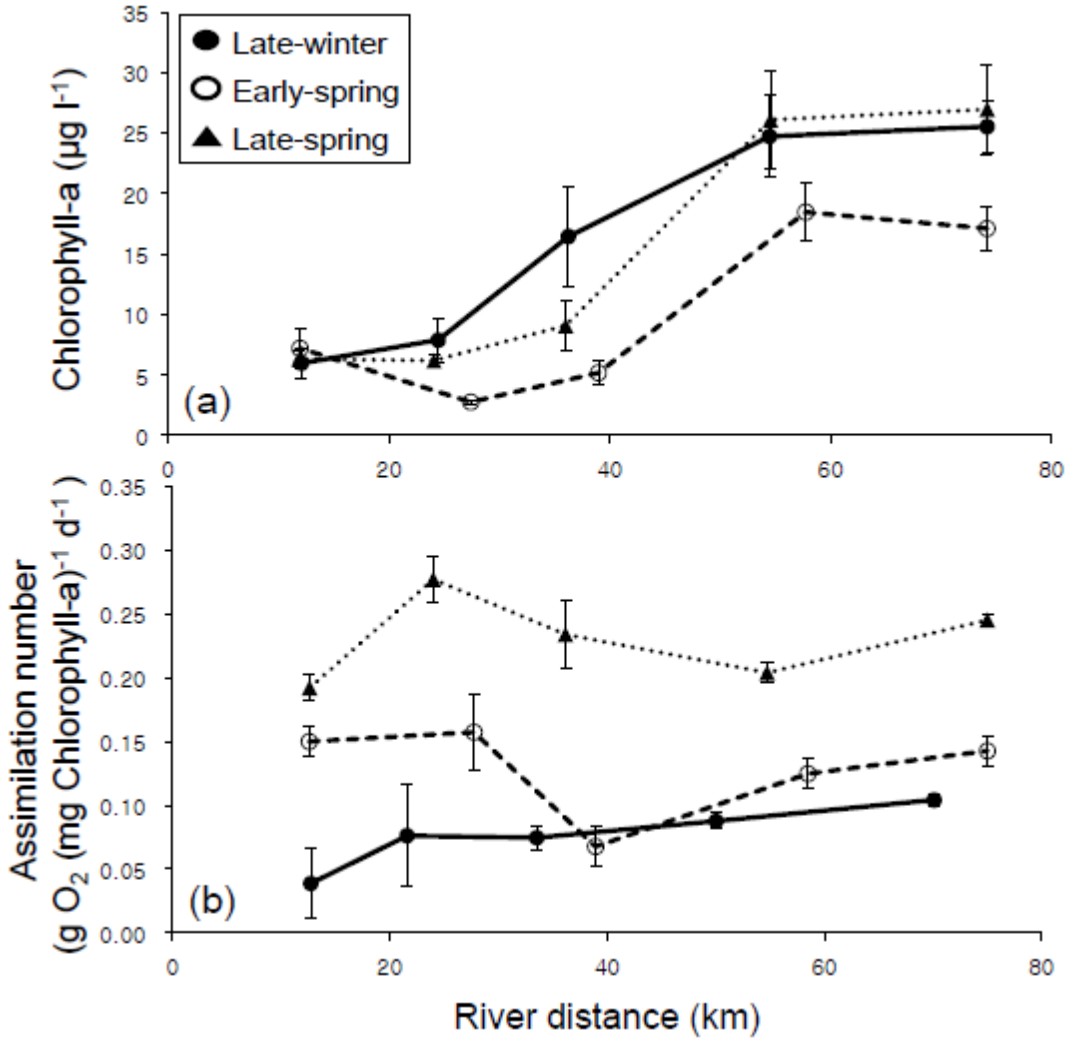

Figure 9: The two-year mean (± SE) of depth-averaged chlorophyll-a concentration (a) and gross primary production per chlorophyll-a at the surface (assimilation number) (b).

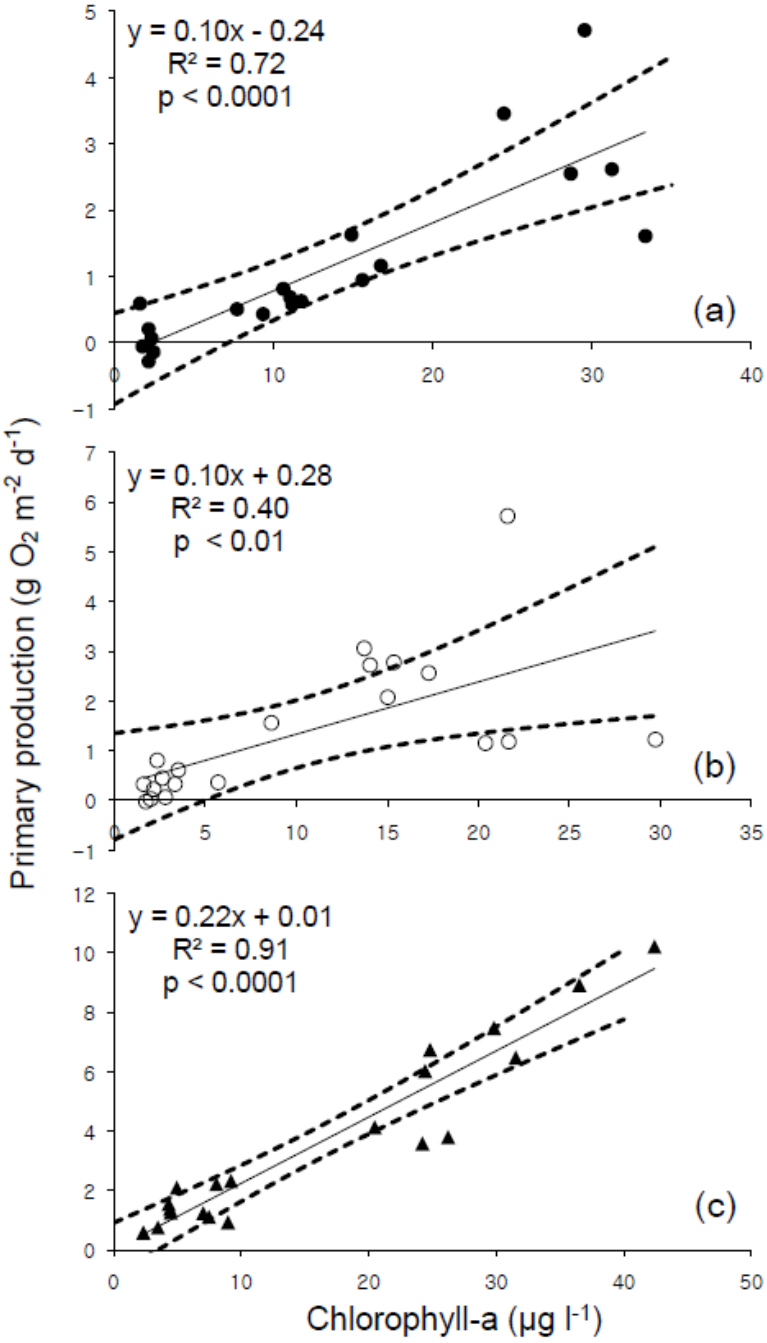

Figure 10: Regression analysis between gross primary production (y-axis) and surface chlorophyll-a concentration (x-axis) in late-winter (a), early-spring (b), and late-spring (c) in 2007 and 2008. The best fit line is calculated using a least-squares method and the two dotted lines indicate the 95 % prediction bounds (n = 20). None of the y-intercepts were significantly different from 0 ($p > 0.05$).

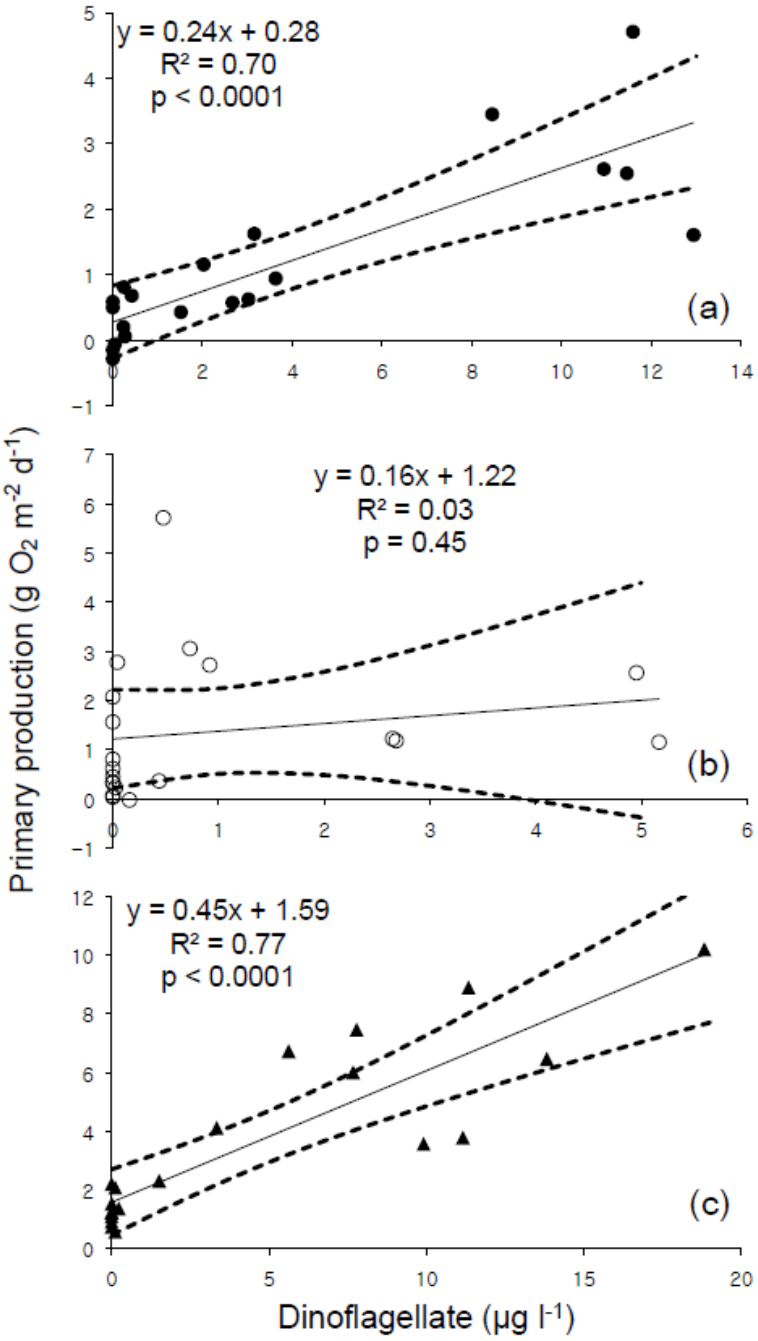

Figure 11: Regression analysis between gross primary production (y-axis) and surface peridinin concentration (x-axis) in late-winter (a), early-spring (b), and late-spring (c) in 2007 and 2008. The best fit line is calculated using a least-squares method and the two dotted lines indicate 95 % prediction bounds (n = 20). The y-intercept was not significantly different from 0 in late-winter ($p > 0.05$) but was significantly different in early and late-spring ($p < 0.05$).

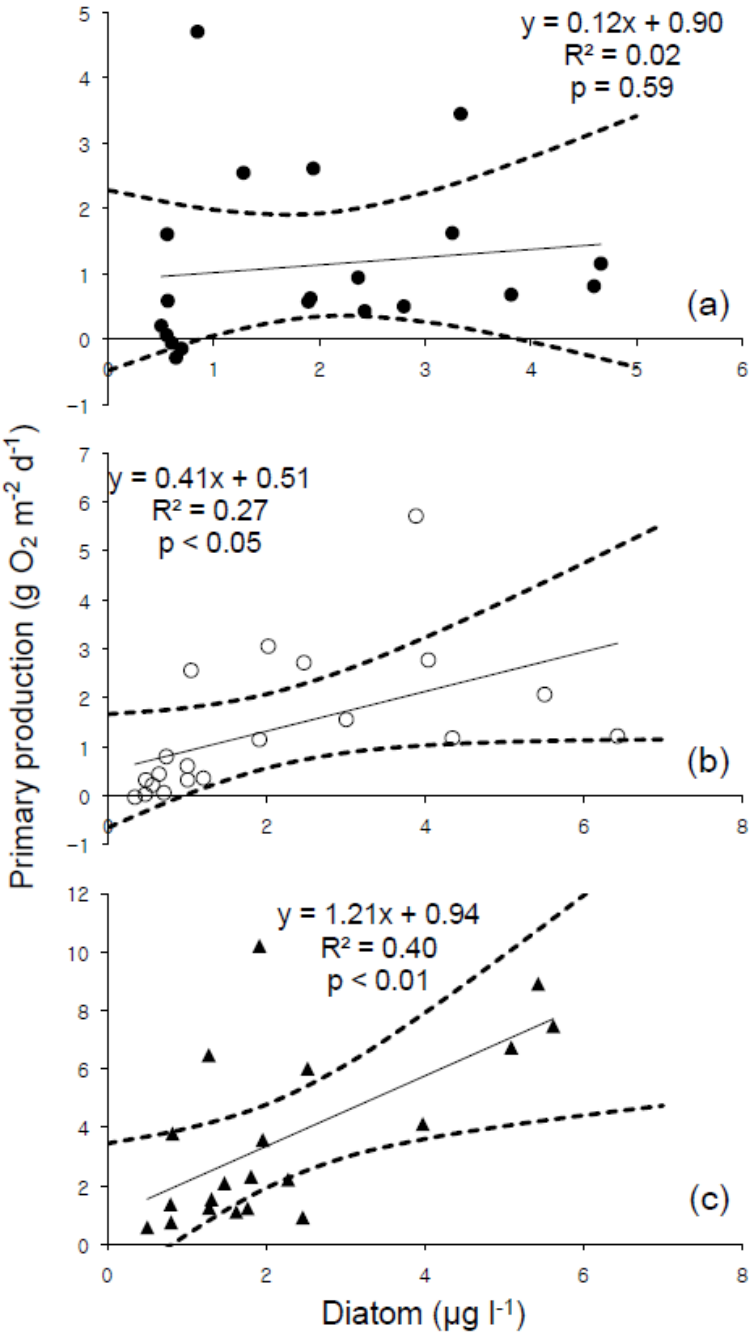

Figure 12: Regression analysis between gross primary production (y-axis) and surface fucoxanthin concentration (x-axis) in late-winter (a), early-spring (b), and late-spring (c) in 2007 and 2008. The best fit line is calculated using a least-squares method and the two dotted lines indicate 95 % prediction bounds (n = 20). None of the y-intercepts were significantly different from 0 ($p > 0.05$).

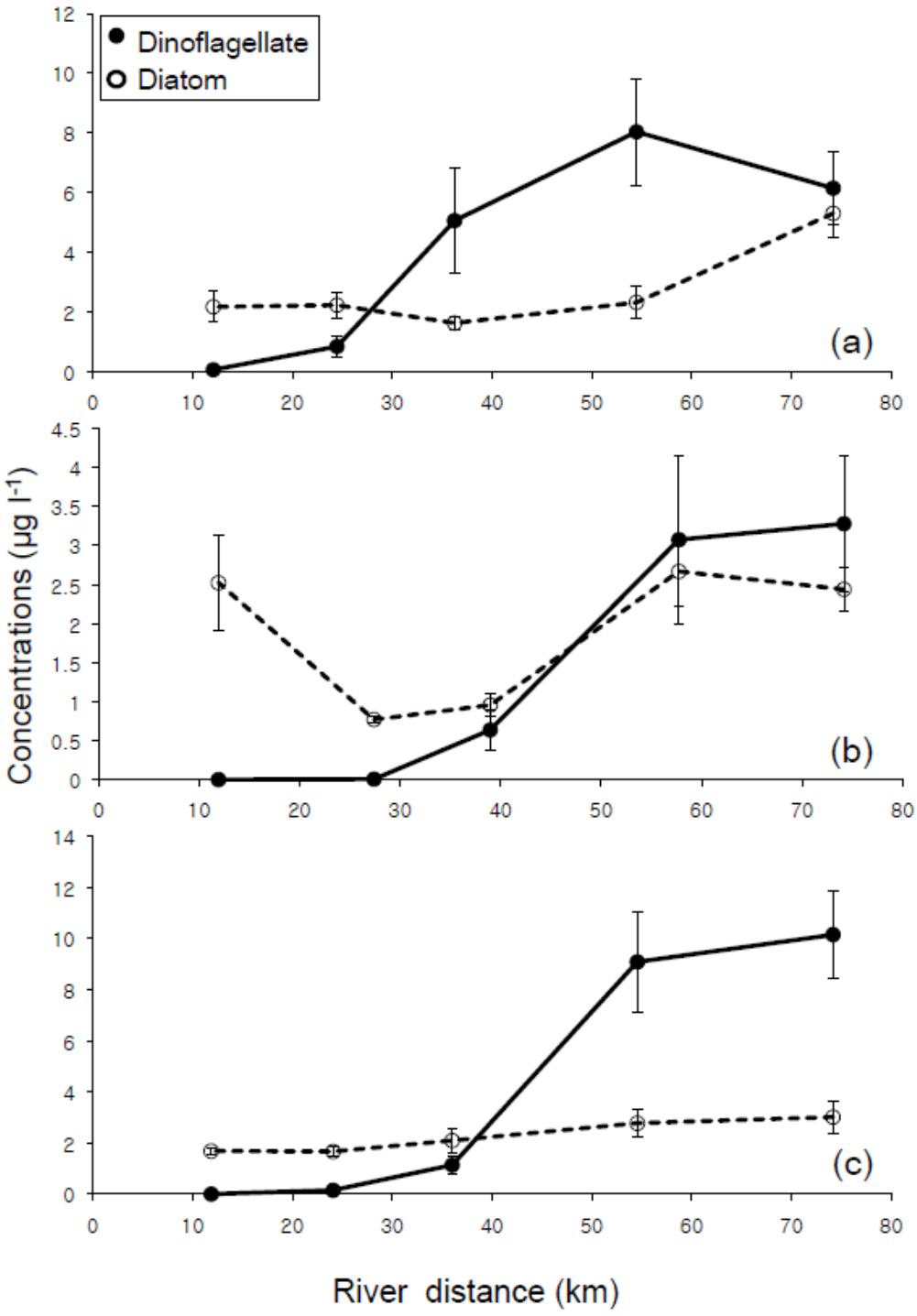

Figure 13: Mean surface concentrations (± SE) of peridinin (black circles) and fucoxanthin (empty circles) in late-winter (a), early-spring (b), and late-spring (c) in 2007 and 2008. The estuarine turbidity maxima were located between 30 and 40 river-km (n = 12).

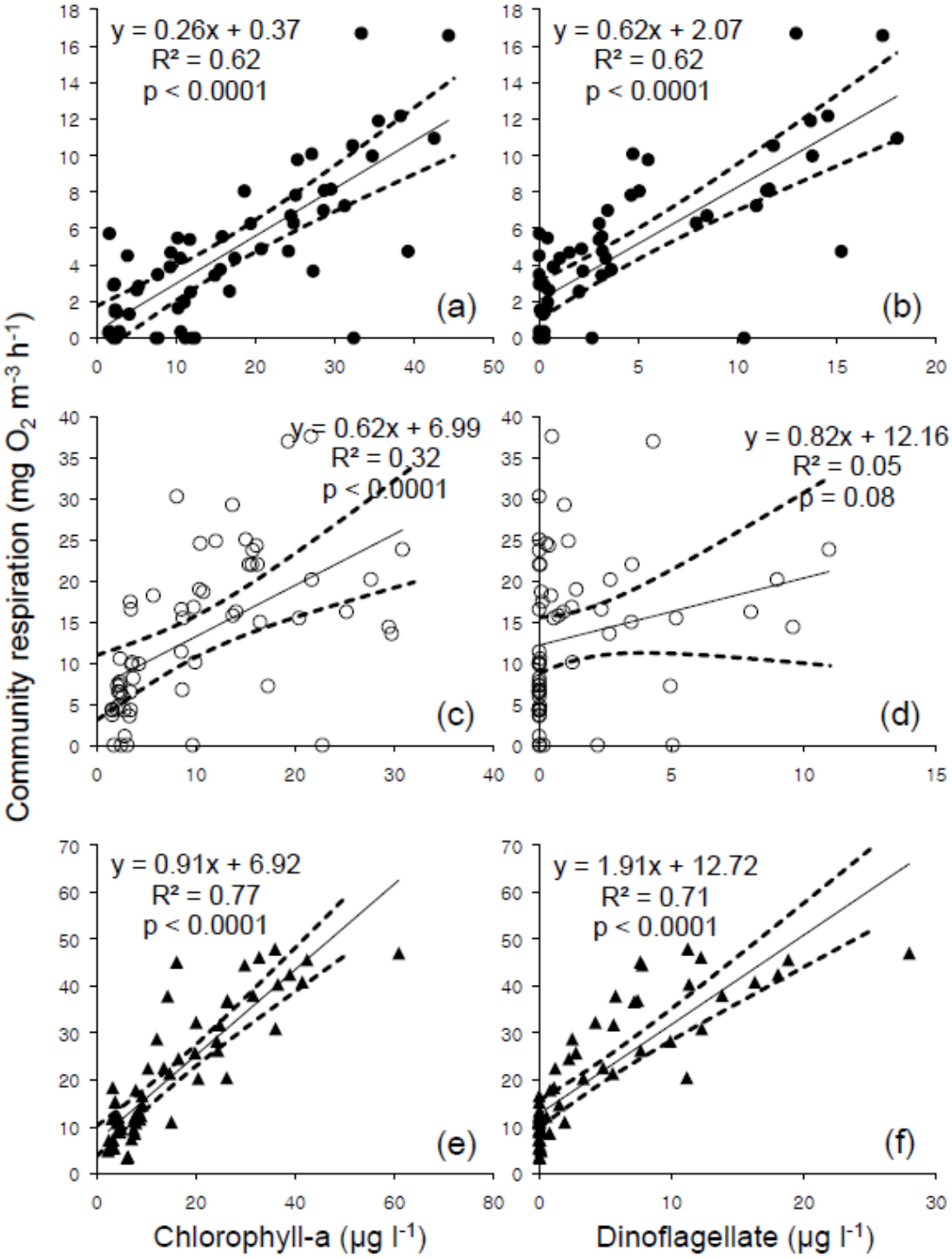

Figure 14: Regression analysis between community respiration (y-axis) and chlorophyll-a and peridinin concentrations (x-axis) in late-winter (a & b), early-spring (c & d), and late-spring (e & f) in 2007 and 2008. The best fit line is calculated using a least-squares method and the two dotted lines indicate 95 % prediction bounds (n = 60). All of the y-intercepts were significantly different from 0 ($p < 0.001$) except chlorophyll-a in late-winter (a; $p > 0.05$).

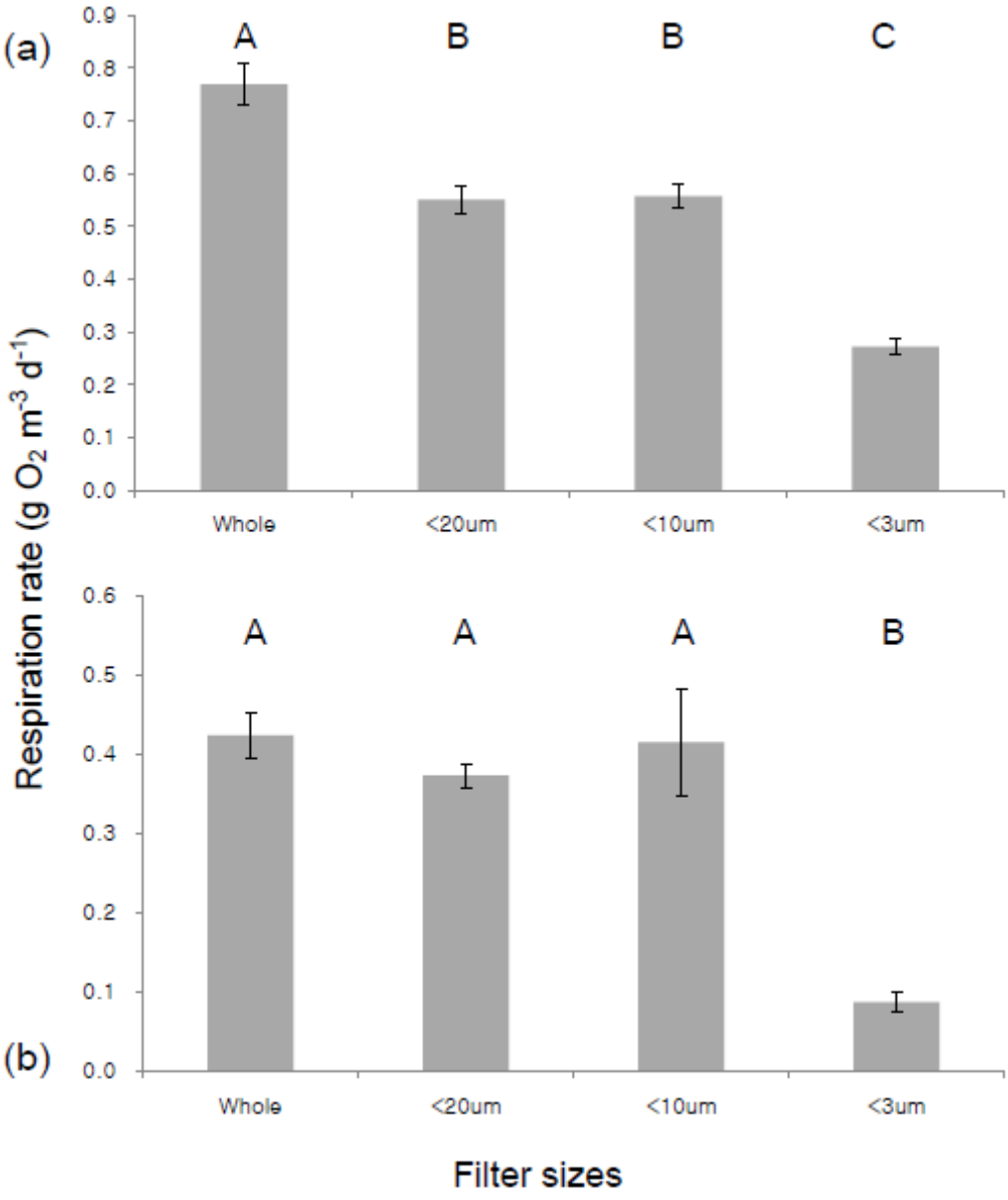

Figure 15: Size-fractionated respiration rates (± SE) in early-spring at the downstream end-member station (a) and in late-spring in the ETM (b). Tukey's Studentized Range test was used to investigate statistical differences between groups. Graphs followed by different subscripts are significantly different ($p < 0.05$).

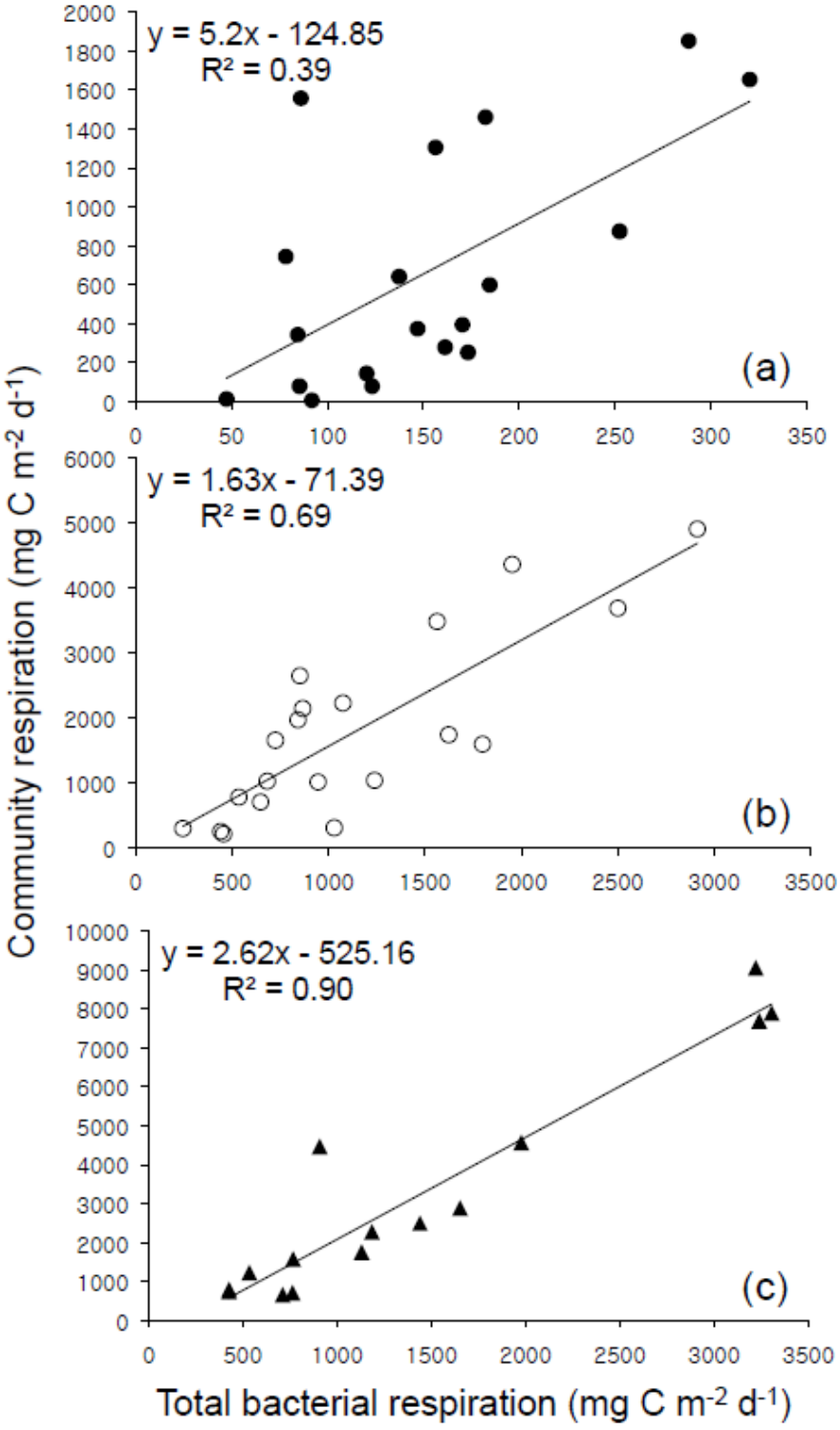

Figure 16: The relationships of depth integrated total bacterial respiration rates, which were computed from total bacterial production rates by using bacterial growth efficiency, with depth integrated community respiration rates in late-winter (a), early-spring (b), and late-spring (c) in 2007 and 2008.

Appendix I: Testing a linear respiration rate for 24 h

Unfiltered and filtered respiration rates were measured in this study with the assumption of constant decreases of dissolved oxygen concentrations over time. To find out whether or not this assumption was valid, a series of experiments were conducted to determine whether or not respiration rates were linear for 24 h in the oligohaline region of Chesapeake Bay.

Stations for these experiments were randomly selected at the freshwater end-member, ETM surface, ETM bottom, and seawater end-member in April, May, and October of 2008. The same sampling, incubation, and oxygen measurement procedures as those described above for determining community respiration were used for testing the linearity of oxygen decrease. A set of triplicate 60 ml BOD bottles were fixed at the beginning (0 h) and every 6 h over a 24 hr period (6, 12, 18, and 24 h). Linear regression analysis was used to estimate the coefficient of determination of each experiment.

The mean of coefficients of determination in the ETM was 0.92, in contrast to $r^2 = 0.97$ in all other areas (Fig. AI.1). The lower coefficient of determination in the ETM may have been caused by the heterogeneous distribution of heterotrophic organisms between triplicates or TSS inhibition of photometric titration sensor. In general, however, constant decreases of oxygen concentration over 24 h were observed in these experiments.

Figure

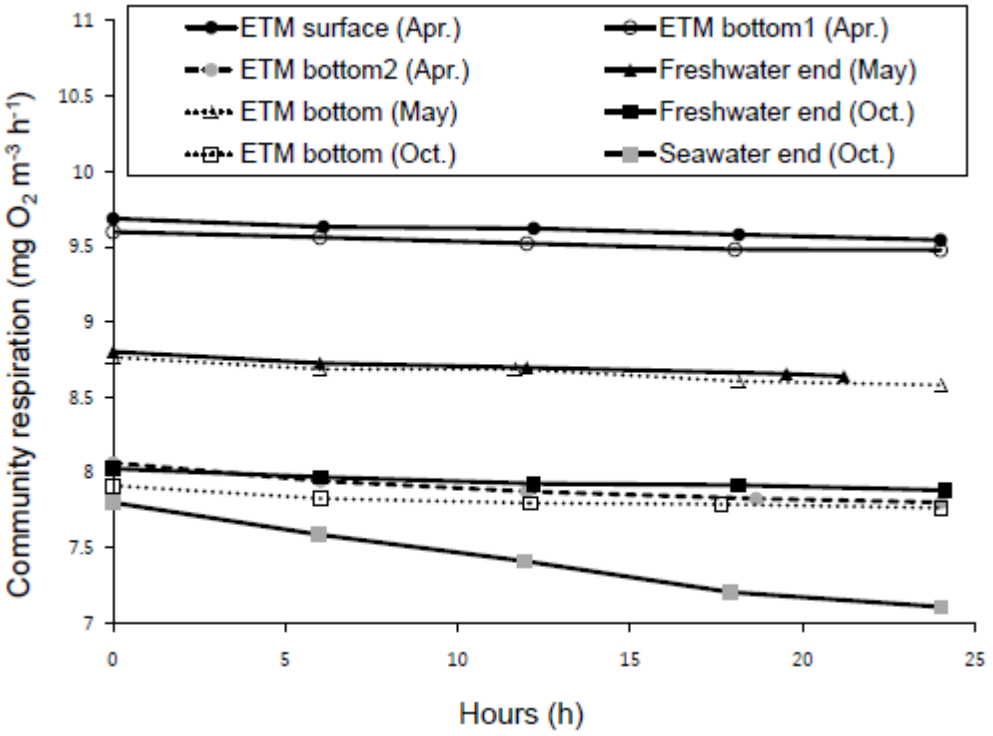

Figure AI.1: Linear respiration experiment for 24 h in different months and locations to test the linearity of respiration. The mean of coefficients of determination in the ETM resulted in $r^2 = 0.92$, in contrast to $r^2 = 0.97$ in all other areas excluding ETM results.

Appendix II: Net biological and physical production of phytoplankton pigments in the upper Chesapeake Bay: a box-modeling analysis

Introduction

Phytoplankton biomass and primary production are important sources of organic matter for secondary production and highly controlled by physical forces in the oligohaline Chesapeake Bay. Year-to-year variations in water properties, primary production, and secondary production are tightly coupled to the variation of the Susquehanna River discharge (Schubel & Pritchard 1986, Boynton & Kemp 2000). The coupled relationship suggests that there are direct influences of physical mechanisms on the concentration of phytoplankton in the Bay.

Phytoplankton biomass, which is derived either from internal growth or physical transports, can be used in combination with salt- and water-balance computations (box-modeling analysis), to estimate the relative contributions of phytoplankton growth and transport in the oligohaline Chesapeake Bay. In this Appendix II, a set of linear equations based on the conservation of water volume and salt mass is used to calculate net production (or consumption) of phytoplankton pigments in terms of carbon. Although it only generates net rates of biomass, it provides useful insights into prevailing forces (i.e., biology versus physics) that control phytoplankton pigment concentrations in a specific area. The purpose of this

modeling effort is to quantify the net flux of carbon biomass in different regions of the oligohaline Chesapeake Bay and to compare these fluxes with community metabolism estimated by measuring oxygen changes.

Methods

The oligohaline region of Chesapeake Bay is longitudinally separated into three regions representing the upstream of estuarine turbidity maximum (ETM), the ETM, and the downstream of the ETM. From the Susquehanna River mouth, the three regions are named Box1, Box2, and Box3, respectively, and they are located from 12 to 25, 26 to 42, and 43 to 74 river-km, respectively, along the main shipping channel of Chesapeake Bay. Box2 and Box3 are additionally separated into surface (Box2S & Box3S) and bottom layers (Box2B & Box3B) by the pycnocline, which is assumed to be 7 m based on the average depth of the pycnocline during our axial surveys. Box1 has only a surface layer because the water column is shallow and vertically well-mixed in this region (Fig. AII. 1). Cronin and Pritchard (1975) reported volumes and areas of the Chesapeake Bay segments every 5-nautical miles longitudinally and volumes and areas of each box are reported in Table AII. 1.

The average salinities of the surface and bottom layers were obtained from the average of axial CTD surveys over the box depths which were measured in February 22 & 26, April 9 & 15, and May 8 & 14, 2007 (Table AII. 2). Susquehanna River discharge, which was assumed to be the only source of freshwater into the upper Chesapeake Bay, was obtained from the United States Geological Survey station at Conowingo Dam, Maryland. A backward average method was used to calculate daily

river discharges to account for the diminishing effect of past discharge variations by 5 % decline per day from present day over the past 20 days. The backward average takes long-term effects of river discharge into the consideration.

The box-modeling computes advective and non-advective (diffusive) exchanges of water and salt between boxes. The salt and water balances for surface (Eqs. 1 & 2, respectively) and bottom layers (Eqs. 3 & 4, respectively) are calculated from following equations:

$$V_m \frac{ds_m}{dt} = Q_{m-1}s_{m-1} + Q_{vm}s'_m - Q_m s_m + E_{vm}(s'_m - s_m) + E_{m-1,m}(s_{m-1} - s_m) + E_{m,m+1}(s_{m+1} - s_m) \quad (1)$$

$$Q_m = Q_{m-1} + Q_{vm} + Q_{fm} \quad (2)$$

$$V'_m \frac{ds'_m}{dt} = Q'_{m+1}s'_{m+1} - Q_{vm}s'_m - Q'_m s'_m - E_{vm}(s'_m - s_m) \quad (3)$$

$$Q'_m = Q'_{m+1} - Q_{vm} \quad (4)$$

where the terms are defined as follows: V_m = volume of the surface box; V'_m = volume of the bottom box; Q_m = advective surface transport to downstream; Q_{m-1} = advective surface transport from upstream; Q'_{m+1} = advective bottom transport from downstream; Q_{vm} = vertical advective transport; Q_{fm} = freshwater input; $E_{m-1,m}$ and

$E_{m,m+1}$ = horizontal non-advective exchange; E_{vm} = vertical non-advective exchange; s_m = salinity of surface layer; s'_m = salinity of bottom layer (see Hagy et al. (2000) for details).

Net biological production (or consumption) of non-conservative materials, phytoplankton pigments (c), in the surface (P_m) and bottom layer (P'_m) is calculated by modifying the Eqs. (1) and (2) with the addition of P_m (Eqs. 5) or P'_m (Eqs. 6) terms. Also, the salinity terms are replaced with the concentration of non-conservative material (c) which is phytoplankton pigments in terms of carbon in this study:

$$V_m \frac{dc_m}{dt} = Q_{m-1}c_{m-1} + Q_{vm}c'_m - Q_m c_m + E_{vm}(c'_m - c_m) + E_{m-1,m}(c_{m-1} - c_m) + E_{m,m+1}(c_{m+1} - c_m) + P_m \quad (5)$$

$$V'_m \frac{dc'_m}{dt} = Q'_{m+1}\, c'_{m+1} - Q_{vm}c'_m - Q'_m\, c'_m - E_{vm}(c'_m - c_m) + P'_m \quad (6)$$

Phytoplankton pigments including chlorophyll-a (Chl-a), peridinin, and fucoxanthin were measured during the same CTD casts that were used for measuring salinity. The method for the pigment analysis can be found in the methods section of Chapter 1. The year 2007 had moderate concentrations of pigments although the distribution of the diatom indicating pigment, fucoxanthin, was different from the distribution in 2008 when riverine diatom concentrations were high upstream. It is assumed that the ratios converting phytoplankton pigments (e.g., Chl-a, peridinin, and

fucoxanthin) to carbon are fixed numbers even though they vary as a function of light, temperature, nutrient-limited growth rate and community composition (Cloern et al. 1995). A Chl-a:C ratio of 0.02 was used, and we assumed the same ratio for peridinin and fucoxanthin to carbon. This is the calculated mean value in San Francisco Bay, which has been applied in other systems (Wienke & Cloern 1987, Vincent et al. 1996). Note that only Chl-a production (or consumption) is reported for Box1 because the box-modeling analysis requires pigment concentrations (c) up-estuary of Box1. The up-estuary Chl-a data were obtained from Chesapeake Bay Program station CB1.1 near Conowingo Dam but the other pigment concentrations were not available from this station. To calculate net production of Chl-a in Box3S and Box 3B, Chl-a data obtained from CB4.1 located below the Chesapeake Bay Bridge were used but, again, the other pigment concentrations were not available from this station. Therefore, to calculate net production of the dinoflagellates and diatoms, one data point from the most downstream station in Box3S and Box3B was excluded and used as the concentration just below the Box3 area.

Results and Discussion

We computed net production (or consumption) of Chl-a, peridinin, and fucoxanthin and the outputs are separated into three categories: 1) Net biological production due to biological effects like photosynthesis, grazing, reproduction, and death of organisms, 2) Net physical production due to the effects of vertical and horizontal advection, and non-advective exchange, and 3) Net total production ($V_m * dc_m / dt$ or $V'_m * dc'_m / dt$), which is the sum of biological and physical production.

Net total production of pigments varies in spatiotemporal scale, and large variations are observed in the net rate of Chl-a and peridinin production. In contrast, net production is relatively constant for fucoxanthin. A much stronger correlation was observed between Chl-a and peridinin ($r = 0.90$, $p < 0.001$, $n=180$) compared to Chl-a and fucoxanthin ($r = 0.30$, $p < 0.001$, $n=180$; Table 2 in Chapter 1). As a result, the variations of net total production were very similar between Chl-a and peridinin.

Chlorophyll-a

The model-calculated net biological production of Chl-a was 863, -268, and -61 and the net physical production was -311, 85, and 117 mg C m^{-2} d^{-1}, in late-winter, early-spring, and late-spring, respectively (Table AII. 3). The high net biological production in late-winter is attributed to the high net primary production rate in Box3B which was 2,159 mg C m^{-2} d^{-1}. Because surface irradiance does not penetrate into the bottom layer (Box2B & Box3B) the high biological production in the bottom layer must be largely derived from phagotrophic phytoplankton, i.e., mixotrophic dinoflagellates as discussed in Chapter 1. Also in late-winter, weakly stratified condition was observed during the field survey, which would cause less efficient trapping in Box2B where the ETM was found. In the model output, landward advection of Chl-a along with the seawater intrusion ($Q'_{m+1}c'_{m+1}$) was very strong in Box2B and Box3B but the vertical advection ($Qv_mc'_m$) to Box2S and Box3S were even stronger, suggesting a strong mixing mechanism between two layers. Thus, it resulted in net physical loss of Chl-a from the bottom to surface layer, i.e., -108 mg C m^{-2} d^{-1} in Box2B and -1,514 mg C m^{-2} d^{-1} in Box3B. Thus, weak stratification was

observed in the ETM and this resulted in a higher vertical flux of Chl-a than horizontal flux in the bottom layer.

Dramatic changes of net biological and physical production were computed in early-spring. This is the season of highest river discharge causing sharp salinity gradients and highest concentration of suspended sediment in the ETM (Sanford 2001; Fig. 3 in Chapter 1). Vertical advection of Chl-a was noticeably decreased in Box2B (837 mg C m^{-2} d^{-1}) in early-spring compared to 2,515 mg C m^{-2} d^{-1} in late-winter, very likely, due to the strong stratification. The decreased vertical advection and increased river discharge caused net physical loss of Chl-a in Box3S (-449 mg C m^{-2} d^{-1}). However, net physical production of Chl-a (818 mg C m^{-2} d^{-1}) was computed for Box2B. This net physical production is attributable to both increasing landward advection in the bottom layer and strong particle trapping mechanism as the salinity gradient became stronger. In contrast, a large net biological consumption was computed in Box2B and Box3B (average of -896 mg C m^{-2} d^{-1}). It agrees with field measurement suggesting that this season had the lowest pigments concentration among the three seasons (Fig. 9 &13 in Chapter 1). As discussed in Chapter 1, rapid salinity changes in the ETM region may impose physiological stress on phytoplankton and the loss of pigment in the region. However, Box2 and Box3 are also regions where mesozooplankton and fish larvae abundance is high in early-spring (Roman et al. 2001, North & Houde 2003). Therefore, besides physiological stress, grazing losses may contribute to the large losses of Chl-a.

Late-spring was the season of highest community metabolism including primary production and community respiration (Fig. 5 & 6 in Chapter 1). Net primary

production (NPP) estimated by measuring oxygen changes in surface samples was 477, 48, and 747 mg C m^{-2} d^{-1} in late-winter, early-spring, and late-spring, respectively. The first two NPP values are comparable to the average net biological production derived from the box model, which were 520 and 151 mg C m^{-2} d^{-1} in late-winter and early-spring, respectively. However, in late spring the measured NPP (747 mg C m^{-2} d^{-1}) was much higher than net biological production computed with the box-model (193 mg C m^{-2} d^{-1}). This discrepancy is likely due to the fact that carbon fluxes mediated by non-pigmented organisms are not accounted for in the box-modeling. These discrepancies will be particularly large when community metabolism is high.

Dinoflagellates

As discussed in Chapter 1, we observed high abundances of two dinoflagellate species in the oligohaline Chesapeake Bay in winter and spring: *Heterocapsa rotundatum* and *Prorocentrum minimum*. These are mixotrophic species that are transported into this region from either down-estuary or from the tributaries of Chesapeake Bay (Tyler & Seliger 1978, Jeong et al. 2005). The dinoflagellates ride the net landward bottom water flow which transports them into the zone of high nutrients and organic matter in the downstream oligohaline region.

In the bottom layer, a net positive biological production was computed only in late-winter (1,235 mg C m^{-2} d^{-1}) which must be caused by heterotrophic growth in these mixotrophic dinoflagellates (Table AII. 4). In contrast, net biological consumption was computed in both the surface and bottom layers in early-spring

which may have been caused by high grazing losses on dinoflagellates from mesozooplankton. In late-spring, net biological production was positive in the surface layer (108 mg C m^{-2} d^{-1}) but was negative in the bottom layer (-277 mg C m^{-2} d^{-1}). This may also have been due to the grazing impacts of mesozooplankton. In contrast, very high primary production in the surface layer would cause net biological production.

Net physical production or consumption in the bottom layer was mainly controlled by the magnitude of vertical advection. Although there was a high landward advection of peridinin in late-winter, higher vertical advection canceled out the effect of the landward input and resulted in net physical consumption (-881 mg C m^{-2} d^{-1}) in the bottom layer. In contrast, dampened vertical advection due to stratification resulted in net physical production in early-spring (108 mg C m^{-2} d^{-1}) and late-spring (265 mg C m^{-2} d^{-1}) in the bottom.

Diatoms

Compared to the net changes of Chl-a and dinoflagellates, the production (or consumption) of diatoms was less significant which is consistent with the low pigment concentrations (Fig. 13 in Chapter 1). However, a high net biological consumption was computed for diatoms (-635 mg C m^{-2} d^{-1}) in late-winter in the bottom layer (Table AII. 5). This was not observed with dinoflagellates. This suggests that the contribution of diatoms to the organic pool of ETM region could be more important than dinoflagellates in winter.

Physiological stress caused by rapid salinity changes is hypothesized to be the primary cause of diatom disappearance in the ETM region. Net biological consumption of fucoxanthin was -29 mg C m^{-2} d^{-1} in the Box2S and -61 mg C m^{-2} d^{-1} in the Box2B in late-winter. However, no more net biological consumption was observed in early- and late-spring in the same boxes. In fact, low diatom concentrations were observed upstream in early- and late-spring 2007 and thus diatoms seemed to originate mainly from downstream in 2007. Presumably, marine diatoms derived from downstream of the ETM where high concentrations of zooplankton are found can be grazed prior to reaching the ETM region. In contrast, the mortality of riverine diatoms may be more influenced by salinity changes. Regardless, net biological production in the surface layer appears to be caused by photosynthesis in spring.

Net physical transport of diatoms is less pronounced than Chl-a and dinoflagellates except in late-winter when a net physical import of diatoms is computed in the bottom layer (714 mg C m^{-2} d^{-1}). This high supply of organic matter along with net biological consumption could be an important source of organic matter for fueling heterotrophic processes in winter.

Conclusion

The purpose of this analysis is to examine and compare biological and physical production (or consumption) of phytoplankton carbon sources. In general, the box-model analysis succeeds in capturing the main physical transports in the oligohaline Chesapeake Bay. For instance, the model predicts restricted vertical

advection when river discharge is high in Box2B in early-spring. Also, increased trapping efficiency resulted in net physical production of phytoplankton in the ETM region.

The box model results suggest that in late-winter a high biomass of dinoflagellates was advected into the bottom layer downstream of the ETM. These dinoflagellates appear to have depended heavily upon phagotrophic production, and they were also advected vertically into the surface layer. Diatoms were also advected into the bottom layer where they appear to have been heavily consumed and may therefore have provided organic matter for heterotrophs. These results have several important implications for food web dynamics in ETM region. Mesozooplankton grazing is relatively weak in late-winter compared to late-spring. Therefore, in late-winter phytoplankton biomass, and specifically mixotrophic dinoflagellates, may accumulate and produce organic matter by both heterotrophic and autotrophic mechanisms in the bottom and surface layers, respectively. Furthermore, detritus from phytoplankton may enhance the quality of organic matter in the region. In early- and late-spring, intense grazing by mesozooplankton on phytoplankton appears to be an important cause of net biological consumption. Continuous physical advection of dinoflagellates into the bottom layer where turbidity is highest may help dinoflagellates consume microbes by enhancing encountering rate between the prey and predator, and also provide dinoflagellate prey for mesozooplankton (MacKenzie & Leggett 1991). Also, higher surface irradiance and warmer temperatures in spring should enhance phytoplankton photosynthesis and the production of organic matter available for secondary producers.

In conclusion, the box-modeling analysis provides quantitative estimates of net biological and physical production and loss of phytoplankton pigments in the ETM region, which is a zone of dynamic bio-physical interactions. These results compliment and contribute to the community metabolism studies described in Chapter 1 providing, in particular, quantitative information on physical influences that help advance understanding of the mechanisms driving the high secondary production in the ETM region.

Tables

Box Volumes (m^3)

	Box 1	Box 2	Box 3
Surface	3.18×10^8	5.15×10^8	1.71×10^9
Bottom		5.44×10^7	6.48×10^8

Box Areas (m^2)

	Box 1	Box 2	Box 3
Surface	8.36×10^7	1.34×10^8	3.55×10^8
Bottom		3.32×10^7	6.29×10^7

Table AII.1: The volume and area of five simulated boxes. Cronin & Pritchard (1975) reported the values of the entire Chesapeake Bay by 5-nautical mile along the shipping channel of the Bay. The volumes in this table include shallow regions. The area is the surface area of each box.

Surface Layer					
	Box1	Box2S	Box3S	OceanS	Discharge
2/22/2007	0.6	3.9	9.3	10.3	237
2/25/2007	1.1	5.4	9.7	11.5	
2/26/2007	1.7	5.3	10.2	11.7	
4/9/2007	0	0.8	4.2	5.6	1,425
4/12/2007	1.2	3.8	6.7	8.5	
4/15/2007	0.1	2.9	6.5	7.1	
5/8/2007	0.9	2.5	6	7.5	969
5/11/2007	1.1	3.4	7.6	7.6	
5/14/2007	0.2	3.2	7.4	9	

Bottom layer				
	Box1	Box2B	Box3B	OceanB
2/22/2007	.	5.6	10.9	12.4
2/25/2007	.	7.4	13.2	12.8
2/26/2007	.	9	13.3	13.9
4/9/2007	.	7.4	13.3	14.4
4/12/2007	.	7.1	13.4	15.5
4/15/2007	.	6.7	13.5	13.5
5/8/2007	.	12	15.6	16
5/11/2007	.	9.8	13.9	16.9
5/14/2007	.	7.8	15.3	13.1

Table AII.2: The mean of salinity (unit: PSU) at surface and bottom layer is calculated using CTD data measured during research cruises in February 22 & 26, April 9 & 15, and May 8 & 14, 2007. River discharges (unit: $m^3 s^{-1}$) at the Susquehanna River mouth are obtained from USGS station at Conowingo Dam (http://waterdata.usgs.gov/md/nwis/dv/?site_no=01578310&PARAmeter_cd=00060,00065), and the 20-d backward average is calculated to account for flushing rate of river discharge.

Late-winter Chlorophyll-a

	Box1	Box2S	Box3S	Average	Total Average
Total	323	1326	-23	542	551
Net biology	430	1230	-100	520	863
Net physics	-108	96	77	22	-311
		Box2B	Box3B	Average	
Total	na	486	645	565	
Net biology	na	594	2159	1376	
Net physics	na	-108	-1514	-811	

Early-spring Chlorophyll-a

	Box1	Box2S	Box3S	Average	Total Average
Total	38	65	-44	20	-183
Net biology	12	35	406	151	-268
Net physics	25	31	-449	-131	85
		Box2B	Box3B	Average	
Total	na	10	-984	-487	
Net biology	na	-808	-984	-896	
Net physics	na	818	0	409	

Late-spring Chlorophyll-a

	Box1	Box2S	Box3S	Average	Total Average
Total	18	279	50	116	56
Net biology	-221	460	339	193	-61
Net physics	239	-181	-290	-77	117
		Box2B	Box3B	Average	
Total	na	75	-142	-34	
Net biology	na	-284	-597	-441	
Net physics	na	359	456	407	

Table AII.3: Net production results of chlorophyll-a (unit: mg C m^{-2} d^{-1}) are reported in late-winter, early-spring, and late-spring.

Late-winter Peridinin

	Box1	Box2S	Box3S	Average	Total Average
Total	na	627	21	324	339
Net biology	na	570	-3	283	759
Net physics	na	58	25	41	-420
		Box2B	Box3B	Average	
Total	na	247	461	354	
Net biology	na	318	2151	1235	
Net physics	na	-71	-1690	-881	

Early-spring Peridinin

	Box1	Box2S	Box3S	Average	Total Average
Total	na	-11	-184	-98	-182
Net biology	na	-24	-96	-60	-217
Net physics	na	13	-88	-38	35
		Box2B	Box3B	Average	
Total	na	-14	-520	-267	
Net biology	na	-365	-384	-375	
Net physics	na	351	-136	108	

Late-spring Peridinin

	Box1	Box2S	Box3S	Average	Total Average
Total	na	46	-7	19	4
Net biology	na	94	122	108	-84
Net physics	na	-48	-130	-89	88
		Box2B	Box3B	Average	
Total	na	13	-36	-11	
Net biology	na	-171	-383	-277	
Net physics	na	184	347	265	

Table AII.4: Net production results of dinoflagellates indicating pigment, peridinin (unit: mg C m^{-2} d^{-1}) are reported in late-winter, early-spring, and late-spring.

Late-winter Fucoxanthin

	Box1	Box2S	Box3S	Average	Total Average
Total	na	-39	44	2	41
Net biology	na	-29	19	-5	-320
Net physics	na	-10	24	7	361
		Box2B	Box3B	Average	
Total	na	-16	174	79	
Net biology	na	-61	-1208	-635	
Net physics	na	46	1382	714	

Early-spring Fucoxanthin

	Box1	Box2S	Box3S	Average	Total Average
Total	na	22	117	69	59
Net biology	na	13	176	94	33
Net physics	na	8	-59	-25	26
		Box2B	Box3B	Average	
Total	na	8	90	49	
Net biology	na	25	-81	-28	
Net physics	na	-17	171	77	

Late-spring Fucoxanthin

	Box1	Box2S	Box3S	Average	Total Average
Total	na	54	69	61	41
Net biology	na	78	77	77	45
Net physics	na	-24	-8	-16	-5
		Box2B	Box3B	Average	
Total	na	10	31	20	
Net biology	na	7	19	13	
Net physics	na	3	11	7	

Table AII.5: Net production results of diatom indicating pigment, fucoxanthin (unit: mg C m^{-2} d^{-1}) are reported in late-winter, early-spring, and late-spring.

Figure

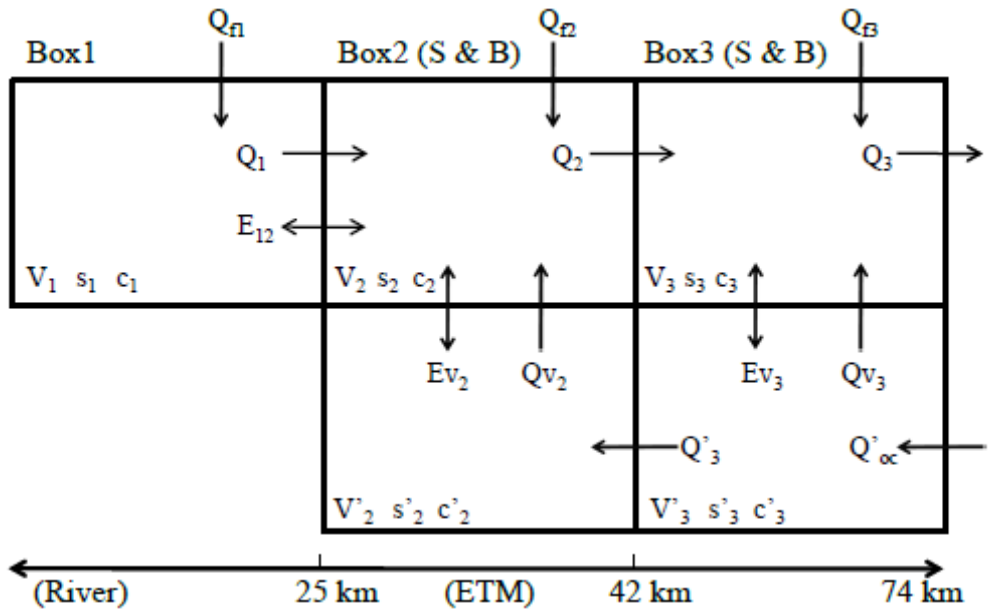

Figure AII.1: Schematic diagram of the box-model structure. The oligohaline region of Chesapeake Bay has longitudinally separated into three regions representing the upstream, ETM, and downstream. From the Susquehanna River mouth, the three regions are named as Box1, Box2, and Box3 and locate from 12 to 25, 26 to 42, and 43 to 74 river-km, respectively, along the main shipping channel of Chesapeake Bay. Box2 and Box3 are additionally separated into surface (e.g., Box2S & Box3S) and bottom layers (e.g., Box2B & Box3B) by pycnocline depth which is assumed to be 7 m. Box1 has only surface layer because water column is shallow and vertically well-mixed. The definitions of terms are defined as follows: V_m = volume of the surface box; V'_m = volume of the bottom box; Q_m = advective surface transport to the downstream; Q_{m-1} = advective surface transport from the upstream; Q'_{m+1} = advective bottom transport from the downstream; Q_{vm} = vertical advective transport; Q_{fm} = freshwater input; $E_{m-1,m}$ and $E_{m,m+1}$ = horizontal non-advective exchange; E_{vm} = vertical non-advective exchange; s_m = salinity of surface layer; s'_m = salinity of bottom layer.

Appendix III: Simulating food web dynamics using a mass-balanced STELLA model

Introduction

Estuarine secondary production in the oligohaline Chesapeake Bay has been estimated by measuring the abundance of copepods and fish larvae, and it has been shown that this region has higher levels of productivity than that of the meso- and polyhaline regions (Roman et al. 2001, North & Houde 2003). The estuarine turbidity maximum (ETM) area, where copepods and fish larvae are most abundant, contains the highest concentrations of total suspended sediment (TSS) in Chesapeake Bay, which limits light penetration and primary production (Fisher et al. 1999). Surprisingly, direct measurements show that respiration rates are low in the ETM despite the high concentrations of copepods, fish larvae, TSS and organic matter loading (Chapter 1 of this thesis). Rather, secondary production and respiration increase dramatically downstream of the ETM region.

This raises an important question: what controls secondary production in the oligohaline region of Chesapeake Bay, i.e., where does the labile organic matter come from? High concentrations of TSS found in the oligohaline Chesapeake Bay are often composed of aggregates of organic matter, bacteria, and clay-like sediment that can be consumed by mesozooplankton (Boak & Goulder 1983). Although the nutritional value of the aggregates is strongly dependent of the fraction of organic matter and bacteria abundance, mesozooplankton food selection experiments support the

possibility that aggregates are important food sources for supporting secondary production (David et al. 2006). Another possible explanation is that secondary production could be driven by high concentrations of mixotrophic dinoflagellates (Chapter 1 of this thesis). Mixotrophic dinoflagellates can switch between autotrophic and heterotrophic modes of nutrition (Stoecker et al. 1997), i.e., they not only graze on microbes, which are abundant in the oligohaline area, but also produce labile organic matter photosynthetically.

The purpose of the model described in this appendix is to simulate the estuarine food web dynamics and community metabolism in the oligohaline Chesapeake Bay to determine where the labile organic matter comes from that fuels secondary production. Community metabolism, including autotrophic production and community respiration, were measured using the oxygen technique (Chapter 1 of this thesis). This model provides insight into the potential contribution of each component of the ecosystem to the community metabolism. The model can also be used to quantify energy flow (i.e., primary production, prey-predator interactions, sinking) between compartments of the pelagic ecosystem.

Model description

The model is a simple NPZD (nutrient – phytoplankton – zooplankton - detritus) formulation with the addition of mixotrophic dinoflagellates that was coded using STELLA (High Performance Systems, Inc.) software (Fig. AIII. 1). The modeling effort was focused on simulating the period of high river discharge and secondary production, i.e., from late winter to late spring. Although low phosphorus

is known to limit primary production in this region (Fisher et al. 1992), we have assumed in this simple modeling exercise that none of nutrients limit the growth of phytoplankton and mixotrophic dinoflagellates in order to maximize primary and secondary production.

Three spatial domains within the oligohaline region were used to simulate the estuarine food web: upstream of the ETM, the ETM region, and downstream of the ETM region. From the Susquehanna River mouth, the three regions are located from 12 to 25, 26 to 42, and 43 to 74 river-km, respectively, along the main shipping channel of Chesapeake Bay. Major differences between three domains are, first, the presence or absence of mixotrophic dinoflagellates. The dinoflagellate indicating pigment, peridinin, was very low in the ETM and disappeared upstream (Fig. 13 in Chapter 1). This was in contrast to very high subsurface concentrations of peridinin downstream all the time. In this model, therefore, we assumed that mixotrophic dinoflagellates are only present downstream of the ETM. Secondly, average light levels (I_{ave}) in a mixed layer were assumed to be different in the three regions (Fig. 4 in Chapter 1). Light levels were calculated using the following procedure. The Chesapeake Bay Program (www.chesapeakebay.net) has been monitoring water quality data including the depth of pycnocline and light attenuation coefficient (k_d) at stations CB2.1, CB3.1, and CB3.3C, respectively, representing the upstream, ETM, and downstream regions. The monthly averages of long-term k_d and depths of the mixed layer (i.e., above pycnocline) measured from 1990 to 2006 were input into the following equation to calculate average irradiance levels over the mixed layers (Stickney et al. 2000):

$$I_{ave} = (\int I_0 \times e^{-kd*Z} dz) / Z$$

where I_0 is monthly average of surface irradiance obtained from Fisher et al. (2003) and Z is the depth above pycnocline. Linear interpolation was used between monthly average light levels to provide continuous time. Water temperature was obtained from a NOAA weather monitoring station at Tolchester Beach, Maryland (www.tidesandcurrents.noaa.gov). All model parameters used in the main-run solution are provided in Table AIII. 1.

Since nutrients were assumed to not limit primary production, carbon (μM C) was used as the model currency. To make the carbon biomass of phytoplankton and dinoflagellates comparable to the actual chlorophyll-a measurements (μg l^{-1}), a Chlorophyll-a to carbon ratio (Chla:C) of 0.02 was used as a conversion factor (Cloern et al. 1995). Also, we used a photosynthetic quotient of 10/12 (moles of CO_2 assimilated : moles of O_2 produced) to convert community metabolism from carbon to oxygen unit (Smith & Kemp 1995).

Phytoplankton (P)

Observations during winter-spring cruises in 2007 and 2008 confirmed that there were two major phytoplankton groups: diatoms and dinoflagellates. Since we have a separate mixotrophic dinoflagellates compartment (M), the phytoplankton compartment (P) represents diatoms, cryptophytes, and all small autotrophic organisms other than mixotrophic dinoflagellates. Despite the lower concentrations of

diatoms and cryptophytes compared to dinoflagellates, we consistently measured these two pigments at all stations, and so "phytoplankton" is assumed to exist in all three regions. In this model, the growth of phytoplankton is controlled by light and temperature but not by nutrients. Although low phosphorus concentrations were observed in our measurements (Crump et al. in preparation), these low concentrations prevailed over the entire oligohaline region. Therefore, any phosphorus limitation should not cause any spatial variations in phytoplankton production and the model is much simpler without considering this potential limitation. Phytoplankton production and biomass are consumed by several processes, such as phytoplankton senescence, and zooplankton and dinoflagellate grazing. The following equations summarize phytoplankton production and consumption processes:

$$dP / dt = production_p - senescence_p - grazing_{zp} - grazing_{mp} \quad (1)$$

where

$$production_p = \text{temperature- and light-dependent phytoplankton production}$$
$$= (U_p * (1.066^{temp})) * (1 - e^{-I / Ik}) * \text{phytoplankton} \quad (2)$$

$$senescence_p = \text{senescence of phytoplankton}$$
$$= S * \text{phytoplankton}^2 \quad (3)$$

$$grazing_{zp} = \text{zooplankton grazing on phytoplankton}$$
$$= (G_z * \text{zooplankton} * PF_{zp} * \text{phytoplankton}) / Q_z$$

(4)

Q_z = zooplankton grazing partition

= $(PF_{zp} * \text{phytoplankton}) + (PF_{zm} * \text{dinoflagellate}) + (PF_{zpoc} * \text{POC})$

$+ (PF_{zz} * \text{zooplankton}) + ZK_s$

(5)

grazing_{mp} = grazing of dinoflagellates on phytoplankton

= $(G_{rm} * \text{dinoflagellate} * PF_{mp} * \text{phytoplankton}) / Q_m$

(6)

G_{rm} = realized maximum grazing of dinoflagellate

=If $(U_m * (1.066^{temp}) / AE_{mp}) * (1 - e^{-I / Ik}) > G_m$

Then G_m

Else $(U_m * (1.066^{temp}) / AE_{mp}) * (1 - e^{-I / Ik})$

(7)

Q_m = dinoflagellate grazing partition

= $(PF_{mp} * \text{phytoplankton}) + (PF_{mm} * \text{dinoflagellate}) + (PF_{mpoc} *$

$\text{POC}) + MK_s$

(8)

Zooplankton (Z)

Estuarine copepods are assumed to be one of the major predators consuming phytoplankton, dinoflagellates, particulate organic matter (POC), and other zooplankton and they provide the energy link to larval fish. In the following equations, zooplankton have grazing effects on all compartments. Loss terms for zooplankton

are self-predation and mortality. The following equations summarize zooplankton processes:

$$\begin{aligned} dZ / dt &= \text{grazing on phytoplankton, dinoflagellates, and POC + predation – zooplankton mortality – zooplankton respiration} \\ &= GE_{zp} * grazing_{zp} + GE_{zm} * grazing_{zm} + GE_{zpoc} * grazing_{zpoc} + GE_{zz} * predation_z - predation_z - mortality_z - respiration_z \end{aligned} \quad (9)$$

where

$$\begin{aligned} grazing_{zm} &= \text{grazing of zooplankton on dinoflagellate} \\ &= (G_z * zooplankton * PF_{zm} * dinoflagellate) / Q_z \end{aligned} \quad (10)$$

$$\begin{aligned} grazing_{zpoc} &= \text{grazing of zooplankton on POC} \\ &= (G_z * zooplankton * PF_{zpoc} * POC) / Q_z \end{aligned} \quad (11)$$

$$\begin{aligned} predation_z &= \text{predation of zooplankton on zooplankton} \\ &= (G_z * zooplankton * PF_{zz} * zooplankton) / Q_z \end{aligned} \quad (12)$$

$$\begin{aligned} mortality_z &= \text{mortality of zooplankton} \\ &= P_z * zooplankton^2 \end{aligned} \quad (13)$$

$$respiratoin_z = Zoo_R * zooplankton \quad (14)$$

Mixotrophic dinoflagellate (M)

Mixotrophic dinoflagellates have been categorized into three different feeding types (Stoecker 1997 & 1998). Here we use a "Type II" mixotrophic dinoflagellate formulation (Stoecker 1997 & 1998) which is primarily autotrophic but ingests microbes or small phytoplankton to supplement nutrients for achieving the maximum photosynthetic rate. However, in this model, nutrients are not limiting so that dinoflagellate grazing is dependent only on light availability. Since the phagotrophic function of the dinoflagellate is for supplementing autotrophic nutrition, the realized grazing rate (G_{rm}) should not exceed the maximum grazing rate (G_m) of the dinoflagellate (Eq. 7; see Stickney et al. (2000) for details). *Prorocentrum minimum* and *Heterocapsa rotundatum* were observed downstream oligohaline region in 2007 and 2008 (Keller et al. in preparation) and these species are found to supplement inorganic nutrients by grazing (Stoecker 1997, Jeong et al. 2005). The maximum phototrophic growth rate (U_m) and the maximum grazing rate (G_m) of dinoflagellates in this study are based on literature values (Stickney et al. 2000). Although dinoflagellates may not ingest POC directly due to size restrictions, we assume in this model that the POC compartment carries both particle-attached and free-living bacteria and that these are readily available for dinoflagellate ingestion.

dM / dt = dinoflagellate primary production + grazing on phytoplankton and bacteria – grazed by zooplankton – dinoflagellate mortality - dinoflagellate respiration

$$= \text{production}_m + AE_{mp} * \text{grazing}_{mp} + AE_{mpoc} * \text{grazing}_{mpoc} - \text{grazing}_{zm} - \text{mortality}_m - \text{respiration}_m \quad (15)$$

where

production_m = temperature- and light-dependent dinoflagellate production

$$= (U_m * (1.066^{temp})) * (1 - e^{-I / Ik}) * \text{dinoflagellate} \quad (16)$$

$$\text{grazing}_{mpoc} = (G_{rm} * \text{dinoflagellate} * PF_{mpoc} * POC) / Q_m \quad (17)$$

$$\text{mortality}_m = P_m * \text{dinoflagellate}^2 \quad (18)$$

$$\text{respiratoin}_m = Mixo_R * \text{dinoflagellate} \quad (19)$$

Particulate organic carbon (POC) & dissolved inorganic carbon (DIC)

POC is detrital organic matter that also include attached bacteria and are the aggregates of clay-like sediment, degraded plankton, zooplankton excretion, and terrestrial organic carbon. POC is consumed by heterotrophs and respired through bacteria respiration (remineralization rate) in the model. Although bacterial processes are not separately computed, these are incorporated into the POC compartment and they are assumed to mediate detrital remineralization into the DIC compartment. Meanwhile, carbon uptake by autotrophic organisms such as phytoplankton and

dinoflagellates cause the removal of DIC from the estuarine carbon pool but inorganic carbon is not a limiting factor controlling primary production in the model.

$$\frac{dPOC}{dt} = (1 - AE_{zp}) * grazing_{zp} + (1 - AE_{zm}) * grazing_{zm} + (1 - AE_{zz}) * predation_z + (1 - AE_{mp}) * grazing_{mp} + (1 - AE_{mpoc}) * grazing_{mpoc} + (S * phytoplankton^2 * B) + P_z * zooplankton^2 + P_m * dinoflagellate^2 - AE_{zpoc} * grazing_{zpoc} - grazing_{mpoc} - Bact_R * POC \quad (20)$$

$$\frac{dDIC}{dt} = (AE_{zp} - GE_{zp}) * grazing_{zp} + (AE_{zpoc} - GE_{zpoc}) * grazing_{zpoc} + (AE_{zz} - GE_{zz}) * predation_z + (AE_{zm} - GE_{zm}) * grazing_{zm} + (S * phytoplankton^2 * (1 - B)) + Mixo_R * dinoflagellate + Zoo_R * zooplankton + Bact_R * POC - production_p - production_m \quad (21)$$

Results and discussion

The model was run for 150 d (from January to May) upstream, in the ETM, and downstream to compare with primary production and community respiration estimated by measuring oxygen changes. Changes in the light intensity in the water column (calculated as discussed above) incorporates the effects of suspended sediment and other forms of organic matter and they are similar to the changes in euphotic depth that were measured during field studies, i.e., euphotic depth was deeper downstream of the ETM. Light levels gradually increase from January to May in all three regions due, in part, to increasing light at the surface (Fig. AIII. 2).

Phytoplankton biomass, excluding mixotrophic dinoflagellates, increased from the end of April upstream and in the ETM region (Fig. AIII. 3a). This also happened downstream of the ETM but the onset was earlier, in the middle of March. The biomass was always highest downstream and ranged from 5.0 to 43.2 μmol C l^{-1} which is equivalent to the chlorophyll-a concentration from 1.2 to 10.4 μg l^{-1}. The earlier increase downstream is attributed to higher light levels and weaker zooplankton grazing pressure on phytoplankton (figure now shown), so the grazing rate was approximately 4-fold lower downstream than upstream and in the ETM despite of highest zooplankton biomass downstream (Fig. AIII. 3b).. It suggests that zooplankton downstream prefers other energy sources as prey and selectively grazes on the preferred items.

Zooplankton biomass was distinct downstream compared to the other two regions (Fig. AIII. 3b). In January and February, zooplankton upstream and in the ETM could not obtain enough organic matter from phytoplankton and so mostly depended on POC as a food source (figure now shown). In contrast, zooplankton downstream obtained organic matter from both POC and dinoflagellates as well from day 1 (Fig. AIII. 4a), and the peak zooplankton biomass of 9.2 μmol C l^{-1} was observed in March, which is one-month prior to the peak dinoflagellate biomass. Meanwhile, as phytoplankton production increased from the end of April, zooplankton consumed phytoplankton and increased in biomass up to 4.7 μmol C l^{-1} upstream and 4.6 μmol C l^{-1} in the ETM at the end of May. Zooplankton downstream still obtained the majority of their organic matter from dinoflagellates (M) in May.

The ratio of M, POC, and phytoplankton (P) as food sources is 6 : 3 : 1 downstream in May and the zooplankton concentration reached 6.2 μmol C l^{-1}.

The dinoflagellate biomass reached the maximum value of 143.0 μmol C l^{-1} which is equivalent to 34.3 μg l^{-1} in April (Fig. AIII. 3c). In January, the small peak of dinoflagellate biomass is attributed to dinoflagellate ingestion of bacteria (parts of POC in the model) and the ingestion rate reached to 48.5 μmol C l^{-1} d^{-1}.

The downstream area where dinoflagellates were abundant appears to have a different food web structure compared to upstream and the ETM. Zooplankton there consumed mostly dinoflagellates (Fig. AIII. 4a). More importantly, mixotrophic dinoflagellates played an important role consuming bacteria, generating autotrophic organic matter, and finally supplying organic matter for zooplankton downstream (Fig. AIII. 4b). Dinoflagellate autotrophic production increased from March and autotrophic production was always higher than phagotrophic production. As the Type II dinoflagellate is assumed to be primarily autotrophic, photosynthesis was a major energy uptake mechanism but the bacteria ingestion was equally important especially during winter when light levels are low. In contrast, upstream and in the ETM POC and bacteria are important sources of organic matter during winter for zooplankton but phytoplankton become a more important source for zooplankton during spring (data not shown). This omnivorous capability of zooplankton is a dynamic organism resulting in high secondary production in the oligohaline but it would become only possible with the mixotrophic capability of dinoflagellates because this supplies the largest fraction of organic matter for zooplankton.

Community metabolism and assessing error

The trend of community metabolism having the highest rates downstream during late spring is consistent with the field measurements (Fig. AIII. 5a & b; Fig. 5 & 6 in Chapter 1). However, in general, the magnitude of the rates in the model is approximately 4-fold higher than the field measurements. Consequently, net ecosystem metabolism is slightly net autotrophic upstream and in the ETM in the model which is different from the measurements and the model produces approximately 4-fold higher net heterotrophy downstream (Fig. AIII. 5c; Fig. 7 in Chapter 1).

These discrepancies with actual measurements may be caused by the simplified food web structure, and/or the environment-independent respiration (remineralization) rates, and/or the lack of advection of organic matter. First, POC is assumed to include bacteria biomass so that heterotrophic organisms can graze on POC in the model. Since this assumption has obvious risks (i.e., all POC may be considered as labile organic matter and therefore bacteria concentration may appear to be extraordinarily high), sensitivity analysis was used to find realistic assimilation efficiency, growth efficiency, and grazing preference of heterotrophic processes on POC within the ranges of the previous study (Stickney et al. 2000). However, these efforts of differentiating quality and quantity between terrestrial organic matter and bacteria appear not to be accomplished without having two separate compartments. As a result, the POC contribution to the pool of organic matter and the bacteria prey source for heterotrophs appear to be overestimated. Secondly, the respiration equation for zooplankton, dinoflagellates, and bacteria are all simple linear functions of

biomass. However, estuarine community respiration is highly correlated with environmental factors such as temperature, organic matter, and nutrients (Caffrey 2004, Apple et al. 2006). Therefore, the method of computing respiration in this model is probably too simple to calculate the spatiotemporal distribution of respiration rates in the oligohaline estuary where the changes in water properties are most rapid (e.g., salinity, temperature, nutrients). Lastly, the advection of terrestrial and aquatic organic matter was not included in the model and there was no exchange of organic matter between the three areas. It has been shown that landward advection of seawater carries a subsurface maximum concentration of dinoflagellates (Tyler & Seliger 1978), which appear to be an important link of energy flow between bacteria and mesozooplankton in the box model (Appendix II). However, the STELLA model cannot simulate this physical transport of organic matter and organisms. In addition, the heterotrophic functions of mixotrophic dinoflagellates and zooplankton may be still active under the pycnocline where light does not penetrate, whereas in the model these processes only occur in the surface layer.

Conclusion

Although the model has some limitations in its ability to simulate realistic community metabolism and biomass of diverse organisms, it succeeds, nevertheless, in providing insights into the spatiotemporal differences in community metabolism and the importance of mixotrophic dinoflagellates that link energy flows. The model results support the idea that the physiological advantages of mixotrophic dinoflagellates, in combination with the omnivorous capability of zooplankton, give

rise to the high secondary production downstream. The contribution of phytoplankton (excluding dinoflagellates) is low downstream but is important upstream and in the ETM. Further analyses will be required to separate the roles of POC and bacteria in the estuarine food web but it especially appears to be important during winter when primary production is low. These spatial and temporal differences in the contribution of each compartment must dynamically interact between regions and times, which suggests that improved model results (and important insights) might be gained with the addition of physical terms such as advection or non-advective exchange of organic matter.

Table

Description	Symbol	Value	Units
Assimilation efficiency of zoop on phytop	AEzp	0.75	Dimensionless
Assimilation efficiency of zoop on POC	AEzpoc	0.38	Dimensionless
Assimilation efficiency of zoop on mixo	AEzm	0.75	Dimensionless
Assimilation efficiency of zoop on zoop	AEzz	0.75	Dimensionless
Assimilation efficiency of mixo on phytop	AEmp	0.75	Dimensionless
Assimilation efficiency of mixo on POC	AEmpoc	0.75	Dimensionless
Growth efficiency of zoop on phytop	GEzp	0.35	Dimensionless
Growth efficiency of zoop on POC	GEzpoc	0.10	Dimensionless
Growth efficiency of zoop on mixo	GEzm	0.40	Dimensionless
Growth efficiency of zoop on zoop	GEzz	0.30	Dimensionless
Maximum phytoplankton growth rate	Up	2.00	d^{-1}
Maximum dinoflagellate growth rate(autotrophic)	Um	1.40	d^{-1}
Mixotroph maximum grazing rate	Gm	0.60	d^{-1}
Zooplankton maximum grazing rate	Gz	3.20	d^{-1}
Phytoplankton senescence rate	S	0.05	d^{-1}
Partitioning of phytoplankton senescence	B	0.50	Dimensionless
Preference of zoop for phytop	PFzp	0.25	Dimensionless
Preference of zoop for mixo	PFzm	0.55	Dimensionless
Preference of zoop for POC	PFzpoc	0.05	Dimensionless
Preference of zoop for zoop	PFzz	0.15	Dimensionless
Preference of mixo for phytop	PFmp	0.60	Dimensionless
Preference of mixo for POC	PFmpoc	0.40	Dimensionless
Zooplankton mortality rate	Pz	0.12	d^{-1}
Mixotroph mortality rate	Pm	0.01	d^{-1}
Saturation constant for zooplankton grazing	ZKs	0.80	umol C kg^{-1}
Saturation constant for mixotroph grazing	MKs	0.50	umol C kg^{-1}
Light saturation parameter for phytoplankton	Ik	40.00	W m^{-2}
Detritus remineralization rate (bacteria respiration)	$Bact_R$	0.05	d^{-1}
Mixo respiration coefficient	$Mixo_R$	0.05	Dimensionless
Zoop respiration coefficient	Zoo_R	0.05	Dimensionless

Table AIII.1: Model parameters used in the mainrun in the downstream. (phytop: phytoplankton; POC: particulate organic matter; mixo: mixotrophic dinoflagellates; zoop: zooplankton).

Figures

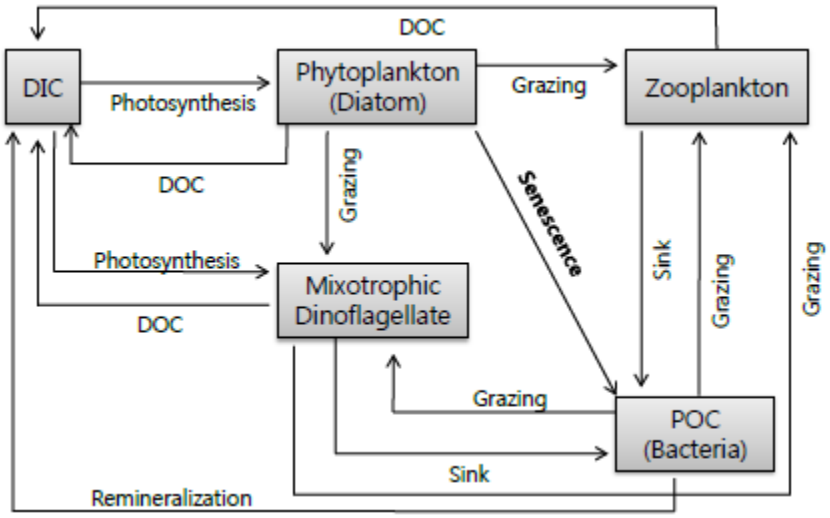

Figure AIII.1: Conceptual diagram of estuarine food web as it was modeled. The model used simple NPZD (nutrient – phytoplankton – zooplankton - detritus) relationship with the addition of mixotrophic dinoflagellates. (DIC: dissolved inorganic carbon; DOC: dissolved organic carbon; POC: particulate organic matter)

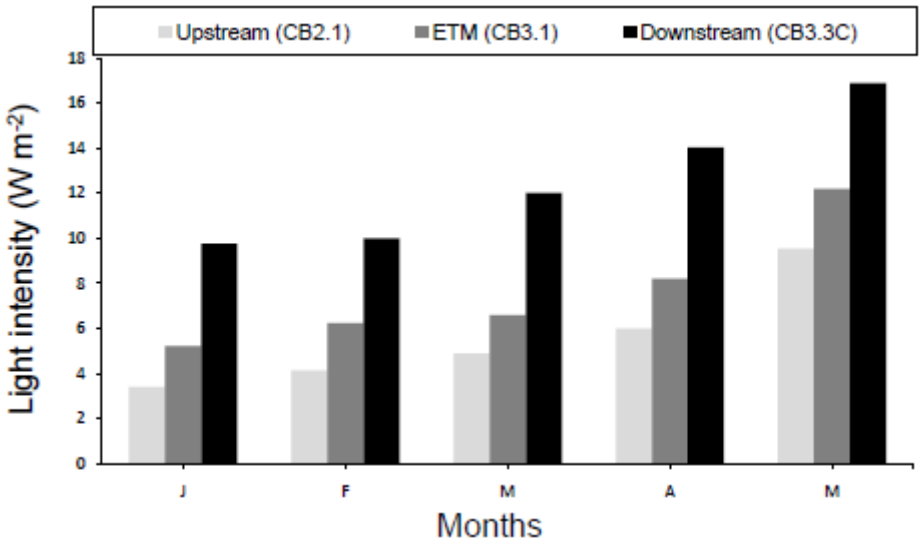

Figure AIII.2: Average light intensity in the mixed layer depth. The average light was computed from January to May at the upstream, ETM, and downstream region. The light levels are gradually increasing from January to May in the three regions because of in part the seasonal increasing of light strength on the surface.

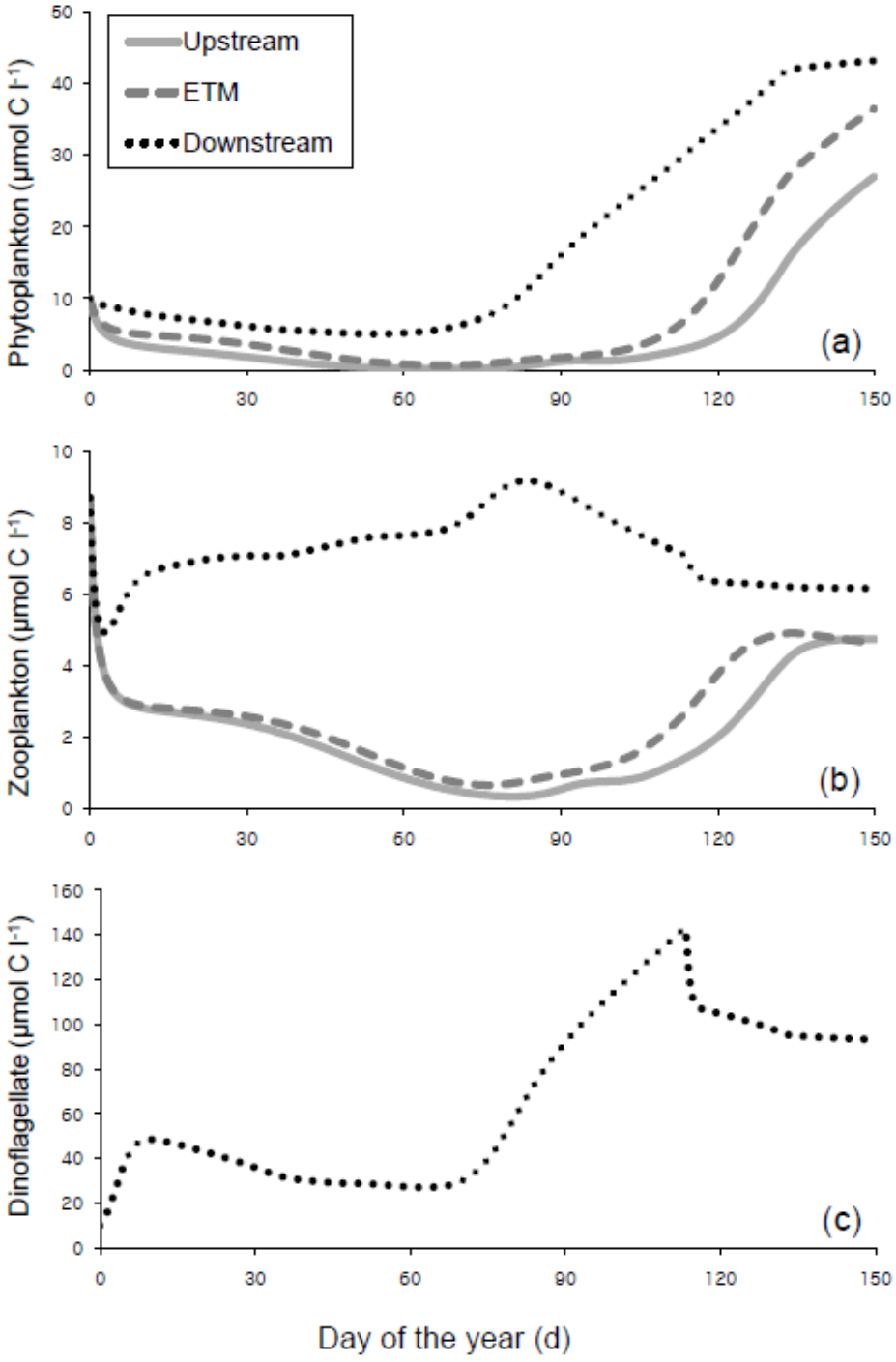

Figure AIII.3: Simulated phytoplankton (a), zooplankton (b), and dinoflagellate (c) biomass in the upstream, ETM, and downstream from winter to spring. Phytoplankton increased from the end of April in the upstream and ETM but from the middle of March in the downstream. Zooplankton biomass was more spatially contrast between the downstream and other two regions. The pattern of dinoflagellate biomass aligned best with that of dinoflagellate primary production and reached the maximum value in April.

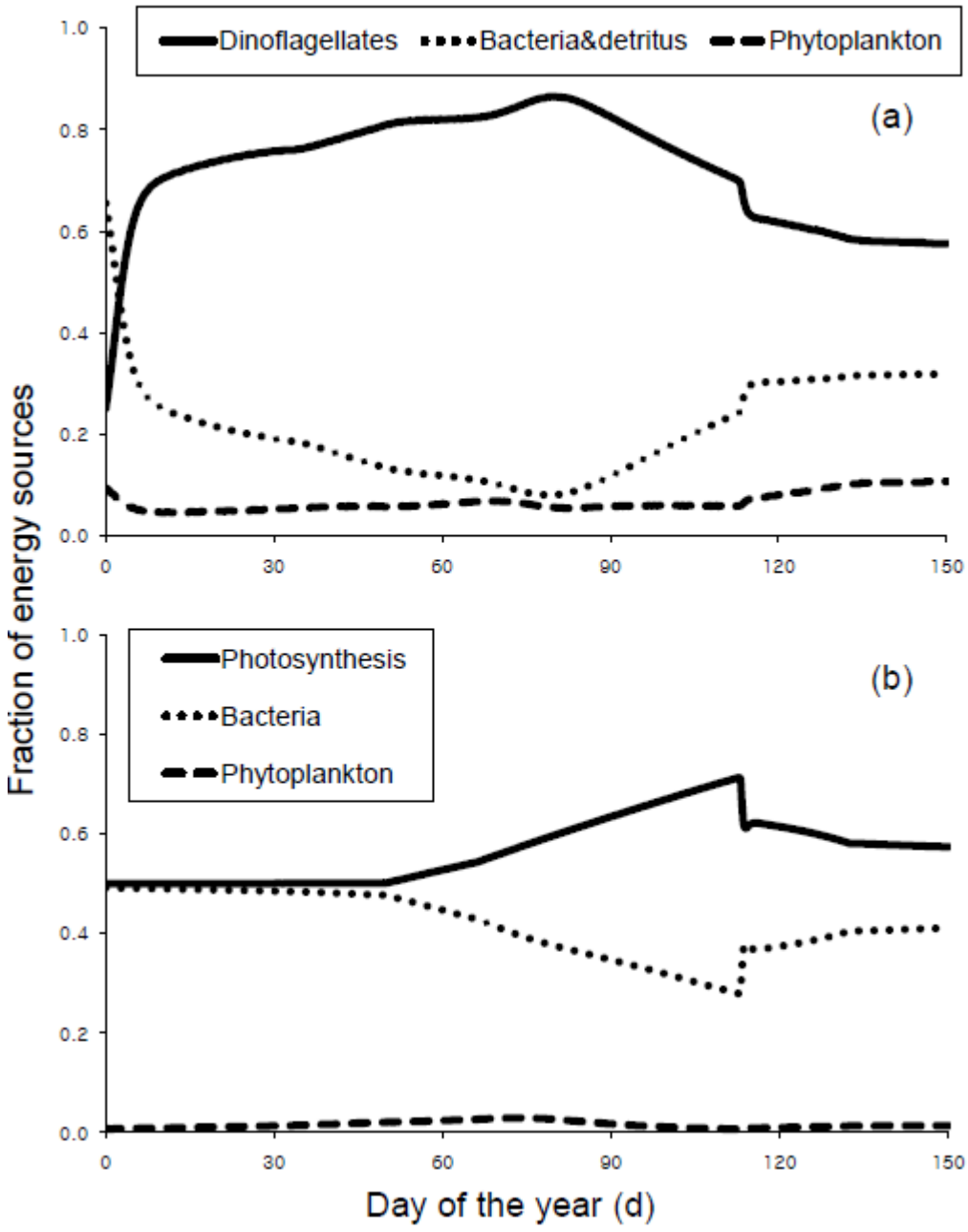

Figure AIII.4: The fraction of energy sources for zooplankton (a) and mixotrophic dinoflagellate (b) in the downstream from winter to spring. Zooplankton had a high preference on dinoflagellate as a prey source from winter. The energy uptake for mixotrophic dinoflagellates is composed mainly of photosynthesis and bacteria ingestion.

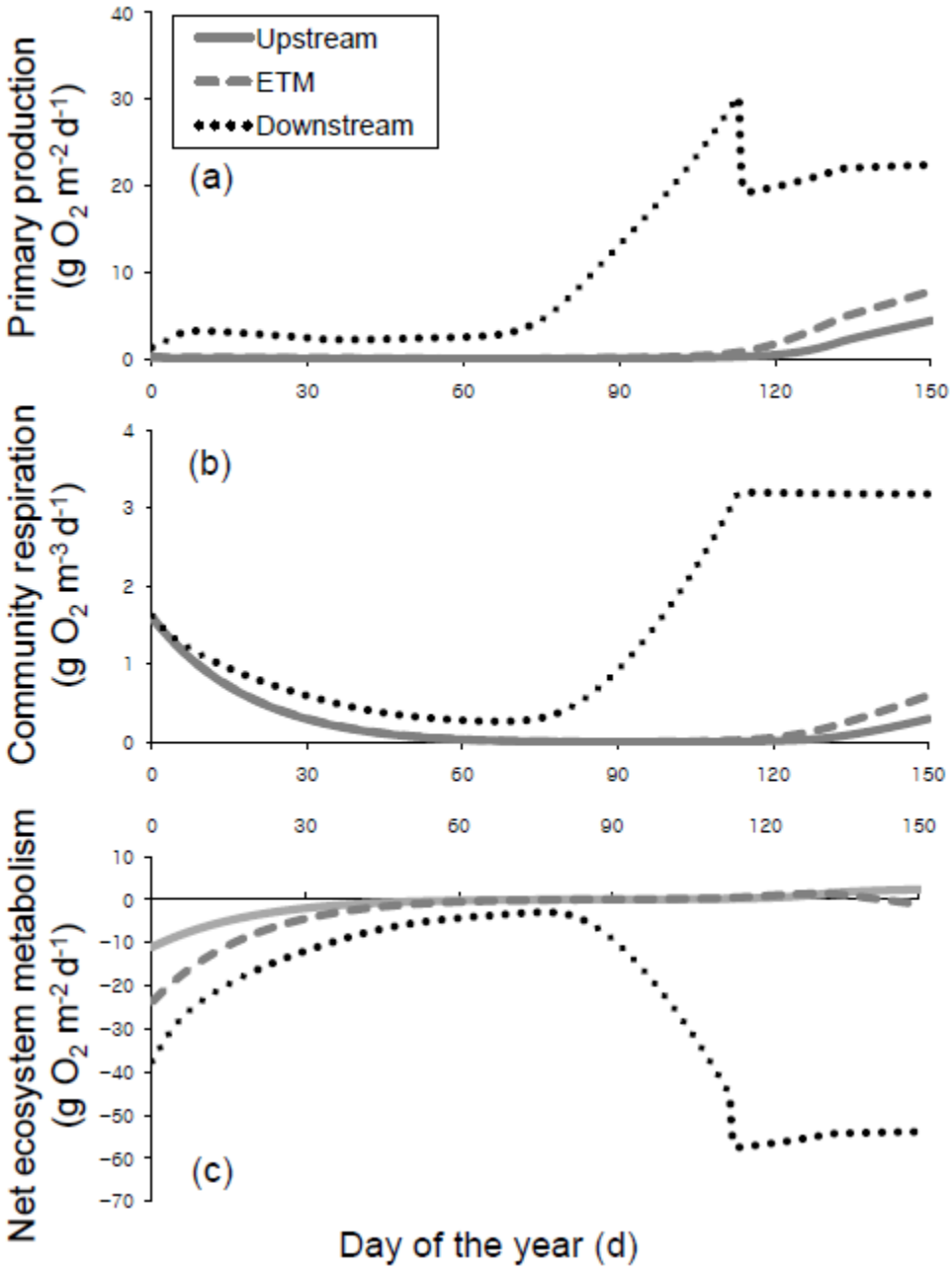

Figure AIII.5: Primary production (a), community respiration (b), and net ecosystem metabolism (c) in the oligohaline of Chesapeake Bay from winter to spring. To calculate net ecosystem metabolism, which is estimated by subtracting community respiration from gross primary production, community respiration rates were multiplied by the depth of mixed layer at the upstream (7 m), ETM (15 m), and downstream (24 m). The trend of community metabolism having highest rates in the downstream during late spring is aligned with the field measurements.

Summary and Synthesis

The plankton community metabolism method, which incorporates systematic responses of the ecosystem to nutrients and organic matter enrichment, was extensively used in this thesis to investigate effective energy transfer mechanisms resulting in high copepod and fish larvae production in the upper Chesapeake Bay. Autotrophic oxygen production and heterotrophic oxygen consumption were both high downstream of estuarine turbidity maximum (ETM) in winter and spring, whereas the two plankton metabolisms were always lower in the ETM and upstream. Because respiration rates were always higher than primary production rates at all stations, the upper Chesapeake Bay was found to be net heterotrophic, suggesting that there was a higher the amount of organic matter imported and consumed by heterotrophs than the amount of organic matter exported and produced by autotrophs. Net heterotrophy is, in fact, a common feature of eutrophied ecosystems where anthropogenic organic matter loading is high. It shows that estuarine food webs in the upper Chesapeake Bay strongly depend on detrital organic matter, which supports a detrital-based food web.

The highest concentration of suspended sediments was clearly observed in the transition zone where seawater meets freshwater near the bottom in winter and spring of the upper Chesapeake Bay. The highest organic matter oxidation was expected in the ETM region since aggregation, flocculation, and retention mechanisms are strongest there which should enhance the quality and quantity of organic matter.

However respiration rate measurements revealed that this was not the case. In addition, bacterial production rates were also lower in the ETM and upstream compared to downstream. These observations suggest that the ETM was not the most effective region of carbon and energy transfer to higher trophic levels. Furthermore, although there were seasonal and spatial variations in the relative importance of organic matter generated either from bacteria or phytoplankton, higher primary production than bacterial production, especially, in late-spring revealed that autochthonous organic matter was still an important source of organic matter.

Strong correlations between plankton community metabolism and phytoplankton pigments, including chlorophyll-a and peridinin, indicate that dinoflagellates were the key organisms that transfer carbon and energy into higher secondary producers in the upper Chesapeake Bay. It is argued that this is due to the physiological advantages of the dinoflagellates, which are mixotrophs, and the physical conditions. Specifically, phagotrophic capability allows mixotrophic dinoflagellates to take up carbon energy or nutrients, which are necessary for growth or photosynthesis, by consuming bacteria and small phytoplankton. Subsurface concentration maxima of dinoflagellates below the pycnocline were consistently observed during the winter-spring period even though the organisms could not perform photosynthesis because light levels were very low. However, bacterial production rates were high downstream where the maximum dinoflagellate concentrations were observed and it suggests that bacteria may be an important carbon and energy source for phagotrophic dinoflagellates. In addition, statistical analysis revealed that cryptophyte pigment concentrations were positively correlated

with dinoflagellate pigment concentrations, so the dinoflagellates appeared to consume cryptophytes as well. In terms of the physical influences, there were two likely physical mechanisms that allowed dinoflagellates to photosynthesize in the surface layer. First, net landward transport of seawater in the bottom layer should carry high concentration of dinoflagellates from the mouth of Chesapeake Bay to the just above the Chesapeake Bay Bridge where water depths decrease rapidly. Then, vertical advection generated due to the hydrodynamic response to a rapid depth decrease force dinoflagellates to move into the surface layer, thus moving them from depth where they function primarily as heterotrophs to near the surface where they function primarily as autotrophs. Secondly, net seaward transport of freshwater from Chesapeake Bay tributaries should also supply dinoflagellates into the mainstem bay. Regardless of where they were originated from, high concentration of dinoflagellates and strong correlations of the pigment concentration with primary production and respiration indicate that dinoflagellates were one of the most active primary and secondary producers in the upper Chesapeake Bay.

Although plankton community metabolism was always lower in the ETM than downstream, it is hypothesized that the influence of the ETM was still important, contributing to high downstream metabolism. At least two sources of diatoms originated from either the Susquehanna River or the downstream mesohaline region, and the latter includes Chesapeake Bay tributaries. The abrupt disappearance of diatoms in the ETM region appeared to be caused by salinity stress, and the same stress would influence bacteria as well, which presumably originated from the same sources. The supply of particulate and dissolved organic matter from these dead

organisms should help to support a detritus-based food web which can be utilized by downstream secondary producers. This suggests that the function of ETM is more like a conveyor belt accumulating high concentrations of nutritious organic matter that is ultimately utilized by downstream organisms.

Two mathematical models were developed that simulate community metabolism and energy transfer pathways. These also suggest that the mixotrophic capability of dinoflagellates not only controlled the seasonal and spatial variations of plankton community metabolism, but also transferred organic matter from lower trophic levels into higher trophic levels in winter and spring. First, a non-conservative box model captured observed environmental conditions, such as increases in mixing between surface and bottom layers in winter and decreases in mixing in spring due to weak and strong stratification, respectively. In terms of biological production, the model revealed that phagotrophic production of dinoflagellates in the bottom layer was higher than the sum of any biological loss terms in winter. In spring, however, biological mortality became higher than the dinoflagellate production in the bottom layer. In addition, a simple NPZD (nutrient-phytoplankton-zooplankton-detritus) model with the addition of a mixotrophic dinoflagellate compartment suggested that dinoflagellates obtained the majority of their energy by first by photosynthesizing and second by consuming bacteria. Zooplankton, on the other hand, obtained the majority of their energy by consuming first mixotrophic dinoflagellates and second detrital organic matter colonized by bacteria. As a result, carbon flows from bacteria to dinoflagellates to zooplankton to fish larvae appears to be a very important energy transfer pathway in the upper Chesapeake Bay.

In summary, a series of high-resolution spatial surveys in the upper Chesapeake Bay revealed that high secondary production downstream of the ETM resulted from a combination of biological, chemical, and physical processes that favored mixotrophic dinoflagellate production and transfer of this production to higher trophic levels. This thesis has focused on processes in a relatively narrow and deep area of upper Chesapeake Bay. Shallow littoral areas, where benthic biogeochemical processes are active, were not included in this analysis. In fact, biotic responses to the nutrient inputs may be more immediate and pronounced due to the close proximity of the sources in the shallow areas. Therefore, further study is needed to measure the metabolic processes occurring in the shallow littoral zone. Also, further study of micro- and mesozooplankton grazing ability will allow better quantification of carbon and energy flows from low to high trophic levels. Finally, a computation model which integrates biological processes with physical advection of organic matter between estuarine regions will allow a more realistic simulation of community metabolism and energy transfer mechanisms of upper estuaries.

Appendix IV: tables & figure

Late-winter

	Salinity	GPP	T.Resp	Pico.Resp	Temp.	TSS	Euphotic.	Chl-a	Dinofla.	Diatom	Crypto.	Cyano.
GPP	0.62	-	*0.41*	*-0.10*	*-0.54*	*0.29*	*0.35*	*0.76*	*0.73*	*0.15*	*0.78*	*0.20*
	0.0035		*0.0778*	*0.6920*	*0.0168*	*0.2210*	*0.1395*	*0.0002*	*0.0003*	*0.5487*	*<.0001*	*0.4043*
T.Resp	0.51	0.59	-	*0.37*	*-0.54*	*0.53*	*-0.47*	*0.69*	*0.76*	*-0.24*	*0.48*	*0.28*
	0.0222	0.0057		*0.1228*	*0.0171*	*0.0186*	*0.0429*	*0.0011*	*0.0002*	*0.3189*	*0.0387*	*0.2426*
Pico.Resp	0.23	0.07	0.42	-	*-0.40*	*0.59*	*-0.54*	*0.29*	*0.36*	*-0.19*	*0.29*	*0.70*
	0.3314	0.7765	0.0627		*0.0873*	*0.0082*	*0.0169*	*0.2231*	*0.1276*	*0.4295*	*0.2362*	*0.0008*
Temp.	0.47	-0.09	-0.17	-0.24	-	*-0.42*	*0.15*	*-0.83*	*-0.78*	*-0.12*	*-0.56*	*-0.42*
	0.0379	0.7204	0.4637	0.3088		*0.0742*	*0.5266*	*<.0001*	*<.0001*	*0.6373*	*0.0128*	*0.0771*
TSS	-0.02	0.22	0.45	0.57	-0.38	-	*-0.46*	*0.41*	*0.56*	*-0.32*	*0.74*	*0.87*
	0.9396	0.3519	0.0462	0.0091	0.0995		*0.0483*	*0.0842*	*0.0133*	*0.1789*	*0.0003*	*<.0001*
Euphotic.	0.74	0.64	0.10	-0.19	0.44	-0.32	-	*-0.14*	*-0.19*	*0.25*	*0.07*	*-0.40*
	0.0002	0.0022	0.6674	0.4327	0.0539	0.1652		*0.5809*	*0.4416*	*0.3036*	*0.7633*	*0.0888*
Chl-a	0.60	0.85	0.78	0.37	-0.31	0.32	0.37	-	*0.93*	*0.18*	*0.68*	*0.38*
	0.0056	<.0001	<.0001	0.1129	0.1823	0.1750	0.1125		*<.0001*	*0.4580*	*0.0014*	*0.1112*
Dinofla.	0.63	0.84	0.83	0.42	-0.24	0.42	0.37	0.96	-	*-0.18*	*0.78*	*0.43*
	0.0028	<.0001	<.0001	0.0667	0.3109	0.0653	0.1103	<.0001		*0.4619*	*<.0001*	*0.0662*
Diatom	0.02	0.13	-0.20	-0.18	-0.09	-0.32	0.18	0.16	-0.13	-	*-0.11*	*-0.06*
	0.9305	0.5906	0.4039	0.4407	0.6981	0.1659	0.4388	0.5060	0.5964		*0.6622*	*0.7981*
Crypto.	0.74	0.87	0.65	0.36	0.01	0.49	0.58	0.81	0.87	-0.06	-	*0.61*
	0.0002	<.0001	0.0018	0.1228	0.9651	0.0292	0.0076	<.0001	<.0001	0.8112		*0.0056*
Cyano.	-0.59	-0.24	-0.11	0.41	-0.57	0.71	-0.66	-0.11	-0.11	-0.06	-0.11	-
	0.0057	0.3073	0.6547	0.0706	0.0083	0.0004	0.0017	0.6450	0.6527	0.7920	0.6535	

Table AIV. 1: Correlation matrix of salinity and environmental and biological variables at surface with gross primary production in late-winter. In italics (upper right): partial correlation coefficients excluding salinity influence if any. n = 20. First row of each parameter is correlation coefficient and second row is p value. (GPP: gross primary production; T.Resp: total community respiration; Pico.Resp: picoplankton respiration; Temp.: temperature; TSS: total suspended sediment; Euphotic.: euphotic depth; Chl-a: chlorophyll-a; Dinofla.: dinoflagellate; Crypto.: cryptophyte; Cyano.: cyanobacteria)

Early-spring

	Salinity	GPP	T.Resp	Pico.Resp	Temp.	TSS	Euphotic.	Chl-a	Dinofla.	Diatom	Crypto.	Cyano.
GPP	0.62	-	*0.68*	*0.29*	*0.55*	*-0.34*	*0.35*	*0.31*	*-0.25*	*0.31*	*0.84*	*0.48*
	0.0038		*0.0012*	*0.2321*	*0.0155*	*0.1501*	*0.1400*	*0.1934*	*0.3106*	*0.1910*	*<.0001*	*0.0369*
T.Resp	0.60	0.80	-	*0.31*	*0.51*	*0.10*	*0.08*	*0.42*	*-0.30*	*0.57*	*0.54*	*0.68*
	0.0049	<.0001		*0.1916*	*0.0252*	*0.6847*	*0.7599*	*0.0769*	*0.2058*	*0.0110*	*0.0182*	*0.0013*
Pico.Resp	0.25	0.37	0.39	-	*0.18*	*0.08*	*0.08*	*-0.19*	*-0.37*	*0.03*	*0.03*	*0.31*
	0.2915	0.1058	0.0876		*0.4663*	*0.7498*	*0.7413*	*0.4277*	*0.1208*	*0.9066*	*0.9039*	*0.1944*
Temp.	-0.08	0.38	0.36	0.15	-	*-0.21*	*0.32*	*0.06*	*-0.50*	*0.34*	*0.42*	*0.66*
	0.7295	0.1001	0.1223	0.5244		*0.3901*	*0.1786*	*0.8209*	*0.0302*	*0.1485*	*0.0736*	*0.0023*
TSS	-0.68	-0.62	-0.35	-0.11	-0.10	-	*-0.81*	*-0.27*	*-0.03*	*-0.22*	*-0.26*	*0.05*
	0.0009	0.0037	0.1271	0.6336	0.6862		*<.0001*	*0.2677*	*0.9001*	*0.3700*	*0.2866*	*0.8254*
Euphotic.	0.65	0.61	0.44	0.22	0.19	-0.89	-	*0.07*	*-0.29*	*0.20*	*0.37*	*-0.14*
	0.0018	0.0042	0.0529	0.3481	0.4236	<.0001		*0.7879*	*0.2245*	*0.4204*	*0.1160*	*0.5657*
Chl-a	0.78	0.64	0.68	0.08	-0.03	-0.66	0.54	-	*0.43*	*0.82*	*0.22*	*0.39*
	<.0001	0.0026	0.0010	0.7434	0.8995	0.0017	0.0135		*0.0652*	*<.0001*	*0.3555*	*0.0968*
Dinofla.	0.55	0.18	0.13	-0.16	-0.46	-0.40	0.18	0.66	-	*-0.09*	*-0.20*	*-0.28*
	0.0114	0.4498	0.5809	0.5003	0.0420	0.0842	0.4575	0.0017		*0.7244*	*0.4027*	*0.2372*
Diatom	0.49	0.52	0.69	0.15	0.26	-0.47	0.45	0.83	0.21	-	*0.15*	*0.62*
	0.0273	0.0192	0.0007	0.5374	0.2718	0.0345	0.0460	<.0001	0.3749		*0.5513*	*0.0046*
Crypto.	0.70	0.91	0.73	0.19	0.24	-0.61	0.66	0.65	0.27	0.44	-	*0.21*
	0.0006	<.0001	0.0003	0.4111	0.3074	0.0041	0.0016	0.0020	0.2554	0.0546		*0.3805*
Cyano.	0.27	0.53	0.69	0.36	0.61	-0.15	0.08	0.45	-0.08	0.65	0.34	-
	0.2457	0.0156	0.0008	0.1215	0.0046	0.5355	0.7533	0.0478	0.7441	0.0018	0.1459	

Table AIV. 2: Correlation matrix of salinity and environmental and biological variables at surface with gross primary production in early-spring. In italics (upper right): partial correlation coefficients excluding salinity influence if any. n = 20. First row of each parameter is correlation coefficient and second row is p value.

Late-spring

	Salinity	GPP	T.Resp	Pico.Resp	Temp.	TSS	Euphotic.	Chl-a	Dinofla.	Diatom	Crypto.	Cyano.
GPP	0.80	-	*0.89*	*0.07*	*-0.04*	*-0.43*	*0.30*	*0.87*	*0.78*	*0.14*	*-0.25*	*0.13*
	<.0001		*<.0001*	*0.7703*	*0.8646*	*0.0643*	*0.2171*	*<.0001*	*<.0001*	*0.5636*	*0.3042*	*0.6031*
T.Resp	0.84	0.96	-	*0.10*	*0.05*	*-0.50*	*0.26*	*0.88*	*0.82*	*0.08*	*-0.44*	*0.03*
	<.0001	<.0001		*0.6960*	*0.8376*	*0.0278*	*0.2812*	*<.0001*	*<.0001*	*0.7315*	*0.0596*	*0.9126*
Pico.Resp	0.56	0.48	0.51	-	*0.03*	*0.08*	*0.11*	*-0.01*	*-0.21*	*0.66*	*-0.26*	*0.70*
	0.0102	0.0302	0.0209		*0.9126*	*0.7392*	*0.6680*	*0.9525*	*0.3835*	*0.0020*	*0.2731*	*0.0009*
Temp.	-0.44	-0.37	-0.34	-0.23	-	*0.06*	*-0.03*	*-0.02*	*-0.05*	*0.10*	*0.07*	*-0.08*
	0.0526	0.1034	0.1388	0.3377		*0.8229*	*0.9109*	*0.9216*	*0.8376*	*0.6689*	*0.7774*	*0.7463*
TSS	-0.46	-0.60	-0.63	-0.20	0.24	-	*-0.77*	*-0.39*	*-0.41*	*0.04*	*0.09*	*0.15*
	0.0433	0.0056	0.0031	0.4094	0.2990		*0.0001*	*0.0956*	*0.0821*	*0.8722*	*0.7255*	*0.5434*
Euphotic.	0.51	0.56	0.55	0.36	-0.24	-0.82	-	*0.05*	*-0.01*	*0.33*	*-0.12*	*0.10*
	0.0219	0.0101	0.0122	0.1186	0.2978	<.0001		*0.8338*	*0.9759*	*0.1633*	*0.6333*	*0.6985*
Chl-a	0.79	0.95	0.96	0.44	-0.36	-0.57	0.43	-	*0.94*	*-0.05*	*-0.22*	*-0.01*
	<.0001	<.0001	<.0001	0.0544	0.1175	0.0080	0.0582		*<.0001*	*0.8536*	*0.3604*	*0.9716*
Dinofla.	0.65	0.88	0.89	0.23	-0.32	-0.57	0.33	0.95	-	*-0.37*	*-0.32*	*-0.27*
	0.0017	<.0001	<.0001	0.3211	0.1665	0.0082	0.1576	<.0001		*0.1241*	*0.1833*	*0.2575*
Diatom	0.72	0.63	0.63	0.78	-0.25	-0.30	0.56	0.55	0.28	-	*0.05*	*0.81*
	0.0004	0.0027	0.0028	<.0001	0.2905	0.1959	0.0095	0.0125	0.2400		*0.8291*	*<.0001*
Crypto.	0.10	-0.06	-0.15	-0.16	0.02	0.03	-0.05	-0.05	-0.17	0.11	-	*-0.08*
	0.6605	0.7888	0.5229	0.5017	0.9463	0.9047	0.8444	0.8276	0.4702	0.6389		*0.7472*
Cyano.	0.67	0.60	0.58	0.80	-0.35	-0.21	0.40	0.53	0.29	0.90	0.01	-
	0.0011	0.0054	0.0079	<.0001	0.1313	0.3742	0.0774	0.0161	0.2168	<.0001	0.9584	

Table AIV. 3: Correlation matrix of salinity and environmental and biological variables at surface with gross primary production in late-spring. In italics (upper right): partial correlation coefficients excluding salinity influence if any. n = 20. First row of each parameter is correlation coefficient and second row is p value.

Late-winter	Salinity	T.Resp	P.Resp	Temp.	TSS	Chl-a	Dinofla.	Diatom	Crypto.	Cyano.	Chlide_a	Phide_a	Phytin_a	T.Pheo.	B.P.	Filt.B.P
T.Resp	0.43 0.0005	-	*0.30* *0.022*	*-0.66* *<.0001*	*0.26* *0.047*	*0.73* *<.0001*	*0.74* *<.0001*	*-0.32* *0.012*	*0.56* *<.0001*	*-0.17* *0.189*	*0.14* *0.2745*	*-0.25* *0.0538*	*0.16* *0.2376*	*-0.17* *0.2075*	*-0.17* *0.19*	*-0.35* *0.006*
P.Resp	0.04 0.7631	0.29 0.0271	-	*-0.23* *0.074*	*0.36* *0.005*	*0.19* *0.142*	*0.24* *0.07*	*-0.28* *0.031*	*0.14* *0.274*	*0.03* *0.845*	*-0.32* *0.0125*	*-0.14* *0.2902*	*0.11* *0.4219*	*0.10* *0.449*	*-0.06* *0.658*	*-0.17* *0.191*
Temp.	0.74 <.0001	-0.07 0.5761	-0.13 0.3329	-	*-0.30* *0.022*	*-0.80* *<.0001*	*-0.79* *<.0001*	*0.20* *0.128*	*-0.80* *<.0001*	*0.01* *0.926*	*-0.24* *0.0647*	*0.30* *0.0221*	*-0.24* *0.0699*	*0.29* *0.0245*	*0.37* *0.004*	*0.54* *<.0001*
TSS	-0.10 0.4667	0.19 0.1426	0.36 0.0052	-0.27 0.0369	-	*0.27* *0.04*	*0.32* *0.015*	*-0.22* *0.088*	*0.46* *3E-04*	*0.60* *<.0001*	*-0.03* *0.8404*	*0.21* *0.1026*	*0.62* *<.0001*	*0.47* *0.0002*	*-0.23* *0.078*	*-0.45* *3E-04*
Chl-a	0.60 <.0001	0.79 <.0001	0.18 0.1728	0.02 0.8989	0.16 0.233	-	*0.92* *<.0001*	*-0.08* *0.544*	*0.79* *<.0001*	*-0.03* *0.793*	*0.41* *0.0012*	*-0.19* *0.1579*	*0.43* *0.0007*	*-0.19* *0.1573*	*-0.05* *0.733*	*-0.39* *0.002*
Dinofla.	0.42 0.001	0.79 <.0001	0.23 0.0742	-0.17 0.1947	0.25 0.057	0.92 <.0001	-	*-0.44* *4E-04*	*0.86* *<.0001*	*-0.17* *0.207*	*0.35* *0.0065*	*-0.38* *0.0032*	*0.27* *0.0397*	*-0.31* *0.0182*	*-0.22* *0.093*	*-0.40* *0.002*
Diatom	0.57 <.0001	0.01 0.9368	-0.21 0.1121	0.54 <.0001	-0.24 0.068	0.29 0.024	-0.09 0.486	-	*-0.33* *0.01*	*0.40* *0.002*	*0.25* *0.0554*	*0.62* *<.0001*	*0.35* *0.0067*	*0.39* *0.0026*	*0.47* *2E-04*	*0.12* *0.372*
Crypto.	0.56 <.0001	0.66 <.0001	0.14 0.2786	-0.02 0.8545	0.32 0.012	0.86 <.0001	0.88 <.0001	0.10 0.464	-	*0.07* *0.583*	*0.48* *0.0001*	*-0.23* *0.0799*	*0.33* *0.0101*	*-0.19* *0.1531*	*-0.24* *0.064*	*-0.50* *<.0001*
Cyano.	-0.20 0.1327	-0.24 0.0664	0.02 0.8938	-0.14 0.2941	0.61 <.0001	-0.15 0.268	-0.23 0.0766	0.21 0.1087	-0.05 0.699	-	*0.14* *0.2887*	*0.71* *<.0001*	*0.78* *<.0001*	*0.72* *<.0001*	*0.16* *0.24*	*-0.14* *0.303*
Chlide_a	0.74 <.0001	0.41 0.0011	-0.19 0.1529	0.44 0.0004	-0.09 0.499	0.67 <.0001	0.52 <.0001	0.56 <.0001	0.68 <.0001	-0.05 0.6842	-	*0.37* *0.0044*	*0.33* *0.0111*	*0.13* *0.3187*	*0.16* *0.233*	*-0.12* *0.376*
Phide_a	0.74 <.0001	0.17 0.1946	-0.06 0.6251	0.68 <.0001	0.07 0.583	0.35 0.007	0.08 0.5533	0.77 <.0001	0.29 0.0253	0.32 0.0117	0.72 <.0001	-	*0.66* *<.0001*	*0.85* *<.0001*	*0.34* *0.008*	*0.13* *0.333*
Phytin_a	0.62 <.0001	0.38 0.0028	0.11 0.4107	0.34 0.0088	0.42 8E-04	0.64 <.0001	0.45 0.0003	0.58 <.0001	0.56 <.0001	0.48 0.0001	0.63 <.0001	0.81 <.0001	-	*0.68* *<.0001*	*0.20* *0.137*	*-0.18* *0.184*
T.Pheo.	0.42 0.0008	0.05 0.7163	0.11 0.4124	0.49 <.0001	0.39 0.002	0.12 0.366	-0.08 0.5588	0.53 <.0001	0.10 0.4649	0.56 <.0001	0.39 0.0018	0.83 <.0001	0.74 <.0001	-	*0.24* *0.064*	*0.06* *0.635*
B.P.	0.26 0.0472	-0.04 0.7694	-0.05 0.7236	0.43 0.0006	-0.25 0.057	0.12 0.364	-0.09 0.5092	0.52 <.0001	-0.05 0.7074	0.10 0.4625	0.29 0.023	0.41 0.0011	0.31 0.0166	0.32 0.0122	-	*0.64* *<.0001*
Filt.B.P	0.30 0.0192	-0.17 0.1893	-0.15 0.2445	0.57 <.0001	-0.46 2E-04	-0.12 0.364	-0.22 0.0933	0.27 0.0404	-0.23 0.0813	-0.19 0.153	0.15 0.2558	0.31 0.0175	0.06 0.6731	0.18 0.1639	0.67 <.0001	-

Table AIV. 4: Correlation matrix of salinity and environmental and biological variables at surface, middle, and bottom water with respiration rates in late-winter. In italics (upper right): partial correlation coefficients excluding salinity influence if any. n=60. (T.Resp: total community respiration; P.Resp: picoplankton respiration; Temp.: temperature; TSS: total suspended sediment; Chl-a: chlorophyll-a; Dinofla.: dinoflagellate; Crypto.: cryptophyte; Cyano.: cyanobacteria; Chlide_a: chlorophyllide-a; Phide_a: pheophorbide-a; Phytin_a: Pheophytin-a; T.Pheo.: total pheophytin; B.P.: bacterial production; Filt.B.P.: free-living bacterial production)

Early-spring	Salinity	T.Resp	P.Resp	Temp.	TSS	Chl-a	Dinofla.	Diatom	Crypto.	Cyano.	Chlide_a	Phide_a	Phytin_a	T.Pheo.	B.P.	Filt.B.P
T.Resp	0.32 0.0129	-	*0.35* *0.0061*	*0.45* *4E-04*	*-0.34* *0.008*	*0.49* *<.0001*	*0.06* *0.648*	*0.53* *<.0001*	*0.53* *<.0001*	*0.14* *0.294*	*0.19* *0.1557*	*-0.13* *0.3239*	*0.27* *0.04*	*-0.17* *0.1897*	*0.33* *0.011*	*0.63* *<.0001*
P.Resp	0.06 0.6384	0.35 0.0056	-	*0.32* *0.013*	*-0.16* *0.228*	*-0.01* *0.935*	*-0.34* *0.01*	*0.20* *0.122*	*0.27* *0.04*	*0.14* *0.291*	*0.05* *0.7018*	*-0.08* *0.5237*	*0.15* *0.2461*	*-0.20* *0.1366*	*0.09* *0.512*	*0.32* *0.013*
Temp.	-0.40 0.0016	0.26 0.0439	0.27 0.0362	-	*-0.19* *0.154*	*0.05* *0.684*	*-0.34* *0.008*	*0.40* *0.002*	*0.35* *0.006*	*0.30* *0.02*	*0.16* *0.2261*	*-0.07* *0.618*	*0.35* *0.0071*	*-0.27* *0.0366*	*0.31* *0.015*	*0.68* *<.0001*
TSS	-0.03 0.7932	-0.33 0.0093	-0.16 0.219	-0.16 0.2264	-	*-0.36* *0.006*	*-0.17* *0.208*	*-0.24* *0.063*	*-0.29* *0.024*	*0.74* *<.0001*	*-0.38* *0.0027*	*0.84* *<.0001*	*0.44* *0.0006*	*0.91* *<.0001*	*-0.15* *0.249*	*-0.20* *0.134*
Chl-a	0.53 <.0001	0.56 <.0001	0.02 0.8564	-0.17 0.191	-0.32 0.013	-	*0.71* *<.0001*	*0.71* *<.0001*	*0.44* *4E-04*	*-0.04* *0.741*	*0.63* *<.0001*	*-0.22* *0.1015*	*0.21* *0.1082*	*-0.11* *0.4037*	*0.08* *0.569*	*0.37* *0.004*
Dinofla.	0.56 <.0001	0.23 0.0808	-0.24 0.063	-0.48 <.0001	-0.16 0.232	0.80 <.0001	-	*0.10* *0.45*	*0.01* *0.926*	*-0.25* *0.059*	*0.41* *0.0014*	*-0.19* *0.1522*	*-0.10* *0.433*	*0.01* *0.9672*	*-0.17* *0.21*	*-0.16* *0.23*
Diatom	0.14 0.2936	0.54 <.0001	0.21 0.108	0.31 0.0176	-0.25 0.058	0.67 <.0001	0.16 0.2227	-	*0.33* *0.012*	*0.24* *0.067*	*0.57* *<.0001*	*0.02* *0.8678*	*0.55* *<.0001*	*-0.08* *0.5535*	*0.23* *0.081*	*0.72* *<.0001*
Crypto.	0.54 <.0001	0.60 <.0001	0.26 0.0457	0.06 0.6624	-0.27 0.041	0.60 <.0001	0.31 0.0152	0.35 0.0067	-	*0.02* *0.868*	*0.34* *0.008*	*-0.19* *0.1427*	*0.10* *0.474*	*-0.18* *0.163*	*0.31* *0.018*	*0.45* *3E-04*
Cyano.	0.21 0.1124	0.20 0.1354	0.15 0.2549	0.19 0.1479	0.72 <.0001	0.07 0.574	-0.08 0.5246	0.26 0.0441	0.13 0.3227	-	*-0.17* *0.191*	*0.79* *<.0001*	*0.69* *<.0001*	*0.75* *<.0001*	*0.13* *0.331*	*0.30* *0.022*
Chlide_a	0.63 <.0001	0.34 0.008	0.08 0.5509	-0.14 0.2889	-0.32 0.013	0.75 <.0001	0.62 <.0001	0.53 <.0001	0.56 <.0001	0.00 0.998	-	*-0.25* *0.0545*	*0.08* *0.5424*	*-0.32* *0.015*	*-0.04* *0.765*	*0.25* *0.061*
Phide_a	0.68 <.0001	0.13 0.3334	-0.02 0.8817	-0.32 0.0137	0.59 <.0001	0.23 0.076	0.27 0.0372	0.11 0.4027	0.25 0.0557	0.71 <.0001	0.29 0.0251	-	*0.61* *<.0001*	*0.87* *<.0001*	*0.00* *0.982*	*0.05* *0.689*
Phytin_a	0.55 <.0001	0.39 0.0022	0.16 0.2161	0.05 0.7127	0.35 0.007	0.44 4E-04	0.24 0.0701	0.53 <.0001	0.36 0.0046	0.68 <.0001	0.40 0.0016	0.75 <.0001	-	*0.51* *<.0001*	*0.30* *0.023*	*0.63* *<.0001*
T.Pheo.	0.49 <.0001	0.01 0.9307	-0.14 0.2823	-0.41 0.0011	0.78 <.0001	0.18 0.176	0.28 0.032	0.00 0.9924	0.13 0.3372	0.74 <.0001	0.09 0.4754	0.89 <.0001	0.64 <.0001	-	*-0.06* *0.643*	*-0.09* *0.481*
B.P.	0.17 0.204	0.36 0.0045	0.10 0.4659	0.22 0.0947	-0.16 0.234	0.15 0.247	-0.04 0.7542	0.25 0.0577	0.35 0.0069	0.16 0.2261	0.07 0.5692	0.12 0.3794	0.34 0.0089	0.03 0.8337	-	*0.58* *<.0001*
Filt.B.P	-0.11 0.3964	0.56 <.0001	0.31 0.0147	0.66 <.0001	-0.19 0.142	0.25 0.054	-0.19 0.1395	0.70 <.0001	0.32 0.0129	0.27 0.04	0.12 0.3694	-0.04 0.7775	0.47 0.0002	-0.14 0.3026	0.55 <.0001	-

Table AIV. 5: Correlation matrix of salinity and environmental and biological variables at surface, middle, and bottom water with respiration rates in early-spring. In italics (upper right): partial correlation coefficients excluding salinity influence if any. n=60.

Late-spring	Salinity	T.Resp	P.Resp	Temp.	TSS	Chl-a	Dinofla.	Diatom	Crypto.	Cyano.	Chlide_a	Phide_a	Phytin_a	T.Pheo.	B.P.	Filt.B.P
T.Resp	0.65 <.0001	-	*0.50* *0.0005*	*0.16* *0.291*	*-0.50* *6E-04*	*0.85* *<.0001*	*0.81* *<.0001*	*0.39* *0.008*	*0.13* *0.409*	*0.05* *0.748*	*0.68* *<.0001*	*-0.24* *0.1121*	*-0.10* *0.5154*	*-0.37* *0.0146*	*0.55* *1E-04*	*0.39* *0.009*
P.Resp	0.40 0.0016	0.58 <.0001	-	*0.09* *0.565*	*-0.20* *0.187*	*0.41* *0.005*	*0.22* *0.152*	*0.60* *<.0001*	*0.01* *0.949*	*0.46* *0.002*	*0.46* *0.0015*	*0.06* *0.7221*	*0.26* *0.0926*	*0.07* *0.6362*	*0.53* *2E-04*	*0.59* *<.0001*
Temp.	-0.81 <.0001	-0.46 0.0003	-0.26 0.0477	-	*-0.29* *0.057*	*0.06* *0.678*	*0.11* *0.463*	*-0.11* *0.488*	*-0.09* *0.551*	*-0.26* *0.092*	*0.03* *0.8651*	*-0.30* *0.0451*	*-0.33* *0.0284*	*-0.37* *0.0135*	*0.23* *0.129*	*0.18* *0.238*
TSS	0.05 0.7304	-0.34 0.0077	-0.21 0.1152	-0.22 0.0912	-	*-0.31* *0.039*	*-0.38* *0.011*	*0.00* *1*	*0.06* *0.713*	*0.56* *<.0001*	*-0.22* *0.1478*	*0.85* *<.0001*	*0.72* *<.0001*	*0.60* *<.0001*	*-0.24* *0.11*	*-0.40* *0.008*
Chl-a	0.47 0.0001	0.88 <.0001	0.41 0.0011	-0.39 0.0023	-0.23 0.072	-	*0.93* *<.0001*	*0.54* *2E-04*	*0.24* *0.118*	*0.21* *0.166*	*0.75* *<.0001*	*-0.03* *0.8686*	*0.12* *0.438*	*-0.27* *0.0728*	*0.43* *0.003*	*0.12* *0.449*
Dinofla.	0.43 0.0007	0.84 <.0001	0.27 0.0405	-0.33 0.0106	-0.28 0.031	0.96 <.0001	-	*0.23* *0.136*	*0.07* *0.64*	*-0.04* *0.792*	*0.56* *<.0001*	*-0.15* *0.3181*	*-0.11* *0.4822*	*-0.49* *0.0008*	*0.39* *0.008*	*0.07* *0.635*
Diatom	0.53 <.0001	0.52 <.0001	0.63 <.0001	-0.48 <.0001	0.04 0.783	0.53 <.0001	0.29 0.0235	-	*0.25* *0.107*	*0.62* *<.0001*	*0.70* *<.0001*	*0.33* *0.0304*	*0.54* *0.0001*	*0.48* *0.0011*	*0.31* *0.04*	*0.18* *0.244*
Crypto.	0.09 0.4868	0.22 0.0924	0.05 0.6787	-0.12 0.359	0.02 0.879	0.36 0.005	0.23 0.083	0.32 0.0135	-	*0.17* *0.257*	*0.37* *0.0143*	*0.09* *0.5703*	*0.34* *0.0252*	*0.19* *0.2115*	*-0.18* *0.245*	*-0.31* *0.043*
Cyano.	0.18 0.1618	0.11 0.3947	0.43 0.0007	-0.30 0.0202	0.57 <.0001	0.20 0.127	0.01 0.9571	0.61 <.0001	0.20 0.1301	-	*0.44* *0.0027*	*0.60* *<.0001*	*0.70* *<.0001*	*0.48* *0.0009*	*0.17* *0.266*	*0.03* *0.837*
Chlide_a	0.14 0.2807	0.65 <.0001	0.30 0.0187	-0.08 0.5186	-0.23 0.074	0.81 <.0001	0.75 <.0001	0.38 0.0025	0.43 0.0007	0.23 0.082	-	*0.01* *0.9425*	*0.16* *0.3052*	*0.00* *0.9968*	*0.37* *0.014*	*0.20* *0.19*
Phide_a	0.69 <.0001	0.29 0.0232	0.27 0.0358	-0.73 <.0001	0.65 <.0001	0.28 0.031	0.18 0.1685	0.55 <.0001	0.10 0.4368	0.57 <.0001	0.02 0.909	-	*0.84* *<.0001*	*0.71* *<.0001*	*0.05* *0.727*	*-0.17* *0.259*
Phytin_a	0.59 <.0001	0.34 0.0082	0.34 0.0084	-0.69 <.0001	0.59 <.0001	0.42 9E-04	0.26 0.0413	0.67 <.0001	0.34 0.0083	0.66 <.0001	0.20 0.1217	0.90 <.0001	-	*0.71* *<.0001*	*-0.02* *0.903*	*-0.20* *0.197*
T.Pheo.	0.25 0.0562	-0.09 0.4832	0.15 0.2685	-0.45 0.0003	0.60 <.0001	-0.08 0.527	-0.23 0.0836	0.46 0.0002	0.15 0.239	0.52 <.0001	-0.07 0.5803	0.67 <.0001	0.67 <.0001	-	*-0.14* *0.372*	*-0.11* *0.484*
B.P. (n=45)	0.60 <.0001	0.73 <.0001	0.60 <.0001	-0.44 0.0027	-0.11 0.476	0.64 <.0001	0.60 <.0001	0.54 0.0001	-0.08 0.5975	0.27 0.074	0.40 0.0058	0.49 0.0007	0.42 0.0043	0.10 0.4976	-	*0.68* *<.0001*
Filt.B.P (n=45)	0.57 <.0001	0.62 <.0001	0.65 <.0001	-0.43 0.0033	-0.24 0.108	0.42 0.004	0.37 0.0113	0.44 0.0022	-0.19 0.2077	0.15 0.3101	0.27 0.0711	0.34 0.0206	0.29 0.051	0.11 0.4577	0.79 <.0001	-

Table AIV. 6: Correlation matrix of salinity and environmental and biological variables at surface, middle, and bottom water with respiration rates in early-spring. In italics (upper right): partial correlation coefficients excluding salinity influence if any. n=60.

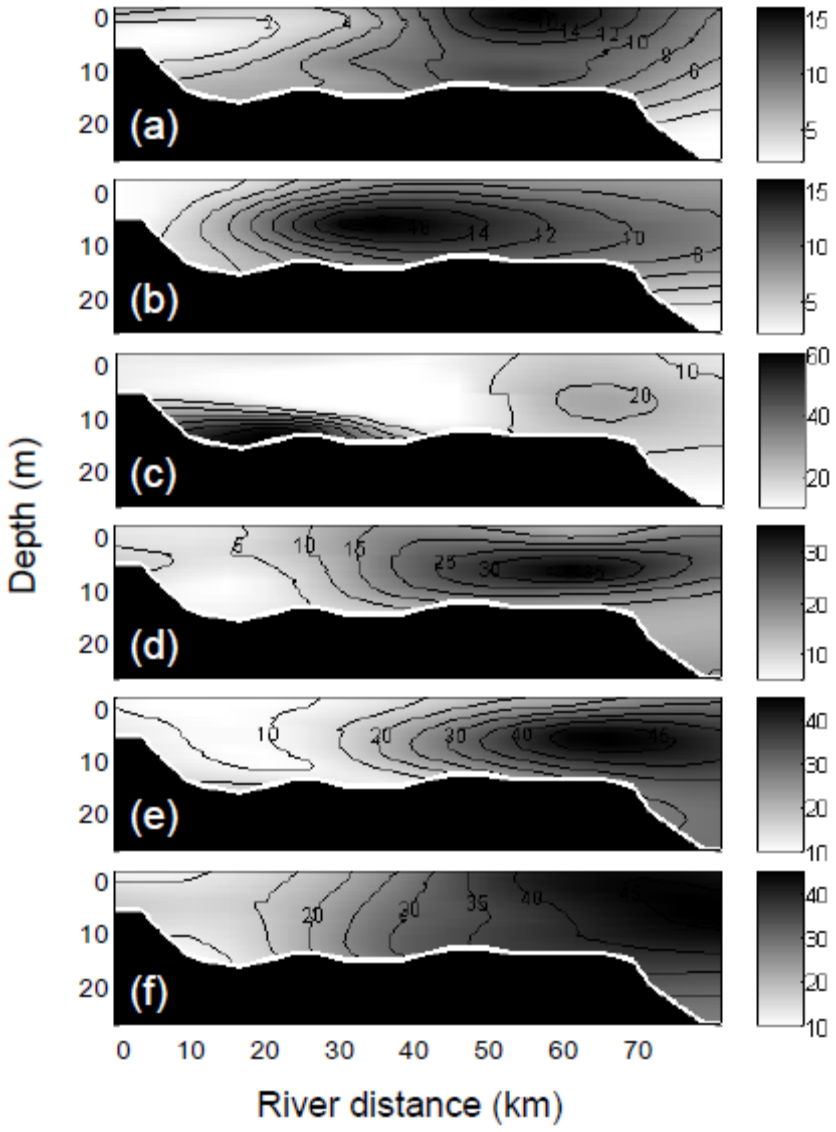

Figure AIV.1 (continued to next page)

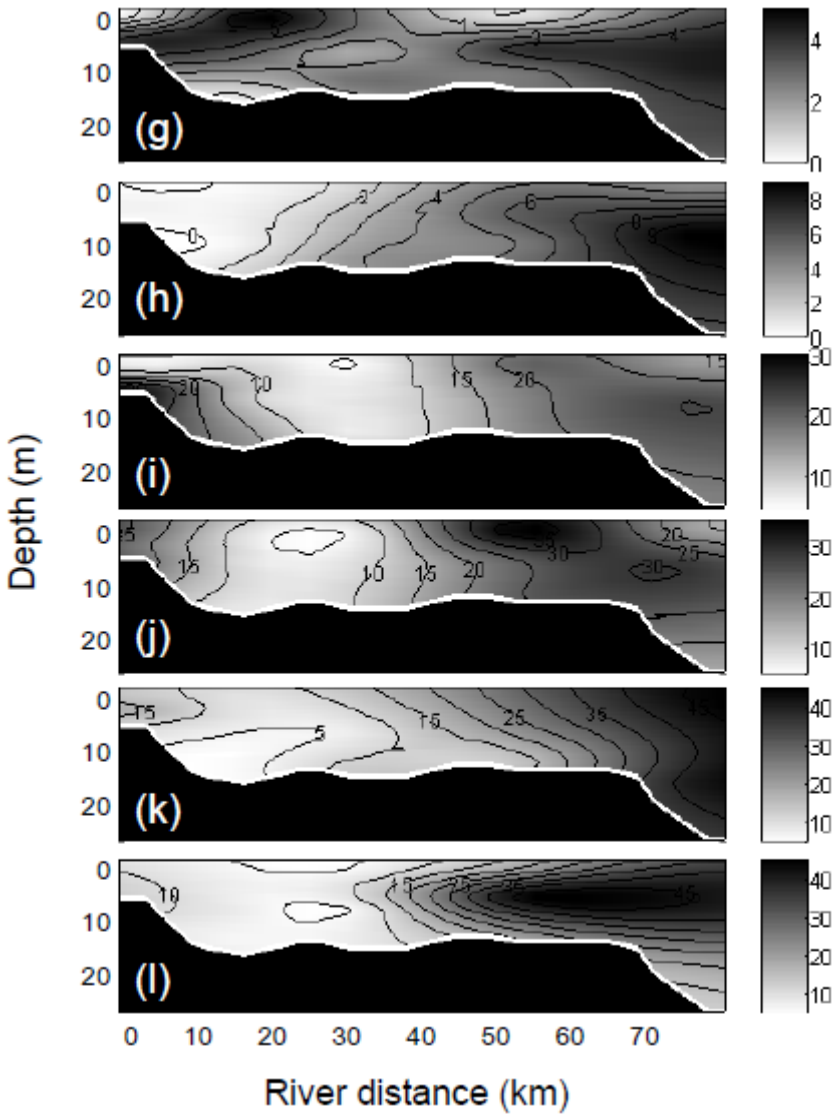

Figure AIV. 1: Contour plots of community metabolism (unit: mg O_2 m^{-3} h^{-1}) at surface, middle, and bottom on two axial surveys per cruise. Late-winter (a & b), early-spring (c & d), and late-spring (e & f) in 2007 and late-winter (g & h), early-spring (i & j), and late-spring (k & l) in 2008. The X-axis of each plot presents distances from the mouth of Susquehanna River (0 river-km) to the Chesapeake Bay Bridge (80 river-km) along the shipping channel.

Complete Reference List

Apple JK, del Giorgio PA, Kemp WM (2006) Temperature regulation of bacterial production, respiration, and growth efficiency in a temperate salt-marsh estuary. Aquat Microb Ecol 43:243–254.

Azam F, Fenchel T, Field JG, Gray JS, Meyer-Reil LA, Thingstad F (1983) The Ecological Role of Water-Column Microbes in the Sea. Mar Ecol Prog Ser 10:257-263.

Baross JA, Crump BC, Simenstad CA (1994) Elevated 'microbial loop' activities in the Columbia River estuarine turbidity maximum. In: Dyer KR, Orth RJ (eds) Changes in fluxes in estuaries: implications from science to management. ECSA/ERF Symp. Olsen & Olsen, Fredenborg, Denmark, p 459-464.

Bauerfeind S (1985) Degradation of phytoplankton detritus by bacteria: Estimation of bacterial consumption and respiration in an oxygen chamber. Mar Ecol Prog Ser 21:27-36.

Boak AC, Goulder R (1983) Bacterioplankton in the diet of the calanoid copepod Eurytemora sp. in the Humber Estuary. Mar Biol 73:139-149.

Boynton WR, Kemp WM (1985) Nutrient regeneration and oxygen consumption by sediments along an estuarine salinity gradient. Marine Ecology Progress Series 23:45-55.

Boynton WR, Kemp WM (2000) Influence of river flow and nutrient loading on selected ecosystem processes: a synthesis of Chesapeake Bay data. In: Hobbie J (ed), A Blueprint for Estuarine Synthesis. p 269-298.

Brand LE (1984) The salinity tolerance of forty-six marine phytoplankton isolates. Est Coast Shelf Sci 18:543-556.

Caffrey JM (2004) Factors controlling net ecosystem metabolism in U.S. estuaries. Estuaries 27:90-101.

Carpenter JH (1965) The accuracy of the Winkler method for dissolved oxygen analysis. Limnol Oceanogr 10:135-140.

Carpenter SR, Cole JJ, Pace ML, Van de Bogert M, Bade DL, Bastviken D, Gille CM, Hodgson JR, Kitchell JF, Kritzberg ES (2005) Ecosystem subsidies: terrestrial support of aquatic food webs from 13C addition to contrasting lakes. Ecology 86:2737-2750.

Cloern JE, Alpine AE, Cole BE, Wong RLJ, Arthur JF, Ball MD (1983) River discharge controls phytoplankton dynamics in the northern San Francisco Bay estuary. Est Coast Shelf Sci 16:415-426.

Cloern JE, Grenz C, Vidergar-Lucas L (1995) An empirical model of the phytoplankton chlorophyll : carbon ratio-the conversion factor between productivity and growth rate. Limnol Oceanogr 40:1313-1321.

Cole BE, Cloern JE (1987) An empirical model for estimating phytoplankton productivity in estuaries. Mar Ecol Prog Ser 36:299-305.

Cole JJ, Caraco NF, Peierls BL (1992) Can phytoplankton maintain a positive carbon balance in a turbid, freshwater, tidal estuary? Limnol Oceanogr 37:1608-1617.

Cowles TJ, Olson RJ, Chisholm SW (1988) Food selection by copepods: discrimination on the basis of food quality. Mar Biol 100:41-49.

Cronin WB, Pritchard DW (1975) Additional statics on the dimensions of the Chesapeake Bay and its tributaries: cross-section widths and segment volumes per meter depth. Chesapeake Bay Institute Special Report 42, Reference 75-3.

Crump BC, Baross JA, Simenstad CA (1998) Dominance of particle-attached bacteria in the Columbia River estuary, USA. Aquat Microb Ecol 14:7-18.

Crump BC, Baross JA (2000) Characterization of the bacterially-active particle fraction in the Columbia River estuary. Mar Ecol Prog Ser 206:13-22.

Crump BC, Peranteau C, Beckingham B, Cornwell JC (2007) Respiratory succession and community succession of bacterioplankton in seasonally anoxic estuarine waters. Appl Environ Microbiol 73:6802-6810.

David V, Sautour B, Galois R, Chardy P (2006) The paradox high zooplankton biomass–low vegetal particulate organic matter in high turbidity zones: what way for energy transfer? J Exp Mar Biol Ecol 333:202-218.

Findlay S, Pace ML, Lints D, Cole JJ, Caraco NF, Peierls B (1991) Weak coupling of bacterial and algal production in a heterotrophic ecosystem: the Hudson River estuary. Limnol Oceanogr 36:268-278.

Fisher TR, Harding LW, Stanley DW, Ward LG (1988) Phytoplankton, nutrients, and turbidity in the Chesapeake, Delaware and Hudson estuaries. Est Coast Shelf Sci 27:61-93.

Fisher TR, Peele ER, Ammerman JW, Harding LW (1992) Nutrient limitation of phytoplankton in Chesapeake Bay. Mar Ecol Prog Ser 82:51-63.

Fisher TR, Gustafson AB, Sellner K, Lacouture R, Haas LW, Wetzel RL, Magnien R, Everitt D, Michaels B, Karrh R (1999) Spatial and temporal variation of resource limitation in Chesapeake Bay. Mar Biol 133:763-778.

Fisher TR, Gustafson AB, Radcliffe GM, Sundberg KL, Stevenson JC (2003) A long-term record of photosynthetically available radiation (PAR) and total solar energy at 38.6°N, 78.2°W. Estuaries 26:1450-1460.

Fuhrman JA, Ammerman JW, Azam F (1980) Bacterioplankton in the coastal euphotic zone: Distribution, activity and possible relationships with phytoplankton. Mar Biol 60:201-207.

Goldman JC (1984) Conceptual role for microaggregates in pelagic waters. Bull Mar Sci 35:462-476.

Griffith P, Shiah F-K, Gloersen K, Ducklow HW, Fletcher M (1994) Activity and distribution of attached bacteria in Chesapeake Bay. Mar Ecol Prog Ser 108:1-10.

Hagy JD, Sanford LP, Boynton WR (2000) Estimation of net physical transport and hydraulic residence times for a coastal plain estuary using box models. Estuaries 23:328-340.

Hansen B, Bjornsen PK, Hansen PJ (1994) The size ratio between planktonic predators and their prey. Limnology and Oceanography 39:395-403.

Harding LW, Meeson BW, Fisher TR (1986) Phytoplankton production in two East Coast estuaries: Photosynthesis-light functions and patterns of carbon assimilation in Chesapeake and Delaware bays. Est Coast Shelf Sci 23:773-806.

Harding LW (1988) The time-course of photoadaptation to low-light in *Prorocentrum mariae-lebouriae* (Dinophyceae). J Phycol 24:274-281.

Heinle DR, Harris RP, Ustach JF, Flemer DA (1977) Detritus as food for estuarine copepods. Mar Biol 40:341-353.

Hitchcock GL (1982) A comparative study of the size-dependent organic composition of marine diatoms and dinoflagellates. J Plankton Res 4:363-377.

Hollibaugh JT, Wong PS (1999) Microbial processes in the San Francisco Bay estuarine turbidity maximum. Estuaries 22:848-862.

Hopkinson CS, Sherr B, Wiebe WJ (1989) Size fractionated metabolism of coastal microbial plankton. Mar Ecol Prog Ser 51:155-166.

Hopkinson CS, Coloso JJ (1995) The relationships among man's activities in watersheds and estuaries: a model of runoff effects on patterns of estuarine community metabolism. Estuaries 18:598-621.

Ichinomiya M, Nakamachi M, Honda M, FUKUCHI M, Taniguchi A (2009) Role of heterotrophic dinoflagellates in the fate of diatoms released from fast ice in coastal water of Lützow-Holm Bay, East Antarctica. Mar Ecol Prog Ser 383:27-36.

Irigoien X, Castel J (1997) Light limitation and distribution of chlorophyll pigments in a highly turbid estuary: the Gironde (SW France). Est Coast Shelf Sci 44:507-517.

Islam MS, Ueda H, Tanaka M (2005) Spatial distribution and trophic ecology of dominant copepods associated with turbidity maximum along the salinity gradient in a highly embayed estuarine system in Ariake Sea, Japan. J Exp Mar Biol Ecol 316:101-115.

Jeong HJ, Park JY, Nho JH, Park MO, Ha JH, Seong KA, Jeng C, Seong CN, Lee KY, Yih WH (2005) Feeding by red-tide dinoflagellates on the cyanobacterium *Synechococcus*. Aquat Microb Ecol 41:131-143.

Johnson MD, Rome M, Stoecker DK (2003) Microzooplankton grazing on *Prorocentrum minimum* and *Karlodinium micrum* in Chesapeake Bay. Limnol Oceanogr 48:238-248.

Kemp WM, Sampou PA, Garber J, Turtle J, Boynton WR (1992) Seasonal depletion of oxygen from bottom waters of Chesapeake Bay: roles of benthic and planktonic respiration and physical exchange processes. Mar Ecol Prog Ser 85:137-152.

Kemp WM, Smith EM, Marvin-Dipasquale M, Boynton WR (1997) Organic carbon balance and net ecosystem metabolism in Chesapeake Bay. Mar Ecol Prog Ser 150:229-248.

Kemp WM, Boynton WR, Adolf JE, Boesch DF, Boicourt WC, Brush G, Cornwell JC, Fisher TR, Glibert PM, Hagy JD, Harding LW, Houde ED, Kimmel DG, Miller WD, Newell RIE, Roman MR, Smith EM, Stevenson JC (2005) Eutrophication of Chesapeake Bay: historical trends and ecological interactions. Mar Ecol Prog Ser 303:1-29.

Kirchman DL (1993) Leucine incorporation as a measure of biomass production by heterotrophic bacteria. In Kemp PF, BF Sherr, EB Sherr, and JJ Cole (eds),

Handbook of methods in aquatic microbial ecology. Lewis Publishers, Boca Raton, FL, p 509–512.

Kleppel GS, Holliday DV, Pieper RE (1991) Trophic interactions between copepods and microplankton: a question about the role of diatoms. Limnol Oceanogr 36:172-178.

Kleppel GS (1993) On the diets of calanoid copepods. Mar Ecol Prog Ser 99:183-195.

Lemaire E, Abril G, De Wit R, Etcheber H (2002) Distribution of phytoplankton pigments in nine European estuaries and implications for an estuarine typology. Biogeochemistry 59:5-23.

Li A, Stoecker DK, Coats DW (2000) Spatial and temporal aspects of *Gyrodinium galatheanum* in Chesapeake Bay: distribution and mixotrophy. J Plankton Res 22:2105-2124.

MacKenzie BR, Leggett WC (1991) Quantifying the contribution of small-scale turbulence to the encounter rates between larval fish and their zooplankton prey: effects of wind and tide. Marine Ecology Progress Series 73:149-160.

Madden CJ, Day JW (1992) Induced turbulence in rotating bottles affects phytoplankton productivity measurements in turbid waters. J Plankton Res 14:1171-1191.

Miller WL, Moran MA (1997) Interaction of photochemical and microbial processes in the degradation of refractory dissolved organic matter from a coastal marine environment. Limnol Oceanogr 42:1317-1324.

Muylaert K, Sabbe K, Vyverman W (2000) Spatial and temporal dynamics of phytoplankton communities in a freshwater tidal estuary (Schelde, Belgium). Est Coast Shelf Sci 50:673-687.

North EW, Houde ED (2003) Linking ETM physics, zooplankton prey, and fish early-life histories to striped bass *Morone saxatilis* and white perch *M. americana* recruitment. Mar Ecol Prog Ser 260:219-236.

North EW, Houde ED (2006) Retention mechanisms of white perch (*Morone americana*) and striped bass (*Morone saxatilis*) early-life stages in an estuarine turbidity maximum: an integrative fixed-location and mapping approach. Fish Oceanogr 15:429-450.

Pace ML, Cole JJ, Carpenter SR, Kitchell JF, Hodgson JR, van de Bogert MC, Bade DL, Kritzberg ES, Bastviken D (2004) Whole-lake carbon-13 additions reveal terrestrial support of aquatic food webs. Nature 427:240-243.

Pace ML, Cole JJ, Carpenter SR, Kitchell JF, Hodgson JR, van de Bogert MC, Bade DL, Kritzberg ES, Bastviken D (2004) Whole-lake carbon-13 additions reveal terrestrial support of aquatic food webs. Nature 427:240-243.

Pace ML, Carpenter SR, Cole JJ, Coloso JJ, Kitchell JF, Hodgson JR, Middelburg JJ, Preston ND, Solomon CT, Weidel BC (2007) Does terrestrial organic carbon subsidize the planktonic food web in a clear-water lake? Limnol Oceanogr 52:2177-2189.

Painchaud J, Lefaivre D, Therriault J-C (1987) Box model analysis of bacterial fluxes in the St. Lawrence Estuary. Mar Ecol Prog Ser 41:241-252.

Parsons T R, Takahashi M, Hargrave B (1984). Biological Oceanographic Processes, 3rd edition. Pergamon Press Inc., New York.

Peterson DH, Festa JF (1984) Numerical simulation of phytoplankton productivity in partially mixed estuaries. Est Coast Shelf Sci 19:563-589

Pomeroy LR (1974) The ocean's food web, A changing paradigm. BioScience 24:499-504.

Preen K, Kirchman DL (2004) Microbial respiration and production in the Delaware Estuary. Aquat Microb Ecol 37:109-119.

Richman S, Bohon SA, Robins SE (1980) Grazing interactions among freshwater calanoid copepods. In: In evolutionand ecology of zooplankton communities. W. C. Kerfoot, ed. U. Press of New England, Hanover, New Hampshire., p 219-233.

Roman MR (1984) Utilization of detritus by the copepod, *Acartia tonsa*. Limnol Oceanogr 29:949-959.

Roman MR, Holliday DV, Sanford LP (2001) Temporal and spatial patterns of zooplankton in the Chesapeake Bay turbidity maximum. Mar Ecol Prog Ser 213:215-227.

Sampou P, Kemp WM (1994) Factors regulating plankton community respiration in Chesapeake Bay. Mar Ecol Prog Ser 110:249-258.

Sanders RW, Porter KG, Caron DA (1990) Relationship between phototrophy and phagotrophy in the mixotrophic chrysophyte *Poterioochromonas malhamensis*. Microb Ecol 19:97-109.

Sanders RW (1991) Mixotrophic protists in marine and freshwater ecosystems. J Eukaryot Microbiol 38:76-81.

Sanford LP, Suttles SE, Halka JP (2001) Reconsidering the physics of the Chesapeake Bay estuarine turbidity maximum. Estuaries 24:655-669.

Schubel JR, Pritchard DW (1986) Responses of upper Chesapeake Bay to variations in discharge of the Susquehanna River. Estuaries 9:236-249.

Sellner KG, Lacouture RV, Cibik SJ, Brindley A, Brownlee SG (1991) Importance of a winter dinoflagellate-microflagellate bloom in the Patuxent River estuary. Est Coast Mar Sci 32:27-42.

Sellner KG, Sawangwong P, Dawson R, Boynton WR, Kemp WM, Garber JH (1992) Fate of dinoflagellates in Chesapeake Bay: is sedimentation likely? Marine Phytoplankton. Smayda TJ (ed), Elsevier, New York, NY, p 825-830.

Sherr EB, Sherr B. (2007) Heterotrophic dinoflagellates: a significant component of microzooplankton biomass and major grazers of diatoms in the sea. Mar Ecol Prog Ser 352:187-197.

Sieburth JM, Smetacek V, Lenz J (1978) Pelagic ecosystem structure: heterotrophic compartments of the plankton and their relationship to plankton size fractions. Limnol Oceanogr 23:1256-1263.

Simon M, Grossart H-P, Schweitzer B, Ploug H (2002) Microbial ecology of organic aggregates in aquatic ecosystems. Aquat Microb Ecol 28:175-211.

Smith EM, Kemp WM (1995) Seasonal and regional variations in plankton community production and respiration for Chesapeake Bay. Mar Ecol Prog Ser 116:217-231.

Smith EM, Kemp WM (2001) Size structure and the production/respiration balance in a coastal plankton community. Limnol Oceanogr 46:473-485.

Smith EM, Kemp WM (2003) Planktonic and bacterial respiration along an estuarine gradient: responses to carbon and nutrient enrichment. Aquat Microb Ecol 30:251-261.

Smith SV, Hollibaugh JT (1997) Annual cycle and interannual variability of ecosystem metabolism in a temperate climate embayment. Ecol Monogr 67:509-533.

Stickney HL, Hood RR, Stoecker DK (2000) The impact of mixotrophy on planktonic marine ecosystems. Ecol Model 125:203-230.

Stoecker DK, Li A, Coats DW, Gustafson DE, Nannen MK (1997) Mixotrophy in the dinoflagellate *Prorocentrum minimum*. Mar Ecol Prog Ser 152:1-12.

Stoecker DK (1998) Conceptual models of mixotrophy in planktonic protists and some ecological and evolutionary implications. Eur J Protistol 34:281-290.

Tackx MLM, Herman PJM, Gasparini S, Irigoien X, Billiones R, Daro MH (2003) Selective feeding of Eurytemora affinis (Copepoda, Calanoida) in temperate estuaries: model and field observations. Est Coast Shelf Sci 56:305-311.

Tyler MA, Seliger HH (1978) Annual subsurface transport of a red tide dinoflagellate to its bloom area: water circulation patterns and organism distributions in the Chesapeake Bay. Limnol Oceanogr 23:227-246.

Valiela I, Foreman K, LaMontagne M, Hersh D, Costa J, Peckol P, DeMeo-Andreson B, D'Avanzo C, Babione M, Sham C, Brawley J, Lajtha K (1992) Couplings of watersheds and coastal waters: Sources and consequences of nutrient enrichment in Waquoit Bay, Massachusetts. Estuaries 15:443-457.

Van den Meersche K, Van Rijswijk P, Soetaert K, Middelburg JJ (2009) Autochthonous and allochthonous contributions to mesozooplankton diet in a tidal river and estuary: integrating carbon isotope and fatty acid constraints. Limnol Oceanogr 54:62-74.

Van Heukelem L, Thomas CS (2001) Computer-assisted high-performance liquid chromatography method development with applications to the isolation and analysis of phytoplankton pigments. J Chromatogr A 910:31-49.

Vincent WF, Dodson JJ, Bertrand N, Frenette J (1996) Photosynthetic and bacterial production gradients in a larval fish nursery: the St. Lawrence River transition zone. Mar Ecol Prog Ser 139:227-238.

Welschmeyer NA, Copping AE, Vernet M, Lorenzen CJ (1984) Diel fluctuation in zooplankton grazing rate as determined from the downward vertical flux of pheopigments. Mar Biol 83:263-270.

White JR, Roman MR (1992) Seasonal study of grazing by metazoan zooplankton in the mesohaline Chesapeake Bay. Mar Ecol Prog Ser 86:251-261.

Wienke SM, Cloern JE (1987) The phytoplankton component of seston in San Francisco Bay. Neth J Sea Res 21:25-33.

Winkler G, Dodson JJ, Bertrand N, Thivierge D, Vincent WF (2003) Trophic coupling across the St. Lawrence River estuarine transition zone. Mar Ecol Prog Ser 251:59-73.

Wofsy SC (1983) A simple model to predict extinction coefficients and phytoplankton biomass in eutrophic waters. Limnol Oceanogr 28:1144-1155.

Xu J, Hood R, Chao SY (2005) A simple empirical optical model for simulating light attenuation variability in a partially mixed estuary. Estuaries 28:572-580.

Sources of Unpublished Data

CBP. 2009. U.S. Environmental Protection Agency. Unpublished data. Chesapeake Bay Program Office, Chesapeake Bay Water Quality Monitoring Program. Annapolis, Maryland. <http://www.chesapeakebay.net>

NOAA. 2009. U.S. National Oceanographic and Atmospheric Administration. Water Temperature. Silver Spring, Maryland. <http://www.noaa.gov>

USGS. 2009. U.S. Geological Survey. Unpublished data. River Discharge. Reston, Virginia. <http://www.usgs.gov>